Modeling Compositionally-Sensitive Reservoirs

By

Kameshwar Singh

A Dissertation for the Partial Fulfillment
of Requirements for the
Degree of Doktor Ingeniør

Department of Petroleum Engineering
and Applied Geophysics

Norwegian University of Science and Technology

May 2002

Acknowledgments

I wish to express my sincerest gratitude to my advisor, Professor Curtis H. Whitson, for his excellent guidance, invaluable suggestions and comments throughout my research work. I also wish to express my sincerest thanks to my co-advisor Dr. Øivind Fevang, Pera, for his technical guidance and fruitful discussions. I am grateful to Dr. Fevang for all his academic and personal help.

Sincere thanks to Professor Michael Golan, Mohammad Faizul Hoda, other colleagues and staff at the Department of Petroleum Engineering and Applied Geophysics for their help during my work.

I would like to thank Tao Yang, Vidar Haugse, and Knut Uleberg for many useful discussions and their helpful comments about my research. I also thank Kathy Herje for her help in proof-reading the thesis for improved readability.

I would like to acknowledge Pera for providing me with financial support to carry out my research, together with companies supporting research projects which led to this thesis and provided a financial foundation for the completion of the dr.ing. degree — Conoco, Ecopetrol, Fortum, Mobil Exploration Norway Inc., Norsk Agip, Norsk Hydro, Norwegian Petroleum Directorate, Phillips, Statoil, and Totalfinaelf.

I am indebted to my father who always encouraged higher studies. I also thank my wife, Sunita, for her encouragement to start the PhD study and her patience and support during the entire work. I am also indebted to my daughter, Sarika, for her understanding.

Trondheim, May 2002
Kameshwar Singh

Summary

This research work provides guidelines for choosing the PVT model (black-oil or EOS compositional) for full-field reservoir simulation of volatile/near-critical oil and gas condensate fluid systems produced by depletion and/or gas injection.

The main issues covered in this dissertation are:

1. Modeling of PVT and flow behavior.

2. Ensuring consistency between black-oil and compositional simulation, particularly for in-place surface volumes.

3. Situations when black-oil models can and should be used, and when compositional models are required.

The first task in this research was to select a wide range of fluid systems varying from medium-rich gas condensate; to near critical fluid; to volatile oil; to slightly volatile oil; to low-GOR oil. In this way, it was desired to have different fluid systems one can expect in any petroleum reservoir.

The one way to get different fluid systems along with corresponding equation-of-state (EOS) models was from published literature. This will require different EOS models for different fluid systems — i.e. a large number of fluid systems and corresponding EOS models. This approach was not considered practical.

Another way was to select a complex fluid system from a complex petroleum reservoir, thereafter derive different fluid systems from the complex fluid system. In this way, only one EOS model would describe all the fluid systems required in this study.

The complex fluid system selected was from an actual North Sea reservoir. This fluid system varied from medium-rich gas condensate to slightly volatile oil, with a critical-fluid gas/oil transition.

The EOS model was obtained by the Pedersen et al. characterization procedure with the SRK EOS. The decanes-plus fraction was split into 9 fractions using a commercial PVT simulation program. The final detailed-EOS model contained 22 components with 12 heptanes-plus fractions.

Since it is impractical to use such a detailed 22-component EOS model in full-field simulation, the detailed-EOS was lumped to fewer components in a stepwise procedure. It was possible to lump the detailed-EOS from 22 components to as

few as 6 components. The lumped-EOS model predicted all PVT properties with reasonable accuracy — even including depletion and gas injection performance for the near critical compositionally grading fluid system. The minimum miscibility pressures predicted with the lumped-EOS were also quite accurate, when compared with the detailed-EOS calculations.

For black-oil simulation models, the black-oil PVT tables can be generated using different PVT experiments. It is recommended to use a depletion-type experiment (CCE, CVD, or DLE) for oil and gas condensate reservoirs. The black-oil PVT tables for compositionally grading reservoirs with undersaturated GOC should be generated from CCE experiment using the GOC fluid. For saturated GOC reservoirs, the oil PVT tables should be generated from the GOC oil and the gas PVT tables should be generated from the GOC equilibrium gas. The surface oil and gas densities should be modified to obtain correct reservoir oil and gas densities at the GOC conditions. Different methods are also described for generating black-oil PVT tables for gas injection, where the black-oil PVT tables are required to be extrapolated to higher pressures.

The aim of the research was also to get consistent in-place surface volumes. The compositionally grading reservoir was initialized using the lumped-EOS model for obtaining initial in-place volumes. Different methods were used for getting compositional gradient for the lumped-EOS model. The lumped-EOS model in-place volumes were compared with the detailed-EOS model in-place volumes. It was possible to get quite accurate in-place volume in the lumped-EOS model with proper selection of the compositional gradient.

The lumped-EOS compositional model in-place volumes were also compared with that of the black-oil model. For the black-oil model initialization, the black-oil PVT tables were generated from the lumped-EOS using the GOC fluid. The compositional gradient in the black-oil model i.e. solution gas-oil ratio and oil-gas ratio versus depth were obtained from the compositional model. The black-oil model in-place volumes were quite accurate with proper selection of the black-oil PVT table and compositional gradient.

For reservoir simulation studies, a 3D dipping reservoir with 99 layers was used. The reservoir had dip angle of 3.8 degree. The permeability from the top layer to the bottom layer were either monotonically increasing or decreasing. The reservoir layer permeabilities were varied based on Dykstra-Parsons model. Different average reservoir permeability was used to quantify the effect of gravity. The simulated reservoir performance was analyzed for different fluid systems for both depletion and injection cases. Furthermore, the possibility for reducing the number of numerical layers without loosing the “accuracy” was examined since it is not practical (due to excessive CPU time) to use 99-layer simulation model for comparison of the production performance from the

compositional and the black-oil models. Different fluid systems and permeability distributions were used for comparing the simulated performance from a model with a reduced number of layers with the results from the model with 99-layer. Based on the analysis, it was found that 10 numerical layers with equal flow capacity were sufficient to reproduce the production performance from the 99-layer.

For comparing black-oil and compositional simulation performance results, the 3D model was used to obtain areal and vertical sweep efficiency correctly. Three different non-communicating geologic units were used, each geologic unit with ten numerical layers and different horizontal permeabilities. The layer permeabilities were distributed in different ways — e.g. highest k at the top, highest k at the bottom or highest k in the middle.

Reservoir performance was analyzed for different simulation cases. Each "reservoir" was simulated using black-oil and compositional models for various depletion and gas injection cases. The simulated performance for the two PVT models was compared for fluid systems ranging from a medium-rich gas condensate to a critical fluid, to slightly volatile oils. The initial reservoir fluid composition was either constant with depth, or a vertical compositional gradient. Both saturated and undersaturated GOC's were considered. The reservoir performance for the two PVT models was also compared for different permeability distributions.

Reservoir simulation results show that the black-oil model can be used for all depletion cases if the black-oil PVT data are generated properly. In most gas injection cases, the black-oil model is not adequate — with only a few exceptions.

Most of the results presented in this dissertation have been presented in the following paper, included as Appendix A:

> Fevang, Ø., Singh, K., and Whitson, C.H. : "Guidelines for Choosing Compositional and Black-oil Models for Volatile Oil and Gas-Condensate Reservoirs," paper SPE 63087 presented at the 2000 Annual Technical Conference and Exhibition, Dallas, Texas, 1-4 October 2000.

Contents

Chapter 1

Fluid Modeling for Reservoir Simulation

1.1 Introduction

Numerical reservoir simulators are widely used for petroleum reservoir performance prediction for full-field development. The reservoir simulator may use black-oil or compositional PVT formulation depending upon the necessity/requirement. The compositional simulation model prediction is considered accurate, but it takes more CPU time and computer memory. The black-oil formulation takes less CPU time and computer memory, but may or may not give performance prediction as accurate as compositional formulation, depending on the recovery mechanism, reservoir and fluid properties.

The aim of this chapter is to model black-oil and compositional PVT consistently and compare the results for these two formulations with respect to initialization. First of all, one reference sample was selected and a 22-component EOS model was used. Secondly the fluid system was obtained varying from rich gas condensate to volatile oil using isothermal gradient calculations. The next step was to reduce the number of components from 22 to fewer components for reservoir simulation. The black-oil and compositional models were initialized to obtain consistent in-place surface volumes.

1.2 PVT Models

In this section, first a reservoir fluid sample was selected. The SRK EOS model was used for fluid description and isothermal gradient calculations performed to get fluid samples from different depths. Lumping was performed to reduce the number of components. The lumped-EOS model results (PVT experiments, numerical simulation, etc.) were compared with that of the detailed-EOS model.

1.2.1 Detailed EOS model

Selection of Reservoir Fluid

The first step in the PVT modeling was to select a reference fluid sample. The fluid sample was selected from a North Sea field[1], a slightly undersaturated gas condensate with initial reservoir pressure of 490 bara at the “reference" depth of 4640 m MSL. The selected reference sample contains 8.6 mol-% C_{7+}, a two-stage

GOR[a] of 1100 Sm^3/Sm^3 and a dewpoint of 452 bara at the reservoir temperature of 163 °C. The reference fluid composition is given in Table A-1[b].

22-Component SRK EOS Model

The Pedersen et al. SRK[2] EOS characterization method was used to generate the "base" EOS model. Decanes-plus was split into 9 fractions using the EOS simulation program PVTsim[3].

The Pedersen et al.[4] viscosity correlation is known to be more accurate in viscosity predictions than the Lohrenz, Bray, and Clark (LBC)[5] correlation, particularly for oils. Therefore, Pedersen predicted viscosities were used as "data" to tune the LBC correlation (using the critical volumes of C_{7+} fractions) in the EOS simulation program PVTx[6]. To cover a range of viscosities that might be expected during a gas injection process, viscosity "data" were also generated using mixtures of the reference fluid and methane and flashing the mixtures at pressures in the range of 100 to 300 bara. This resulted in oil viscosities up to 7 cp, considerably higher than reservoir oil "depletion" viscosities from the reference fluid (maximum 0.5 cp).

For gas viscosities, the difference between the tuned LBC correlation and Pedersen viscosities ranged from -5 to -12%. For oil viscosities, the tuned LBC correlation predicts oil viscosity about 15% lower than Pedersen viscosities up to about 0.35 cp. For higher oil viscosities (0.35 - 1.25 cp), the tuned LBC correlation predicts up to 15% higher oil viscosities than Pedersen viscosities. For still higher oil viscosities ("vaporized" oil), the tuned LBC correlation consistently predicts lower and lower viscosities compared with the Pedersen oil viscosities (Fig. C-1).

Isothermal Gradient Calculation

The basic equations[7] for the isothermal gradient calculations are

$$\mu_i(p_{ref}, z_{ref}, T) = \mu_i(p, z, T) + M_i g(h - h_{ref}) \qquad i = 1,2,...,N \quad \text{.....(1.1)}$$

$$\sum_{i=1}^{N} z_i(h) = 1 \quad \text{.....(1.2)}$$

where μ_i = chemical potential of component i, z_{ref} = homogeneous mixture at pressure p_{ref} at a reference depth h_{ref}, p = pressure, and z = mixture composition at depth h.

Based on isothermal gradient calculations using the "base" 22-component SRK EOS model (Table A-2), the reservoir fluids vary from medium-rich gas

[a] Separator conditions (1) first stage 75 bara & 75 °C (2) second stage 1.0135 bara & 15.56 °C. These separator conditions are used in this work unless otherwise mentioned.

[b] Table A-1 means Table 1 of Appendix A, and so on.

condensate to highly-volatile oil in the depth interval from 4500 to 5000 m MSL, with GORs ranging from 1515 to 244 Sm^3/Sm^3, C_{7+} content ranging from 6.9 to 22 mol-%, dewpoints ranging from 428 to 475 (maximum) bara, and bubblepoint pressure ranging from 475 to 435 bara (Table A-3). The reservoir pressure varies from 484.8 bara at the top to 509.0 bara at the bottom. At the GOC, reservoir pressure is 494.7 bara and (critical) saturation pressure is 473.4 bara i.e. the reservoir is undersaturated by 21.2 bar at the GOC. Variations in reservoir pressure, saturation pressure, and solution GOR are shown in **Fig. 1.1**.

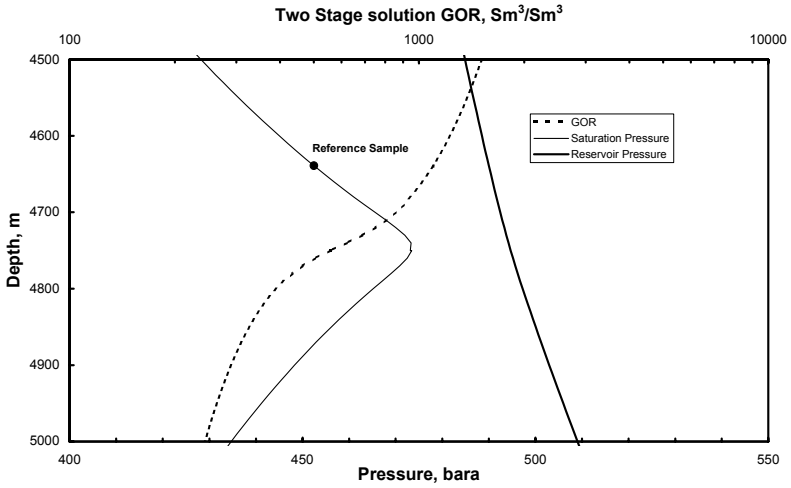

Fig. 1.1 — Reservoir pressure, saturation pressure and solution GOR variation with depth.

Selection of Different Fluid Samples

In this study, different fluid systems were used, all originating directly or indirectly from the compositional gradient calculation using the 22-component EOS model. The fluid systems are:

1. Compositional gradient throughout the entire reservoir, from undersaturated gas condensate at the top to a lower-GOR volatile oil at the bottom.
2. Only the grading gas condensate fluids above the GOC (i.e. remove the underlying oil).
3. Only the grading oil below the GOC (i.e. remove the overlying gas).
4. A gas condensate, initially undersaturated, is taken from a specified depth in the reservoir. This gas condensate fluid is assumed to have constant composition with depth.
5. A relatively low-GOR volatile oil taken at a specified depth in the reservoir. This oil is assumed to have constant composition with depth.

6. A low-GOR oil was "constructed" from the oil taken at 250 m below the GOC, where this oil was further flashed to a pressure of 135 bara with the equilibrium oil having a GOR of 50 Sm^3/Sm^3.

For constant composition fluid systems (4) and (5) above, the fluids were selected at depths 250, 50 and 10 m above and below the GOC, as well as the GOC composition. In this way, seven "samples" were collected from the single compositional gradient calculation as shown in **Fig. 1.2**.

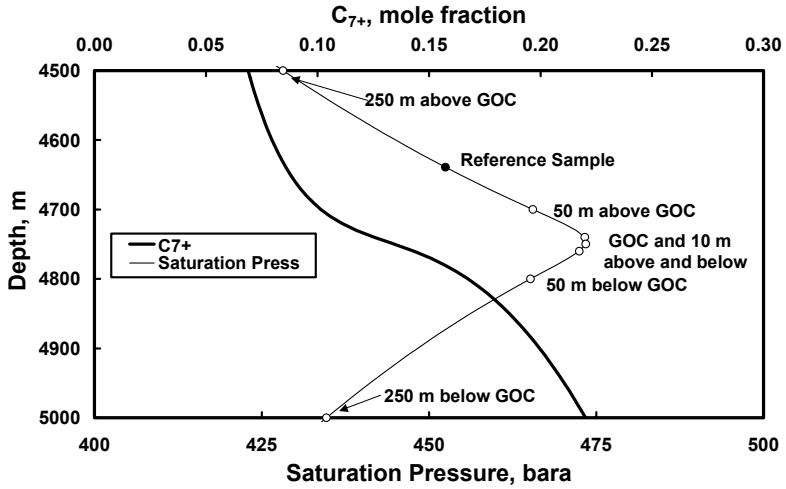

Fig. 1.2 — Saturation pressure and C_{7+} variation with depth and different selected feed locations.

For all further reference, the fluid name was given based on their depth. The feed 4500 represents the reservoir fluid taken from a depth of 4500 m. The fluid from 4500 m represents a medium-rich[a] gas condensate, while richness increases with increasing depth. The fluid at the depth of 4750 m is near critical fluid. The reservoir fluid above 4750 is gas condensate and below is oil. The reservoir fluid compositions from different depths are given in Table B-1.

[a] A "rich" gas condensate implies a fluid with "large" OGR, and a "lean" gas condensate implies a fluid with "low" OGR.

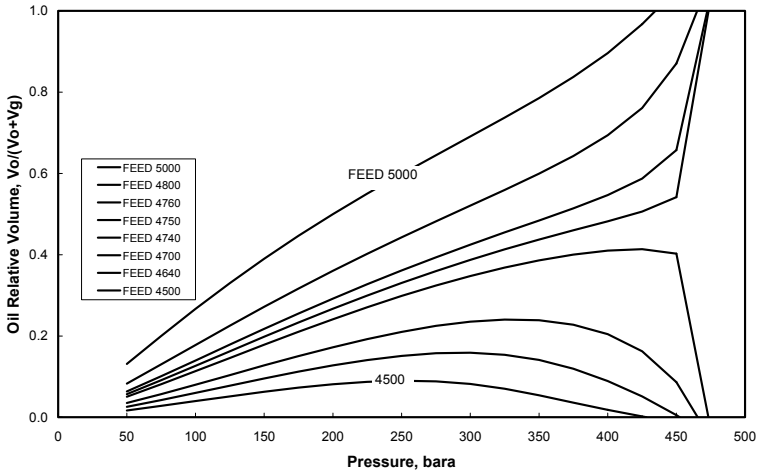

Fig. 1.3 — Oil relative volume from simulated constant composition expansion experiments with different fluids (EOS22).

The oil relative volume curves from CCE experiments for the different fluids are shown in **Fig. 1.3**.

1.2.2 Lumping – Reducing Number of Components

Since it is impractical to conduct full-field simulations using a 22-component model (due to CPU and memory limitations), several "lumped" or reduced-component EOS models were developed – i.e. EOS models with 19-, 12-, 10-, 9-, 6-, 4-, and 3 components.

In the past, several authors have suggested different methods for lumping[7,8,9,10,11].

In this research, the approach for developing lumped-EOS models involves a stepwise-automated regression procedure, whereby the 22-component EOS model is used to calculate PVT experimental data, which are then treated (stored) as "data". At each step in the lumping procedure, a few components are grouped together. The newly-formed component properties are then adjusted to minimize the difference in EOS calculations compared with the original 22-component EOS "data".

The lumping procedure is summarized below:

1. Using the original (22-component) EOS model, simulate a set of PVT experiments, which cover a wide range of pressures and compositions expected in the recovery processes used to produce a reservoir. Eight samples were used for the lumping procedure in this study, ranging from the medium-rich gas condensate, to the near-critical system, and to the downstructure "low"-GOR volatile oil.

2. PVT experiments included constant composition tests, depletion-type experiments (differential liberation and constant volume depletion), separator tests, and multicontact gas injection (swelling) tests. Two quite-different injection gases were used for the swelling test simulations.
3. The simulated PVT properties were used as "data" for the step-wise lumping.
4. At each step in lumping, new lumped-components were formed from existing components. Regression was used to fine tune the newly-formed lumped-component EOS parameters and a selected number of BIPs.
5. Step 4 was repeated a number of times, trying (manually) to select the best grouping at each stage in the lumping process.

The procedure allows the determination of which components are best to group, and at what point during lumping, the quality of EOS predictions deteriorate beyond what is acceptable for engineering calculations.

Generating the 22-Component EOS PVT "Data"

The 22-component EOS model was first used to generate a large set of PVT data. A total of eight feeds (one reference sample and seven generated from the compositional gradient calculation; four gas samples, one near-critical sample, and three oil samples) were used for generating PVT data. Depletion-type PVT tests and separator tests were used, together with swelling-type tests for several injection gases. All calculated PVT results using these feeds were treated as "data" for lumping.

Constant composition expansion (CCE) experiments

For oil samples, the constant composition expansion experiment[7] was used to determine the bubblepoint pressure, the undersaturated oil density, isothermal oil compressibility, total relative volume, and the two-phase volumetric behavior at pressures below the bubblepoint. For gas condensate samples, total relative volume, liquid dropout, and Z-factors were obtained.

Constant composition expansion data were generated for all of the eight fluid samples in the pressure range of 600 to 50 bara with pressure at an interval of 25 bar. Saturation pressures were given somewhat additional weighting in the lumping runs.

Separator tests

Separator tests were performed to determine saturated formation volume factor (FVF), separator oil properties, producing gas-oil ratio, stock-tank oil density, and total produced gas gravity.

Separator test data were generated for all of the eight feeds. A two-stage separator was used, with primary-separator conditions of 75 bara and 75 ^{o}C, and stock-tank conditions of 1.0135 bara and 15.56 ^{o}C. Zero weight factors were used for the

second-stage GOR, while generating data (i.e. only 1st-stage and total GORs were included).

Constant volume depletion (CVD) experiments
To simulate depletion behavior of a gas condensate reservoir, constant volume depletion experiments were simulated. From this experiment, produced gas composition (C_{7+} in particular), relative oil volume, cumulative gas produced, and Z-factors were obtained. CVD tests were simulated for all of the gas condensate samples (4 samples).

Differential liberation expansion (DLE) experiments
For oil samples and the near-critical sample, differential liberation tests were simulated. Saturation pressures, oil formation volume factors, solution gas-oil ratios, oil and gas densities, oil and gas viscosities, and gas Z-factors were obtained from this experiment.

Selection of injection gases for multi-contact swelling experiments
Two gases were selected for studying injection processes – a "rich" primary separator gas and a lean reservoir gas from a North Sea field.

Rich Gas (primary-stage separator gas):
For obtaining the "rich" injection gas, the GOC feed was flashed at primary separator conditions – 75 bara and 75 ^{o}C. The composition of this gas is given in Table A-4. The C_{7+} fraction in this injection gas is 0.49 mol-%. It was found that the primary separator gas from the GOC mixture was more-or-less the same as primary separator gas from any of the reservoir fluid compositions (Table B-2).

Lean Gas:
The lean gas was selected from a North Sea lean-gas reservoir. The composition of the gas is given in Table A-4. The C_{7+} fraction in this injection gas is 0.18 mol-%.

Multi-contact swelling experiments
One sample from the gas zone 10 m above the GOC and another sample from 10 m below the GOC were selected for swelling experiments.

For the reservoir gas sample, primary-stage separator gas was injected step-wise and then CCE experiments were performed for each mixture to obtain PVT data in a "swelling test" process. Similarly, primary-stage separator gas was injected in the reservoir oil sample. The above swelling experiments were repeated with lean injection gas.

A total of 8 CCE, 8 SEP, 5 CVD, 8 DLE and 8 MCV experiments were used for generating the "data" for lumping.

Stepwise Lumping

At each lumping stage, two steps were used. In the first step, the components to be grouped were selected. Then the lumped-component EOS constants A and B, and binary interaction parameters between C_1 and C_{7+} were modified to match the PVT data. Different combinations were used for selecting the components to be grouped. The combinations predicting the PVT data correctly were grouped together. In the first step, only the PVT data fits were considered. In the second step, the oil and gas viscosities were fit; the critical volumes of the newly formed lumped-components were changed to match the oil and gas viscosities.

First, a 19-component EOS model was obtained after grouping C_1+N_2, i-C_4+n-C_4, and i-C_5+n-C_5.

The regression parameters for PVT fits were EOS constants A and B of the newly-formed lumped-components and (collectively) the binary interaction parameters between C_1 and C_{7+}. All simulated tests were used for the PVT fit. For viscosity fits (at each stage in the lumping process), only DLE and MCV viscosity data were used in regression. Viscosity regression parameters were the critical volumes of the newly formed lumped-components.

PVT properties of the 19-component EOS model matched the 22-component EOS model almost exactly.

The 12-component EOS model was obtained by grouping the original twelve C_{7+} fractions into 5 fractions on the basis of (more-or-less) equal mass fraction of the C_{7+} fractions. The heaviest component was kept as the original fraction and other components were grouped into 4 lumped-components. Regression was performed again, where it was found that the 12-component EOS model predicts PVT properties very similar to the 22-component EOS model.

The 10-component EOS model was obtained after reducing C_{7+} fractions from 5 to 3 fractions, based on equal mass fraction of the C_{7+} fractions. Regression was performed and the 10-component EOS model predicts PVT properties, which are comparable with the 22-component EOS model properties.

In the 9-component EOS model, C_2 and CO_2 were grouped together. There is little change from the 10-component EOS. If there is a possibility of CO_2 gas injection (in the actual full field project), then CO_2 should not be grouped with any other component.

Further grouping was done in steps. In each step, one component was grouped with another suitable component and properties were compared with the 22-component EOS model (after regression). From the 9-component EOS model, it was grouped to 8-, 7-, and finally 6 components. In the 6-component EOS, it was necessary to have 3 C_{7+} fractions. The heaviest component was kept as one

component, because grouping with any other component deviated the PVT properties. Hence, the 6-component EOS model contained 3 C_{7+} components and 3 C_{6-} components.

It is required to have 3 gas components in the EOS model, to properly model injection gas and lean gas to near critical fluid description. Similarly it is also necessary to have 3 oil fractions for proper treatment of vaporization, condensation and critical fluid description. So the 6-component EOS model can properly describe the complex fluid system and depletion and gas injection mechanisms. The 22-component EOS (EOS22) model versus the 6-component EOS (EOS6) model PVT properties are shown in Fig. A-3[a] through A-6.

1.2.3 Verification of the Lumped-EOS

CVD Depletion Recovery

As a check on the validity of the lumped-EOS models, depletion recovery factors calculated from CVD tests were used as a verification of how accurate the lumped-models maintained surface oil and surface gas recoveries, when compared with the original EOS22 model. CVD data are used to compute surface oil and gas recoveries at different pressures (based on simplified surface flash). The basic equations[12] used in calculations are given below

$$RF_{\bar{g}} = \left(1 - \frac{(p/z)_d}{(p/z)_i}\right) + \frac{(p/z)_d}{(p/z)_i} \cdot \sum_{k=1}^{N} \left(\frac{\Delta n_p}{n_d}\right)_k \cdot \frac{\left(1 + r_{si} \cdot C_{og}\right)}{\left(1 + r_{sk} \cdot C_{og}\right)} \quad \text{.....(1.3)}$$

$$RF_{\bar{o}} = \left(1 - \frac{(p/z)_d}{(p/z)_i}\right) + \frac{(p/z)_d}{(p/z)_i} \cdot \sum_{k=1}^{N} \left(\frac{\Delta n_p}{n_d}\right)_k \cdot \frac{\left(1/r_{si} + C_{og}\right)}{\left(1/r_{sk} + C_{og}\right)} \quad \text{.....(1.4)}$$

$$r_s \approx \frac{y_{7+}}{y_{7+} - 1} \cdot \frac{1}{C_{og}} \quad \text{.....(1.5)}$$

$$C_{og} = \frac{R.T_{sc}}{P_{sc}} \cdot \frac{\rho_o}{M_o} \quad \text{.....(1.6)}$$

In the above equations, it is assumed that $C_{og}(p)$= constant = C_{ogi}[b].

[a] Fig A-3 means Fig. 3 of Appendix A, and so on.

[b] There will be some difference in recovery if variable $C_{og}(p)$ is used but the difference will be almost same in the two EOS models for a given fluid system.

When deviation in condensate recovery factor is used for comparison, the leanest upstructure gas at 4500 m shows the largest difference between EOS6 and EOS22 as shown in **Fig. 1.4**. The smallest difference in recovery factor between EOS6 and EOS22 is for the near critical fluid compared to the other fluid systems.

However, in terms of reserves, the largest error is in the richest downstructure gas at 4750 m, where a "typical" North Sea HCPV has been used to convert recovery factors to reserves. The differences in reserves between EOS6 and EOS22 for different fluids are shown in **Fig. 1.5**. The IOIP is 333 MSm^3[a] for the feed 4750 and 125 MSm^3 for the feed 4500 for the same reservoir volume and EOS22 model. The difference in recovery between EOS6 and EOS22 is 1.7 MSm^3 for feed 4500 and 6.4 MSm^3 for the near critical feed 4750.

Since the largest difference in reserves is in the downstructure fluids, care must be taken in lumping so that these sample properties are matched properly. It might also be better to give more weighing factor for downstructure gas condensate fluid sample PVT properties, as these samples have the largest IOIP.

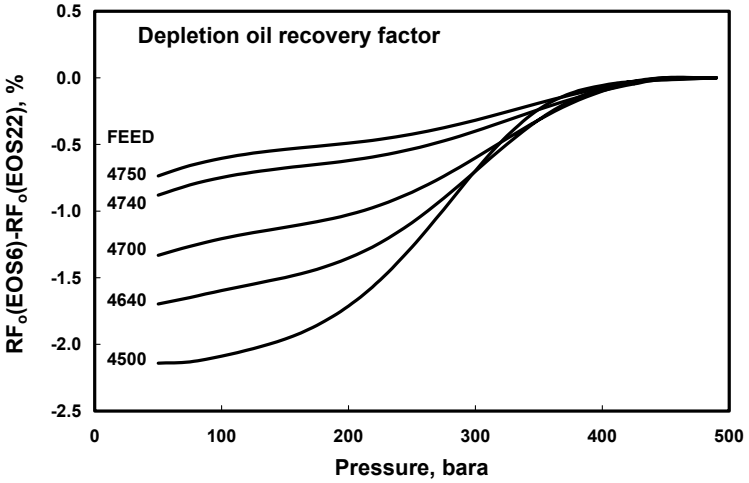

Fig. 1.4 — Difference in CVD oil recovery for different fluid systems – EOS22 vs. EOS6.

[a] $MSm^3 = 10^6\ Sm^3$

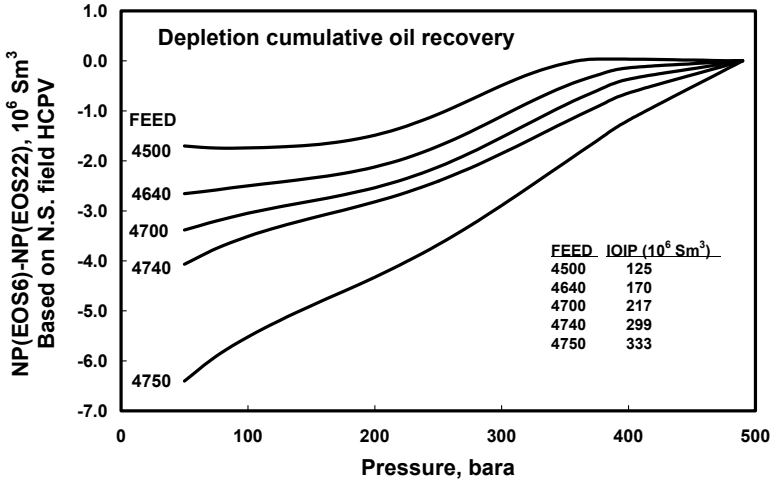

Fig. 1.5 — Difference in total oil recovery for different fluid systems for the same reservoir volume – EOS22 vs. EOS6.

Simulation Performance

The final check for the lumped-EOS was made by simulating the reservoir using a 3D sector model[a] of a reservoir. An equation-of-state based commercial numerical reservoir simulator[13,14] was used for simulating the reservoir. Different reservoir fluid systems were used for comparing the reservoir performance using EOS22 and EOS6 compositional simulation models. The reservoir performance for the near critical fluid (Feed 4750) is given below for depletion and gas injection cases.

Depletion Performance – Near Critical Fluid

The reservoir was simulated using the EOS22 model and the EOS6 model. The production performance is shown in **Fig. 1.6**.

The initial oil production rates in EOS22 and EOS6 compositional simulation models are 1796 and 1762 Sm^3/d respectively i.e. 1.9% less in EOS6. The difference in initial oil production rate is due to difference in the initial solution gas-oil ratios and gas formation volume factors for the near critical fluid in EOS22 and EOS6 models. The two-stage separator solution gas-oil ratios for the near critical fluid in EOS22 and EOS6 models are 557 and 575 Sm^3/Sm^3 respectively i.e. a difference of 3.1%. The two-stage separator gas formation volume factor for the near critical fluid in EOS22 and EOS6 models are 0.005052 and 0.004988 Rm^3/Sm^3 respectively i.e. a difference of -1.1%. The equivalent oil formation volume factor[b] for the near critical fluid for EOS22 and EOS6 models are 2.814 and 2.868 Rm^3/Sm^3 i.e a difference of 1.9%.

[a] See chapter 2 for details of the reservoir model.

[b] The oil formation volume factor (=HCPV/IOIP) is equivalent to B_{gd}/r_s in the gas zone.

The separator solution gas-oil ratio differences for other fluids are shown in Fig. A-3. The oil recovery factor after 10 years of production is 26.9% in both the EOS models as given in Table A-8. Even though there is about 2% difference in the initial oil production rate, the overall performance is similar in EOS6 and EOS22 simulation models.

The computer CPU time taken was 86 minutes for EOS6 simulation model and 590 minutes for the EOS22 simulation model for adaptive implicit method (AIM)[15] for 10 years depletion performance prediction on the same computer. The EOS6 simulation model is about 7 times faster than the EOS22 simulation model in this case.

There are small differences in initial oil and gas production rates, but overall performances are quite similar in EOS22 and EOS6 compositional simulation models. The simulation run is much faster in the EOS6 model. Hence the EOS6 simulation model can be used instead of EOS22 for the reservoir performance prediction under depletion process.

The reservoir performance for the compositional gradient reservoir is shown in Fig. C-2. The reservoir performance for the near critical fluid with high k at the top is shown in Fig. C-3. The reservoir performances are quite similar in the EOS22 and EOS6 models.

Gas Injection Case Performance – Near Critical Fluid

In this case, the lean injection gas was injected to maintain the reservoir pressure and the performance was analyzed. The performance for EOS22 and EOS6 are shown in **Fig. 1.7**.

The initial oil production is about 2% less in EOS6 simulation model compared to EOS22 simulation model. The oil recovery factors are 71.1% in the EOS22 simulation model and 71.3% in the EOS6 simulation model after 15 years of gas injection as shown in Table A-9. The overall performance in both EOS22 and EOS6 simulation models are quite similar. The EOS6 simulation model was about 5 times faster than the EOS22 simulation model. Hence based on overall performance and CPU time, the EOS6 simulation model can be used instead of EOS22 for the reservoir performance prediction in the gas injection case also.

The reservoir performance for the compositional gradient reservoir is shown in Fig. C-4. The reservoir performance for the near critical fluid for partial pressure maintenance is shown in Fig. C-5. The reservoir performances are quite similar in the EOS22 and the EOS6 models.

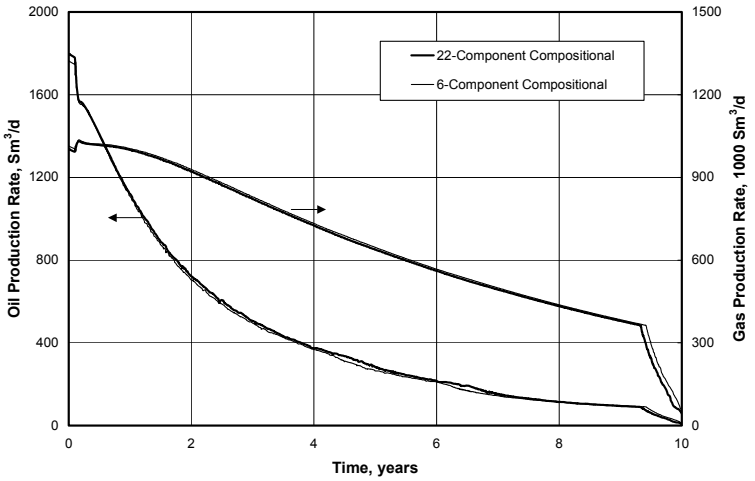

Fig. 1.6 — Depletion recovery – EOS22 vs. EOS6 (near critical fluid with constant composition).

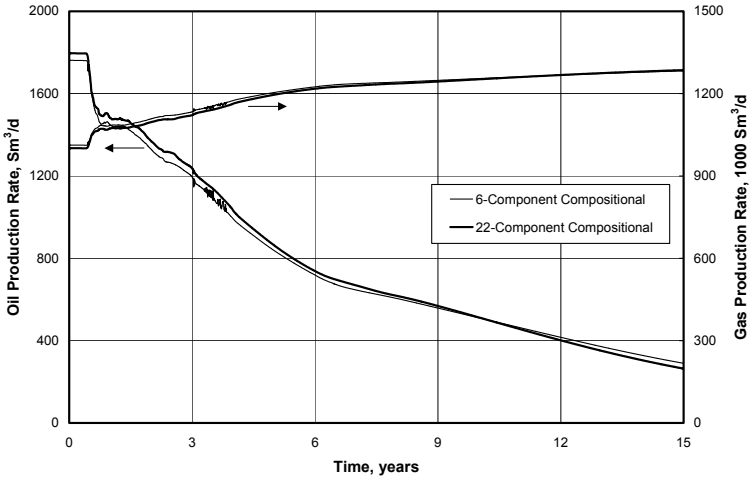

Fig. 1.7 — Gas Injection case – EOS22 vs. EOS6 (near critical fluid with constant composition).

Minimum Miscibility Pressure Comparison

The minimum miscibility pressure (MMP) is an important parameter in gas injection cases. The EOS22 and EOS6 calculated MMPs were compared for reservoir fluid samples taken from different depths.

The MMP was calculated using a proprietary muti-cell algorithm developed by Zick[16,17]. The calculated MMPs are given in **Table 1.1**.

Table 1.1 — MMP calculation from MMPz for different fluid systems.

Fluid Depth, m	MMPz calculated MMP (bara)		
	EOS22	EOS6	% Diff
4500	428.2	431.0	0.64
4640	452.5	453.6	0.25
4700	465.5	465.8	0.06
4740	473.3	473.1	-0.04
4750	473.9	473.9	0.01
4760	476.0	476.2	0.04
4800	488.6	488.0	-0.12
5000	533.5	528.8	-0.87

The rich injection gas was injected in the reservoir fluid samples for calculating MMPs; 200 stages[a] were used for MMP calculations in the MMPz program.

The EOS22 and EOS6 model calculated MMPs are quite similar for almost all reservoir fluid samples. The EOS6 calculated MMP is slightly higher (i.e. 0.6%) than that of the EOS22 for the medium-rich gas condensate fluid, but lower (i.e. 0.9%) for the slightly volatile oil. For the near critical fluid sample, there is no difference in EOS6 versus EOS22 model calculated MMP.

1.2.4 Generating Black-Oil PVT Properties

In the black-oil model, the PVT system consists of two reservoir phases[7] – oil (o) and gas (g) – and two surface components – surface oil ($\bar{o}$) and surface gas ($\bar{g}$). The equilibrium calculations in a black-oil model are made using the solution gas-oil ratio and solution oil-gas ratio, R_s and r_s, respectively, where surface "component K-values" can be analytically expressed in terms of R_s and r_s.

$$K_{\bar{o}} = r_s \frac{R_s + C_o}{1 + r_s C_o} \quad \text{.....(1.7)}$$

$$K_{\bar{g}} = \frac{1}{R_s} \frac{R_s + C_o}{1 + r_s C_o} \quad \text{.....(1.8)}$$

C_o is calculated by

$$C_o = \frac{R T_{sc}}{P_{sc}} \frac{\rho_{osc}}{M_o} \quad \text{.....(1.9)}$$

Where M_o is molecular weight of the surface oil.

[a] The sensitivity of MMP using MMPz to grid cells from 10 to 200 is less than 0.1% for the Feed 4640 with rich gas injection, EOS22.

Black-oil PVT properties have been generated in this study with an EOS model using the Whitson-Torp procedure[18]. In this approach, a depletion-type experiment is simulated – either a CCE, CVD, or DLE test. At each step in the depletion test, the equilibrium oil and equilibrium gas are taken separately through a surface separation process. The surface oil and surface gas products from the reservoir oil phase are used to define the oil FVF B_o and the solution GOR R_s. The surface oil and surface gas products from the reservoir gas phase are used to define the "dry" gas FVF B_{gd} and the solution oil-gas r_s (or R_v).

Undersaturated Oil Reservoirs

For undersaturated oil reservoirs, the black-oil PVT tables can be made by simulating a DLE or CCE experiment using the fluid with the highest solution GOR. The proper separator conditions should be specified for generating the black-oil PVT tables. The undersaturated PVT properties should be calculated up to the maximum initial reservoir pressure or higher. The oil FVF and solution gas-oil ratio for the near critical fluid is shown in **Fig. 1.8**. The black-oil PVT properties are quite similar from CCE and DLE experiments, though there is a small difference at lower pressures.

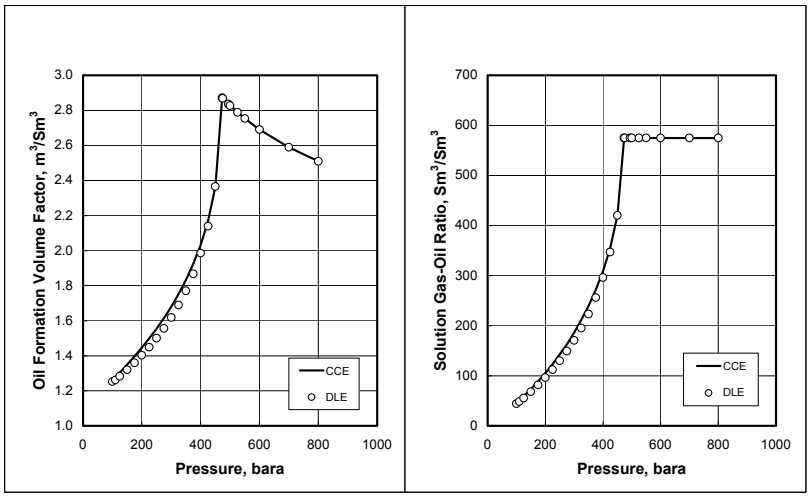

Fig. 1.8 — Oil formation volume factor and solution gas-oil ratio for the near critical oil from CCE and DLE experiments.

Undersaturated Gas Reservoirs

For undersaturated gas reservoirs, the black-oil PVT tables are made by simulating a CVD or CCE experiment using the fluid with the highest solution oil-gas ratio. The undersaturated PVT properties should be calculated up to maximum initial reservoir pressure or higher.

Undersaturated GOC

For reservoirs with an undersaturated GOC, the black-oil PVT tables are made by simulating a CCE experiment with the GOC critical fluid. Some of the nearest-to-critical-pressure data may need to be omitted if $|d(R_s)/dp|$ or $|d(r_s)/dp|$ is too large.

For reservoir simulators[a] that do not support an undersaturated GOC, a "fictitious" saturated GOC has to be introduced. This requires using a "fictitious" saturation pressure for the critical fluid that is slightly higher than the initial reservoir pressure at the undersaturated GOC. The artificial extension of the black-oil PVT table needed for the reservoir simulator can be made using a large change in saturation pressure with a very small change in solution gas-oil ratio and solution oil-gas ratio.

A single black-oil PVT table can also be generated by splicing black-oil tables[b] generated from fluids taken from different depths. Due to non-linear nature of the solution GOR and OGR with saturation pressure curve near the GOC, there might be convergence problems in some reservoir simulators.

Saturated GOC

For saturated reservoirs initially containing both reservoir oil and reservoir gas, the black-oil PVT properties may differ in the "gas cap" and "oil zone" regions. Consistent treatment of this problem may be important. The best approach is to perform a depletion test on the initial GOC reservoir gas alone, retaining only the r_s, μ_g, and B_{gd} properties, and separately performing a depletion test on the initial GOC reservoir oil alone, retaining only the R_s, μ_o, and B_o properties.

It is also necessary to choose a single set of constant surface gas and surface oil densities used to calculate reservoir densities (together with R_s, B_o, r_s, and B_{gd}). Proper selection of surface "component" densities can ensure improved accuracy in the black-oil reservoir density calculations. The reservoir oil and gas densities, based on surface oil and gas densities, can be calculated by the following equations:

---

[a] Consistent extrapolation of the saturated and undersaturated black-oil PVT properties can be made by using a separate program BOPVT written by the author in parallel research to the current work. The BOPVT program uses equation of state for interpolation and extrapolation. It assumes that the reservoir fluid consists of two surface components – surface oil and surface gas. It uses all available input black-oil PVT data and finds EOS parameters for the two components after regression. The final EOS parameters are used in the EOS for interpolation and extrapolation of saturated and undersaturated black-oil PVT properties. The LBC correlation is used for oil and gas viscosities interpolation and extrapolation in the BOPVT program.

[b] The black-oil PVT table is generated from the oil with the lowest saturation pressure (base table). The black-oil PVT properties for the higher saturation pressure oil are appended to the base table. This process is continued until the highest saturation pressure oil black-oil PVT properties are added. Similar approach is used for gas black-oil PVT tables.

$$\rho_{oR} = \frac{\rho_{os} + R_s \rho_{gs}}{B_o} \quad \text{.....(1.10)}$$

$$\rho_{gR} = \frac{\rho_{gs} + r_s \rho_{os}}{B_{gd}} \quad \text{.....(1.11)}$$

It is recommended to use surface oil and surface gas densities that give the correct reservoir oil and reservoir gas densities at the GOC. The above equations can be used to calculate surface oil and gas densities from reservoir oil and gas densities.

$$\rho_{os} = \frac{\rho_{oR} B_o - R_s \rho_{gR} B_{gd}}{1 - R_s r_s} \quad \text{.....(1.12)}$$

$$\rho_{gs} = \frac{\rho_{gR} B_{gd} - r_s \rho_{oR} B_o}{1 - R_s r_s} \quad \text{.....(1.13)}$$

A single black-oil PVT table can be generated by splicing black-oil tables generated from fluids taken from different depths. Due to the non-linear nature of the solution GOR and OGR with saturation pressure curves near the GOC, there might be convergence problems in the reservoir simulators, but it will usually be less severe than that of undersaturated GOC.

Gas Injection Cases

A special problem is addressed in this work – generating black-oil PVT properties needed for gas injection studies in an undersaturated oil reservoir. This involves extrapolation of the saturated oil PVT properties, sometimes far beyond the initial bubblepoint pressure. Several methods can be used for generating the extrapolated saturated black-oil PVT tables, but one in particular has been found consistently better than others.

The black-oil PVT table is generated from the original reservoir oil. Thereafter the injection gas is added to the original oil sample in steps using a multi-contact swelling experiment, until the saturation pressure of the swollen oil is somewhat higher than the maximum (injection) pressure. Afterward, black-oil PVT table is generated from the swollen oil. Finally, the modified black-oil PVT tables used in gas injection processes are made by splicing the black-oil PVT tables for the original reservoir oil and the swollen oil

The modified black-oil PVT tables (both oil and gas) used in the gas injection simulation model can be generated using three different approaches:

A. Original black-oil PVT table + incremental swollen oil properties from the original bubblepoint to the highest pressure.

B. Original PVT table + depletion of the fully-swollen oil to the saturation pressure of the original oil.
C. Original PVT table + one additional data at the fully-swollen saturation point.

The modified black-oil table for lean gas injection in slightly volatile oil is shown in **Fig. 1.9**. The saturation pressure of the original reservoir oil is 435 bara (O2). O1-O2 represents the undersaturated B_o and O2-O3 represents the saturated B_o of the original oil. When 0.05 mole of injection gas is injected in one mole of the original oil, the saturation pressure of the original oil is increased; represented by the triangle near O2. When additional gas is injected, the saturation pressure increases further, shown by the triangles. After 0.40 mole of cumulative gas injection, the swollen oil saturation pressure becomes 558 bara (B2). The black-oil PVT table is generated from the swollen oil (B2). B1-B2 represents the undersaturated B_o and B2-B3-B4 represents the saturated B_o of the swollen oil.

In method A, the saturated B_o is taken from B2 to down, represented by the triangles till O2. In method B, the saturated B_o is taken from B1 to B3, represented by open circles; and then from B3 to O2. In method C, the saturated B_o is taken from B2, next from O2. The undersaturated B_o is taken from B1 to B2 and saturated B_o from O2 to O3 in all three cases.

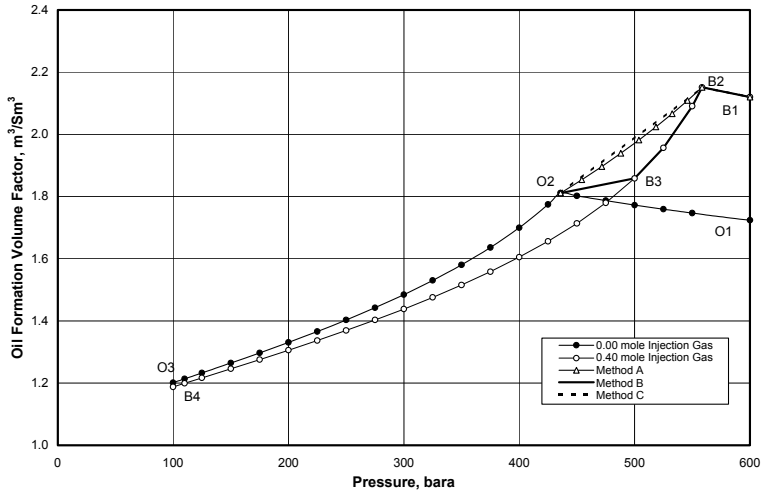

Fig. 1.9 — Extrapolated oil formation volume factor (the lean gas injection in slightly volatile oil).

The modified black-oil PVT data for the different approaches are also shown in Figs. A-31 through A-34 for lean gas injection into a slightly volatile oil. It was found that method B always gives more accurate results compared to other methods.

1.3 Initialization of Reservoir Fluids

To obtain correct and consistent initial fluids in-place (IFIP[a]) for black-oil and compositional models, it is important to initialize the models properly. This involves treatment of (1) fluid contacts and phase definitions, (2) PVT models, (3) compositional (solution-GOR) gradients, and (4) defining the relative importance of IFIP versus ultimate recoveries for the relevant recovery mechanisms.

For comparing different initialization procedures, a simple reservoir model was used. The numerical model has 15x5x3 grid cells. The thickness of the reservoir model considered is 150 m (50 m each layer). The length and width of the reservoir are 3000m and 1000m respectively. The initial water saturation is 26%: The oil-water and gas-oil capillary pressures are assumed negligible. The reservoir has a dip of 3.8 degrees. The top of the reservoir is considered at 4500 m, while the bottom at 4850 m. The GOC is at 4750m.

1.3.1 EOS Models

The reservoir was initialized with the 6-component EOS model and initial fluids in-place were compared with that of the 22-component EOS model. Three different initialization methods were used for the 6-component EOS model.

- Method A – starting with the reference feed, the 6-component EOS model was used to make an isothermal gradient calculation, providing a compositional gradient, based on the 6-component EOS model. In this method, the calculated GOC was somewhat different than with the 22-component EOS model (11.3 m above the actual GOC).

- Method B – starting with the reference feed, use the 6-component EOS model for isothermal gradient calculation and adjust the reservoir pressure at the reference depth such that the calculated GOC equaled the GOC from the 22-component model. The resulting compositional gradient using the 6-component EOS model was then used in the reservoir simulation model, with the correct reservoir pressure at reference depth.

- Method C - use the 22-component EOS model for the gradient calculation, and then manually lumped to obtain the 6-component compositional gradient.

The C_{7+} compositional variation with depth for the above three initialization methods is shown in **Fig. 1.10**.

[a] IFIP = Initial oil in-place (IOIP) and initial gas in-place (IGIP)

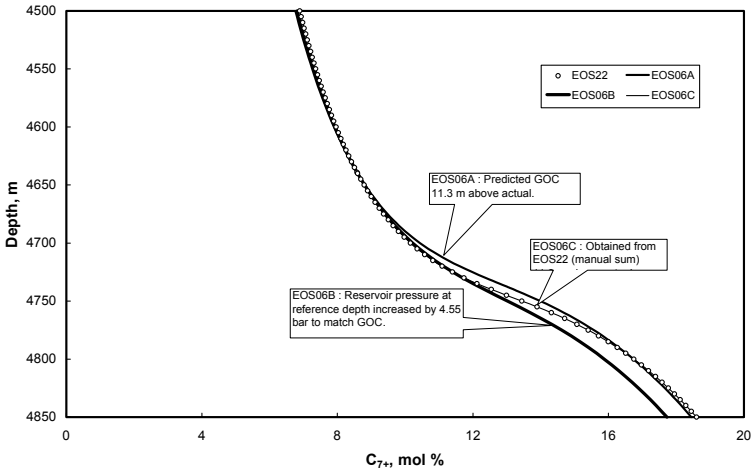

Fig. 1.10 — C_{7+} composition variation with depth under different initialization methods, EOS22 vs. EOS6.

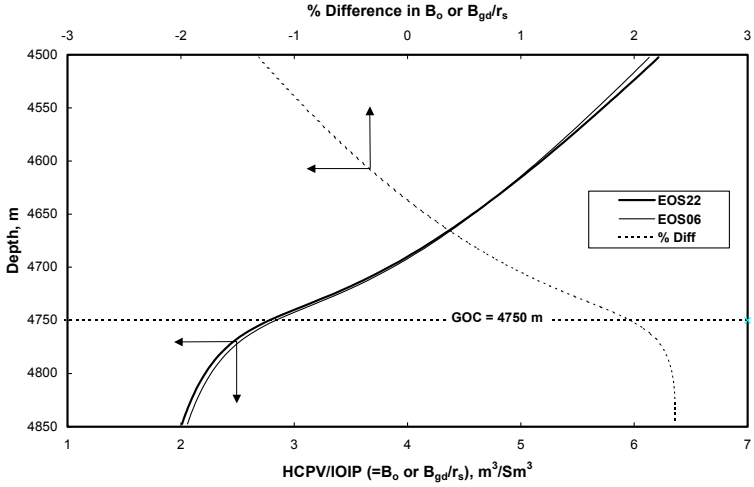

Fig. 1.11 — Oil formation volume factor for EOS22 and EOS6 using the same composition versus depth (compositional gradient from EOS22).

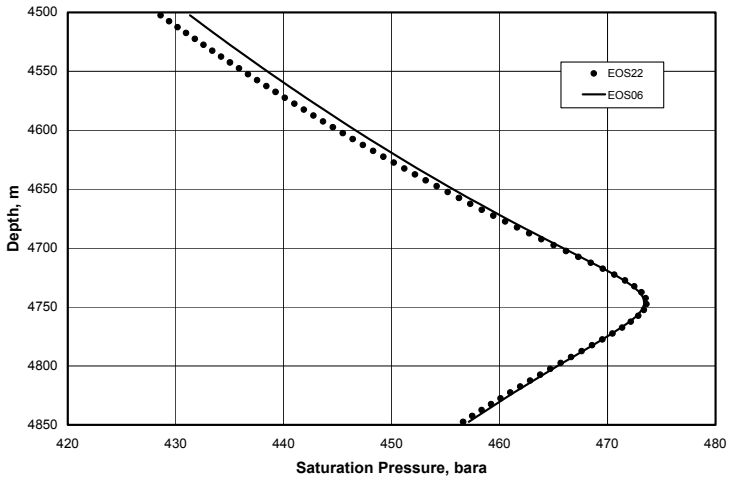

Fig. 1.12 — Saturation pressure versus depth, EOS22 vs. EOS6. The fluid composition with depth is same in both EOS22 and EOS6.

Method C gives the most correct reservoir fluid compositional gradient (when compared with the EOS22 initialization). The IFIP calculated with the different methods are given in **Table 1.2**. The initial oil in-place is 0.9% less in EOS6 (method C) compared to EOS22. This difference in oil in-place is due to the difference in oil formation volume factor in EOS22 and EOS6 for the same fluid composition as shown in **Fig. 1.11**. In the oil zone, the EOS6 model B_o is about 2% higher than that of EOS22 model. In the gas zone, the equivalent B_o ($=B_{gd}/r_s$) is higher for the rich gas condensate, but lower for the medium-rich gas condensate in EOS6 compared to EOS22 model.

Table 1.2 — Initial fluid in-place calculation for different compositional simulation initialization methods.

Initializing Compositional Models				
CASE	**IOIP (10^6 Sm^3)**	**IGIP (10^9 Sm^3)**	**% Error in IOIP w.r.t. EOS22**	**% Error in IGIP w.r.t. EOS22**
EOS22	13.22	11.02	-	-
EOS06A	13.34	11.03	0.94	0.1
EOS06B	12.96	11.13	-1.98	1.0
EOS06C	13.10	11.08	-0.88	0.5

Note:
EOS22 : Gradient calculation using EOS22, starting point reference feed
EOS06A : Gradient calculation using EOS06, starting point reference feed
EOS06B : Gradient calculation using EOS06, after adjustment in reservoir pressure to obtain EOS22 GOC
EOS06C : Gradient calculation using EOS22, starting point reference feed

Method C is recommended for this reservoir, and in general, for initializing lumped-EOS models. This assumes, however, that the saturation pressure gradient and key PVT properties are similar for the detailed-EOS and lumped-EOS models; differences in saturation pressures (**Fig. 1.12**) and PVT properties will potentially have an impact on recoveries. This lumping procedure should minimize these differences and make method C the recommended procedure for all reservoirs.

The initialization method A also seems to give quite accurate fluid in-place compared to EOS22, but this is due to a wrong GOC (GOC shifted up by 11.3 m) – i.e. "cancellation of errors". In general, this method will not always give consistent in-place, therefore method A is not recommended.

In case of saturated gas-oil contact, the detailed-EOS GOC oil and gas composition will be in equilibrium. When detailed-EOS composition is lumped manually to obtain lumped-EOS GOC oil and gas compositions then

- Oil and gas composition at GOC may not be in equilibrium.
- Oil and gas saturation pressures at the GOC may not be equal to the detailed-EOS oil and gas saturation pressures (reservoir pressure).

In the case of the saturated GOC, the saturation pressure at the GOC should be equal to the reservoir pressure at that depth. If the lumped-EOS GOC oil and gas saturation pressure are not equal to the detailed-EOS corresponding saturation pressure, then it is needed to change either the reservoir pressure at the GOC or the GOC oil and gas composition to get saturation pressure equal to the reservoir pressure at the GOC depth in lumped-EOS model. The reservoir pressure should be honored at the GOC depth, because (a) it is an independent measured data, (b) if it is made equal to the saturation pressure, then reservoir pressure at the GOC will vary with EOS model, and (c) the GOC gas saturation pressure and GOC oil saturation pressure may not be equal. The composition of the GOC oil and gas in the lumped-EOS model can be modified to satisfy both conditions (a) oil and gas in equilibrium and (b) saturation pressure equal to reservoir pressure, in the following way:

a. If lumped-EOS GOC oil saturation pressure is less than that of the detailed-EOS, then GOC gas may be injected in the oil to increase the saturation pressure to the reservoir pressure. The oil composition obtained after injecting the GOC gas can be used as the GOC oil composition. The equilibrium gas composition can be obtained from the new GOC oil composition.

b. If the lumped-EOS has a bubblepoint at the GOC, higher than that of the detailed-EOS, then the isothermal flash calculation can be done at the actual GOC conditions and lumped-EOS equilibrium oil and gas compositions can be obtained.

c. The other way is to mix lumped-EOS GOC oil and gas composition in 50-50-mol-% and flash the resulting composition at the detailed-EOS GOC conditions (pressure and temperature) using lumped-EOS. The resulting equilibrium oil and gas compositions can be used as the GOC oil and gas compositions. This approach will always result in oil and gas composition in equilibrium and saturation pressure equal to the reservoir pressure at the GOC conditions.

The method (c) above is recommended for getting the correct saturated GOC oil and gas composition for the lumped-EOS model.

The composition of the saturated GOC oil and gas for a lumped-EOS at the GOC pressure is given in **Table 1.3**. The detailed-EOS model was lumped to 9-components from the original 16-components. When the detailed-EOS GOC oil and gas compositions were lumped manually to get lumped-EOS composition then GOC gas and oil were not in equilibrium (the difference in saturation pressure about 1 bar, GOC pressure 299 bara). When GOC oil and gas were mixed in 50-50 mol-%, the saturation pressure increased by 12 bar from the GOC pressure. After flashing to the GOC pressure, the equilibrium oil and gas were obtained, which were quite similar to the detailed-EOS GOC oil and gas, but flashed oil and gas were in equilibrium.

Table 1.3 — Equilibrium oil and gas composition calculation at saturated GOC.

GOC Oil and Gas Composition (mol %) for Lumped-EOS at GOC Pressure						
Components	Based on manual lumping from detailed-EOS		Based on GOC gas injection in GOC oil		Based on 50-50 mol% of GOC oil & GOC gas	
	GOC gas	GOC oil	GOC gas	GOC oil	GOC gas	GOC oil
F1	56.8333	50.2512	56.5518	50.2803	56.6304	50.2110
F2	13.3425	12.9365	13.3646	12.9385	13.3490	12.9134
F3	10.3269	9.8872	10.3191	9.8892	10.3186	9.8788
F4	7.1085	7.6717	7.1243	7.6692	7.1219	7.6794
F5	3.7938	4.5521	3.8134	4.5487	3.8106	4.5637
F6	4.5289	6.7553	4.6241	6.7455	4.5990	6.7674
F7	3.5201	5.8409	3.6158	5.8307	3.5916	5.8552
F8	0.4782	1.8224	0.5136	1.8164	0.5066	1.8447
F9	0.0680	0.2826	0.0734	0.2817	0.0723	0.2863

1.3.2 Black-Oil Models

For obtaining accurate initial fluids in-place and description of reservoir recovery processes, black-oil PVT tables and "compositional gradients" must be selected carefully.

The compositional gradient in a black-oil model is given by the depth variation of solution GOR (R_s) in the oil zone and the solution OGR (r_s) in the gas zone. The

use of solution GOR and OGR versus depth – instead of saturation pressure versus depth – is important for minimizing "errors" in initial fluids in-place.

The choice of how to generate a proper black-oil PVT table depends on a number of factors, including:

- Whether the purpose is to describe as accurate as possible (a) the actual reservoir PVT behavior or (b) a particular EOS description of PVT behavior – for the purpose of comparing black-oil with compositional simulation results.
- Treatment of compositional gradients, and whether the reservoir has a saturated gas-oil contact or an undersaturated "critical" gas-oil contact.
- Extrapolation of saturated PVT properties to pressures higher than the maximum saturation pressure found initially in the reservoir.
- Choice of the surface gas and surface oil densities to minimize the "errors" in reservoir gas and reservoir oil densities calculated from the black-oil PVT tables and used to compute the vertical flow potential needed for (a) static initialization and (b) dynamic flow calculations.

In this study, assumption was made that a single reference fluid had been obtained by sampling in the gas cap. This sample, based on the isothermal gradient calculation with the EOS22 and EOS6 models, indicated a fluid system with compositional grading through a critical (undersaturated) gas-oil contact.

It was necessary to extrapolate the black-oil PVT properties at least to the maximum saturation pressure of the critical mixture at the gas-oil contact. Three methods of extrapolation were studied, all based on the EOS6 model:

1. Adding incipient (oil) phase composition to the reference sample until the saturation pressure reached the GOC maximum value.
2. Adding the GOC composition from the gradient calculation to the reference sample until the saturation pressure reached the GOC maximum value.
3. Using the GOC composition itself.

For each method, a composition with a saturation pressure equal to the GOC critical fluid saturation pressure was obtained. This composition was then used to generate the black-oil PVT tables using a constant composition expansion experiment (with separator tests conducted separately for each equilibrium phase during the depletion).

To initialize the black-oil model, first it is required to choose a solution GOR&OGR versus depth relation. From the discussions in the previous section, methods A, B, and C were used for generating compositional variation with depth for the 6-component EOS model. From the compositional gradient with depth,

each of the three methods also generates a solution GOR&OGR versus depth relation. When comparing black-oil initialization using the three methods A, B, and C combined with the three methods for generating black-oil PVT properties (1, 2, and 3 above), it was found that method C always gave more accurate and consistent initial fluids in-place; by consistent it is meant that the method provided a more accurate estimation of the 22-component EOS gas-oil contact. The most accurate and consistent IFIP in the black-oil model was achieved using method C for solution GOR&OGR versus depth together with method 3 above for generating the black-oil PVT tables.

The comparative initial fluids in-place are given in **Table 1.4**. The difference in initial fluid in-place is calculated with respect to EOS6 model.

Table 1.4 — Black-oil initialization methods.

Initializing Black-Oil Models				
CASE	IOIP (10^6 Sm^3)	IGIP (10^9 Sm^3)	% Error in IOIP w.r.t. EOS6	% Error in IGIP w.r.t. EOS6
EOS6	13.10	11.08	-	-
BO6 Method 1	12.96	11.17	-1.07	0.8
BO6 Method 2	12.89	11.17	-1.60	0.8
BO6 Method 3	13.02	11.13	-0.61	0.5

The difference in initial oil in-place for method 3 is 0.61%, which is somewhat less than the other two methods.

In case of saturated GOC, GOC equilibrium oil and gas composition are obtained as mentioned above. The oil black-oil PVT properties are obtained by a simulated DLE with the equilibrium oil. The gas black-oil PVT properties are obtained by a simulated CVD experiment with the equilibrium gas.

Solution GOR/OGR Versus Saturation Pressure

The most important aspect of initializing a black-oil model for a reservoir with compositional gradients is the proper use of solution OGR and solution GOR versus depth. These two black-oil PVT properties represent in fact composition and should, accordingly, be used to initialize the reservoir model. It would not make sense, for example, to initialize a compositional simulator with saturation pressure versus depth, and it is equally "illogical" in a black-oil model – with the added disadvantage that the resulting initial fluids in-place can be very wrong!

To quantify the difference in initial fluid in-place using two initialization methods mentioned above, the reservoir was also initialized using saturation pressure versus depth. In that case, in the gas-zone, the gas dewpoint pressure versus depth

was used. In the oil zone, the oil bubblepoint pressure versus depth was used for initializing the reservoir. For this purpose, detailed-EOS model was used for generating black-oil PVT table. The black-oil PVT properties were generated by a simulated CCE experiment with the GOC fluid. The saturation pressure (bubblepoint pressure in oil zone and dewpoint pressure in gas zone) versus depth was obtained by the isothermal gradient calculations. The detailed-EOS compositional model fluid in-place was compared with the black-oil fluid in-place (the solution GOR/OGR versus depth). The initialization with solution GOR/OGR versus depth gave initial fluid in-place close to the EOS model compared to saturation pressure versus depth.

The difference in initial fluid in-place for different initialization methods is given in **Table 1.5**. The difference in initial oil in-place compared to EOS model for saturation pressure versus depth initialization is 11.8% and for solution GOR/OGR versus depth initialization is –0.55%. It is clear that there is a big difference in initial oil in-place for two initialization methods. The difference depends on the fluid properties and thickness of the oil and gas zones.

Table 1.5 — Initial fluid in-place (a) compositional model initialization (b) black-oil model initialization with solution GOR/OGR vs. depth (c) black-oil model initialization with saturation pressure vs. depth.

	Gas Zone		Oil Zone		Oil & Gas Zone	
	IOIP	IGIP	IOIP	IGIP	IOIP	IGIP
	10^6 Sm^3	10^9 Sm^3	10^6 Sm^3	10^9 Sm^3	10^6 Sm^3	10^9 Sm^3
(a) EOS22	9.80	9.48	3.41	1.54	13.21	11.02
(b) Ps vs D	11.70	9.10	3.08	1.64	14.78	10.74
(c) GOR/OGR vs D	9.85	9.50	3.29	1.58	13.15	11.08

If GOR versus B_o relation is the same for all fluids, then there will not be any difference in initial oil in-place in the oil zone for compositional and black-oil model with solution versus depth initialization. The above difference in initial oil in-place in the oil zone is due to (a) small differences in solution GOR versus B_o relation for different fluids as shown in Fig. A-11 and (b) initialization difference in the black-oil and the compositional models for grid cells containing both oil and gas.

The reservoir production performance for the three cases above is shown in **Fig. 1.13**.

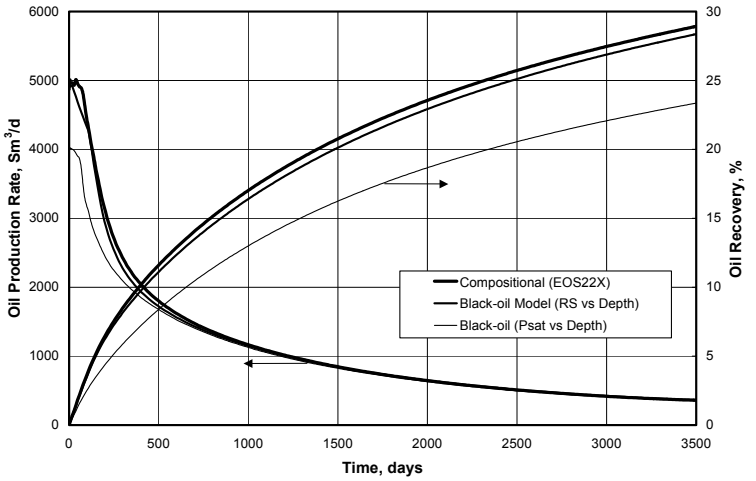

Fig. 1.13 — Depletion performances under different initialization methods (a) compositional model (b) black-oil model with R_s vs Depth (c) black-oil model with saturation pressure vs. depth.

The oil and gas recovery factor for EOS is similar to black-oil initialization using solution GOR/OGR versus depth. However initialization with saturation pressure versus depth, gives quite different oil production performance. Hence the initialization with solution GOR/OGR versus depth gives consistent initial fluid in-place and reservoir performance.

In the oil zone, at a given pressure below bubblepoint pressure of the GOC fluid, the solution GOR is different for the GOC fluid and the fluid with the saturation pressure equal to the selected pressure. When initializing with saturation pressure versus depth, the difference in solution GOR results in difference in oil formation volume factor. The difference in oil formation volume factor results in differences in initial oil in-place compared to compositional model. The difference in solution gas-oil ratio is shown in **Fig. 1.14**.

In the gas zone, at a given pressure below dewpoint pressure of the GOC gas, the solution OGR is different for the GOC fluid and the fluid with the saturation pressure equal to the selected pressure. When initializing with the dewpoint pressure versus depth, the difference in solution OGR versus depth gives differences in initial oil in-place. In the gas zone, initial oil in-place is given by B_{gd}/r_s. The B_{gd}/r_s difference between black-oil and compositional models becomes larger as one goes far from the GOC conditions as shown in **Fig. 1.15**.

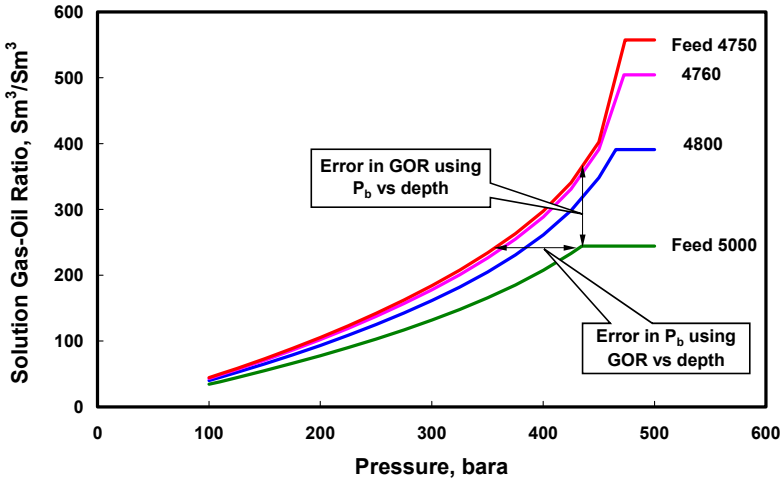

Fig. 1.14 — Initializating black-oil model – (a) solution GOR vs. depth and (b) saturation pressure vs. depth.

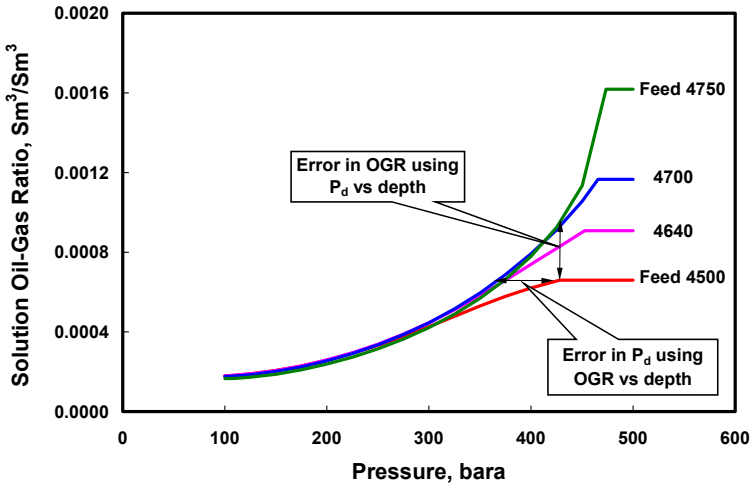

Fig. 1.15 — Initializating black-oil model – (a) solution OGR vs. depth and (b) saturation pressure vs. depth.

In this fluid system case, in the oil zone, saturated B_o at any bubblepoint pressure in black-oil model is higher than that in the compositional model (**Fig. 1.16**). If only the oil zone is initialized, one will always obtain more initial oil in-place in the compositional model, while initializing using bubblepoint versus depth. In the gas zone, the saturated B_{gd}/r_s is lower in the black-oil model than in the compositional model at any pressure. If black-oil model is initialized with dewpoint pressure versus depth, one will always get lower initial oil in-place in the gas zone in the compositional model compared to the black-oil model. If both

oil and gas zone is present, there will be a cancellation effect and the difference in the black-oil and the compositional models in-place may be reduced and one may get misleading close initial fluid in-place while initializing with saturation pressure versus depth.

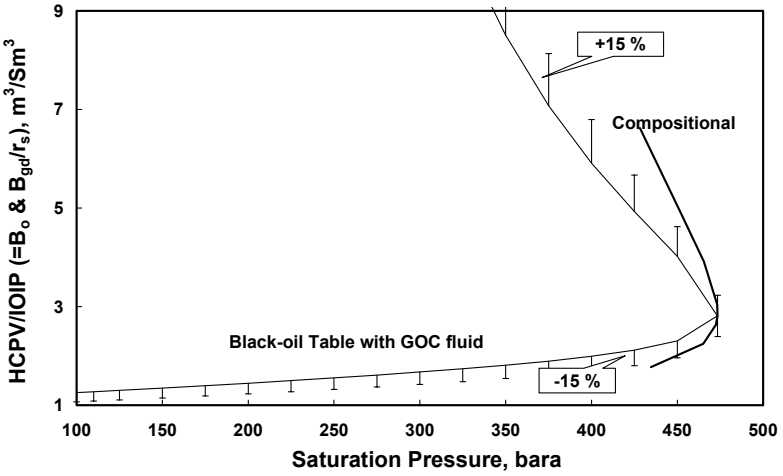

Fig. 1.16 — Saturated oil FVF – (a) The black-oil PVT table generated from the GOC fluid (b) compositional B_O is obtained from the gradient calculation.

A single black-oil PVT table is used to represent the reservoir fluid properties in the grading reservoir, and the GOC fluid is used for generating the black-oil PVT properties. Different black-oil PVT tables cannot be used at different depths because in that case the same fluid will have different properties depending upon its depth, which will happen in the case of gas injection.

Despite a "perfect" initialization of composition with depth in a black-oil model, where solution OGR and solution GOR are taken directly from the compositional EOS model, the saturation pressure versus depth will not be represented properly in the black-oil model. This "error" in saturation pressure versus depth has practically no effect on initial fluids in-place, but it does have a potential effect on depletion recoveries. Figures above show the magnitude of error in saturation pressure that can be expected in a black-oil model initialized with correct solution OGR and solution GOR versus depth.

The error in saturation pressure versus depth usually has little impact on production performance and ultimate recoveries. It may have a short-lived effect on recovery (rates) versus time as the reservoir depletes below the initial saturation pressures, however ultimate recoveries are not usually affected noticeably.

Spliced Black-oil PVT Tables for Undersaturated GOC Reservoirs

The initialization of a compositionally grading reservoir can also be done with a spliced black-oil PVT table. The spliced black-oil PVT table will give correct initial fluid in-place as well as correct saturation pressure. In some cases, due to very non-linear nature of the curve near the GOC, there may be convergence problems in the reservoir simulators. Even if the initial conditions are represented properly, pressure dependent properties are not represented properly. That is, fluid at each depth has its own set of black-oil PVT tables i.e. the pressure dependence of PVT properties is somewhat different for fluids at different depths.

In this case, for generating the black-oil PVT table for oil, the PVT properties of the oil with the lowest bubblepoint pressure is taken. Thereafter one new point is added for oil with higher bubblepoint pressure. The addition is continued until the GOC oil. Similarly a gas black-oil table is generated, starting from the lowest dewpoint pressure gas till GOC gas. The spliced solution GOR/OGR plots are shown in **Fig. 1.17**. The spliced oil black-oil PVT table was generated by splicing oil PVT tables generated from oil from depths 5000, 4800, 4760, and 4750 m. The spliced gas black-oil PVT table was generated by splicing gas PVT tables generated from gas from depths 4500, 4640, 4700, and 4750 m.

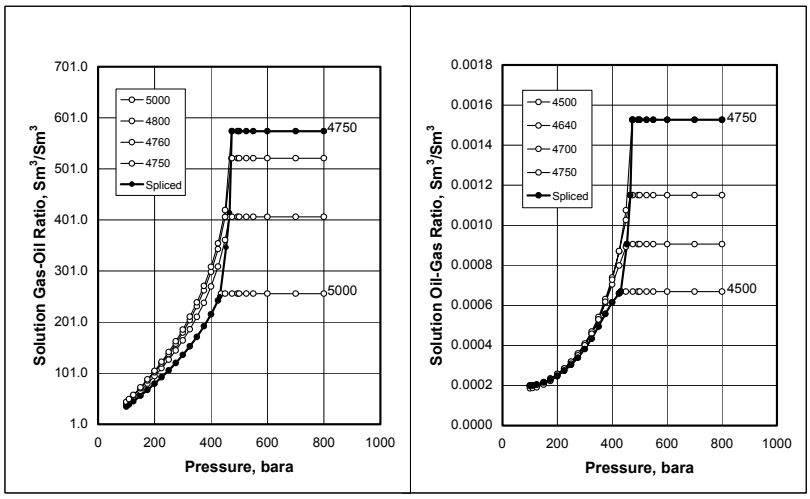

Fig. 1.17 — Spliced black-oil PVT table for undersaturated GOC (a) solution gas-oil ratio vs. pressure (b) solution oil-gas ratio vs. pressure.

If a spliced black-oil PVT table is used, then one obtains the same initial fluid in-place for (a) initializing with saturation pressure versus depth and (b) initializing with solution GOR/OGR versus depth. The initial conditions i.e. saturation pressure and solution GOR/OGR will also be the same in both cases, but the depletion behavior will not be the same in both cases.

Spliced Black-oil PVT Tables for Saturated GOC Reservoirs

In the case of the saturated GOC and the undersaturated reservoirs, the solution GOR/OGR variation with pressure may not be too large. In those situations, the spliced black-oil PVT tables may be used for simulating the reservoir. **Fig. 1.18** shows solution gas-oil ratio for a saturated GOC.

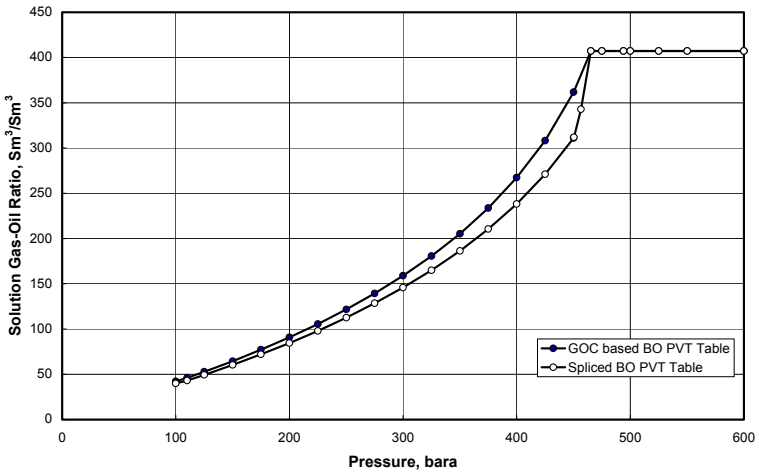

Fig. 1.18 — Solution gas-oil ratio with pressure obtained from (a) black-oil PVT table from GOC equilibrium oil (b) spliced black-oil PVT tables from different depths in the reservoir.

The performance prediction comparison for single black-oil and spliced black-oil PVT tables (effect of error in saturation pressure on production performance) is analyzed for a compositionally grading reservoir. The reservoir is simulated using two black-oil PVT tables (first generated from saturated GOC equilibrium oil and gas; second generated after splicing black-oil PVT tables from different depths). The solution GOR/OGR versus depth is the same in both the cases. The GOC reservoir pressure is 465 bara and at the bottom of the reservoir the saturation pressure is 450 bara, a change of 15 bar over a depth of 50 m i.e. average saturation pressure gradient of 0.3 bar/m in the oil zone. Due to differences in two PVT curves, the initial saturation pressure difference is 25 bar (the bubblepoint for the first set is 425 bara and for the second set is 450 bara) at the bottom of the reservoir.

The choice of using the GOC fluid generated black-oil table or spliced black-oil PVT table depends on the location of the bulk of the reservoir fluid. If most of the reservoir fluid is near the GOC compared to the bottom (or top) of the reservoir, then GOC fluid based black-oil table should be used. In the case of the majority of the oil is at the bottom of the reservoir, the spliced black-oil PVT table should be used for oil properties. If most of the gas is at the top of the reservoir, then the spliced black-oil PVT table should be used for gas properties.

The depletion performance for the above two black-oil PVT tables are compared with the compositional simulation results. The oil production rate and the oil recovery are shown in **Fig. 1.19.** The gas production rate is shown in **Fig. 1.20**. In this case, most of the oil is near the GOC therefore GOC fluid based black-oil PVT table gives better performance compared to spliced black-oil PVT table.

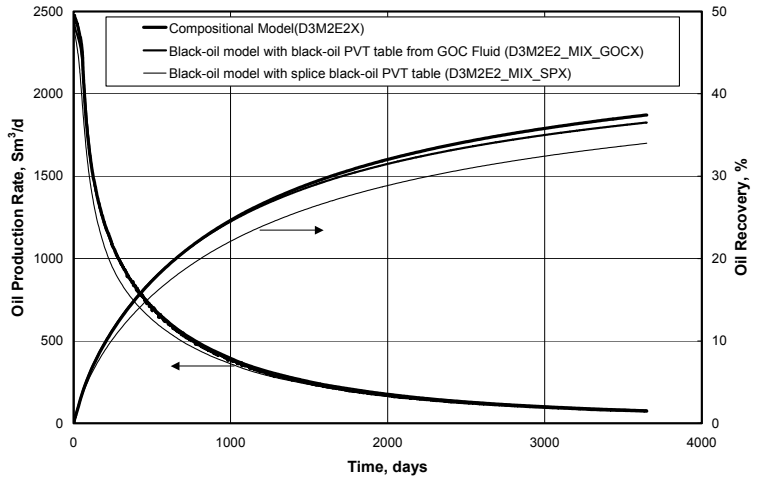

Fig. 1.19 — Reservoir simulation depletion performance (a) compositional simulation (b) GOC fluid generated black-oil PVT table (c) spliced black-oil PVT table (D3M2E2X.DATA, D3M2E2_MIX_GOCX.DATA, D3M2E2_MIX_SPX.DATA).

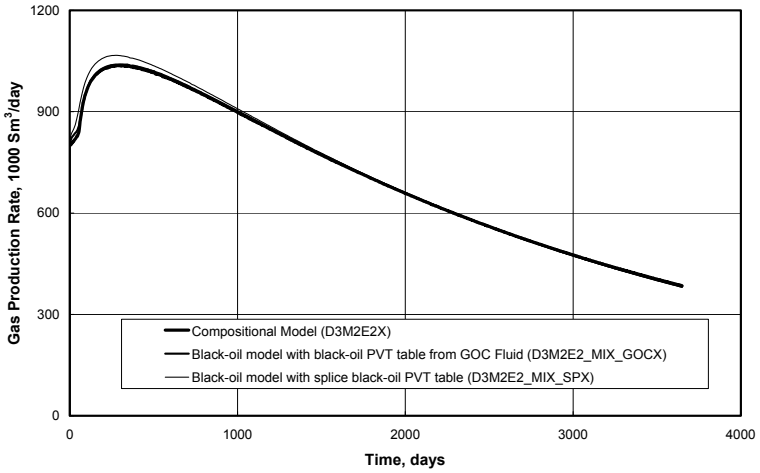

Fig. 1.20 — Reservoir simulation depletion performance (a) compositional simulation (b) GOC fluid generated black-oil PVT table (c) spliced black-oil PVT table (D3M2E2X.DATA, D3M2E2_MIX_GOCX.DATA, D3M2E2_MIX_SPX.DATA).

1.4 Conclusions and Summary of New Contributions

Conclusions in this study are considered to be "general", having been derived using a wide range of realistic fluid systems.

1. An EOS was successfully lumped from a detailed 22-component model to a lumped 6-component EOS model for a complex compositionally grading fluid system, considering depletion and gas injection mechanisms. The lumping procedures used in this complex example should be applicable to practically any petroleum reservoir fluid system.

2. For initializing a lumped-EOS compositional model, the compositional gradient should be calculated from the detailed-EOS compositional gradient, manually lumped at each depth. This procedure ensures consistency between detailed- and lumped-EOS fluid compositions.

3. In general, for black-oil simulation models, the black-oil PVT data should be generated from the fluid with the highest saturation pressure in the reservoir. For a saturated GOC reservoir, the DLE experiment with GOC oil should be used for generating oil PVT properties and a CVD experiment with GOC gas should be used for generating gas PVT properties. For undersaturated GOC reservoirs, the black-oil PVT table should be generated from CCE experiment of the GOC (critical) fluid.

4. In black-oil simulation, the solution GORs (and OGRs) versus depth should be used for initialization. The solution GOR/OGR gradient should be obtained from a compositional model. This will ensure consistency between the black-oil and the compositional simulation models, particularly for in-place surface volumes.

5. Using solution GOR initialization in a black-oil model, though guaranteeing accurate IFIP, may result in inaccurate saturation pressure versus depth. One approach to use solution GOR initialization and still have accurate saturation pressure versus depth involves "splicing" saturated black-oil PVT properties from the fluids along the compositionally grading column. The possible drawback with solution is numerical stability problems in some simulators.

1.5 References

1. Fevang, Ø., Singh, K., and Whitson, C.H. : "Guidelines for Choosing Compositional and Black-oil Models for Volatile Oil and Gas-Condensate Reservoirs," paper SPE 63087 presented at the 2000 Annual Technical Conference and Exhibition, Dallas, Texas, 1-4 October 2000.
2. Soave, G.: "Equilibrium Constants for a Modified Redlich-Kwong Equation of State," Chem. Eng. Sci.(1972), 27, 1197-1203.
3. PVTSim, a general purpose PVT package by Calsep A/S.
4. Pedersen, K. S. and Fredenslund, A.: "An Improved Corresponding States Model for the Prediction of Oil and Gas Viscosities and Thermal Conductivities," Chem. Eng. Sci., 42, (1987), 182.
5. Lohrenz, J., Bray, B. G., and Clark, C. R.: "Calculating Viscosities of Reservoir Fluids From Their Compositions," J. Pet. Tech. (Oct. 1964) 1171-1176; Trans., AIME, 231.
6. Whitson C.H : "PVTx : An Equation-of-State Based Program for Simulating & Matching PVT Experiments with Multiparameter Nonlinear Regression," Version 98.
7. Whitson, C.H. and Brule, M.R.: *Phase Behavior*, Monograph Series, SPE, Richardson, TX (2000).
8. Coats, K. H.: "Simulation of Gas Condensate Reservoir Performance," JPT (Oct. 1985) 1870.
9. Coats, K.H. and Smart, G. T. : "Application of a Regression-Based EOS PVT Program to Laboratory Data", paper SPE 11197.
10. Mehra R.K., Heidemann, R.A., Aziz, K., and Donnelly, J.K. : "A statistical Approach for Combining Reservoir Fluids into Pseudo Components for Compositional Model Studies," paper SPE 11201 presented at the 57th Annual Fall Technical Conference and Exhibition, held in New Orleans, LA, Sep. 26-29, 1982.
11. Joergensen, M., Stenby, E.H. : "Optimization of Pseudo-component Selection for Compositional Studies of Reservoir Fluids," paper SPE 30789 presented at the 70th Annual Technical Conference and Exhibition held in Dallas, Texas, Oct. 22-25, 1995.
12. Whitson, C. H., Fevang, Ø., and Yang, T.: " Gas Condensate PVT – What's Really Important and Why?".
13. Eclipse 300, 1998a Release.
14. Eclipse 100, 1998a Release.
15. Thomas, G.W. and Thurman, D.H.: "Reservoir Simulation Using an Adaptive Implicit Method," SPEJ (Nov. 1983) 69-78.
16. MMPz for Minimum Miscibility Pressures and Compositions, Version 1.0, December 2001, Zick Technologies.
17. Høier, Lars: Miscibility Variations in Compositionally Grading Petroleum Reservoirs, PhD Dissertation, Department of Petroleum Engineering and Applied Geophysics, NTNU, Trondheim, Norway (Aug. 1997).
18. Whitson, C. H. and Torp, S. B.: "Evaluating Constant Volume Depletion Data," JPT (March, 1983) 610; Trans AIME, 275.

Chapter 2

Simulation Studies

2.1 Introduction

This chapter compares simulation results from a black-oil model with a compositional model. The black-oil and the equation of state (EOS) compositional simulation results are compared for various reservoir fluids; with constant composition, compositional grading reservoirs with saturated and undersaturated GOC.

Coats[1,2] compared simulation results from a compositional model and from black-oil model. Coats showed that the depletion performance was very similar for the two simulation models. Coats also showed that a black-oil model could be used to simulate the gas cycling in gas condensate reservoirs as long as the pressure was higher than the initial dewpoint. The simulation model used by Coats had one numerical layer and the reservoir was horizontal (no effect of gravity).

El-Banbi et al.[3] compared simulated reservoir performance from a black-oil and a compositional simulation model for a specific reservoir. The reservoir fluid was a near critical gas condensate. They concluded that a black-oil simulation model could be used to simulate the depletion and water influx processes for gas condensate reservoirs.

In the present study, a 3D multi-layered dipping reservoir with various fluid systems is used. The fluid system varies from low-GOR oil to slightly volatile oil; to volatile oil; to near critical fluid; to rich gas condensate to medium-rich gas condensate. Simulation results are shown for reservoirs with constant composition and for reservoirs with a compositional variation with depth. The reservoir fluids are derived from the complex fluid system described in Chapter 1. The reservoir heterogeneity is described by a Dykstra-Parson coefficient of 0.75. It is a "layer-cake" model i.e. each numerical layer has constant rock properties.

In the first section of this chapter, the simulation model has 99 numerical layers. The permeability from the top layer to the bottom layer are either monotonically increasing or decreasing. Different average reservoir permeability is used to quantify the effect of gravity. The reservoir performance is analyzed for different fluid systems for both depletion and injection cases.

Furthermore, this section examines the possibility for reducing the number of numerical layers without loosing the accuracy, since it is not practical (due to

excessive CPU time) to use 99 layers in the simulation model for comparing the compositional and black-oil model performance. Different fluid systems and permeability distributions are used for comparing the performance from a model with a reduced number of layers with the results from the model with 99-layer. Grid sensitivities in x and y direction are also analyzed. All these simulations are performed with a black-oil model. Based on the results from this section, the comparison between the black-oil model and the compositional model are done using a simulation model with 50x10x10 grid cells.

In the second section of this chapter, the black-oil and the compositional simulation results are compared for different depletion cases. Different fluid systems are used with constant composition. Also results from compositionally grading reservoirs with saturated and undersaturated GOC are shown. The permeability distributions are also varied in the depletion cases.

In the third section of this chapter, the black-oil and the compositional simulation results for different gas injection cases are compared. Both full and partial pressure maintenance cases are considered. Different fluid systems with different permeability distributions are used.

Basic Reservoir and Model Data

For reservoir layering analysis, a 99-layer reservoir with equal thickness, but different permeability is used. Thereafter the number of numerical layers is reduced without loosing the performance accuracy. The basic reservoir properties for 99-layer reservoir are given in Table B-4. The reservoir is divided into 15x5x99 cells. The grid cell size in x- and y-direction is constant, equal to 200 m. Based on the reservoir simulation results, it is found that 50x10x10 grid cells are required to simulate the reservoir properly, each numerical layer with equal flow capacity.

For comparing black-oil and compositional simulation results, the reservoir simulation model contains 50x10x10 grid cells in each geologic unit. The reservoir simulation model contains three geologic units. The thickness of each unit is 50 meters. Each geologic unit generally has ten numerical layers, with equal flow capacity. Each layer has constant permeability. The heterogeneity of each geologic unit is described by a Dykstra-Parsons coefficient of 0.75. The average permeability in each geologic unit is 5, 50, and 200 md (top, middle and bottom). The reservoir has a dip of 3.8 degrees. The size in x- and y-direction is constant, equal to 60 m and 100 m respectively. The basic geologic unit properties are given in Table B-7 and shown in **Fig. 2.1**.

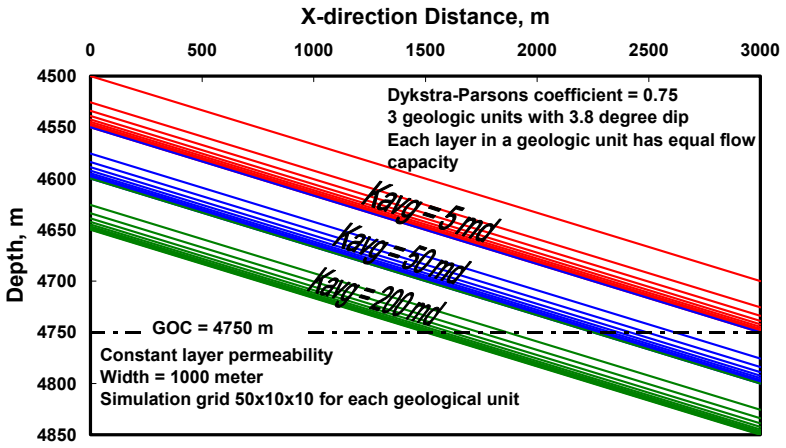

Fig. 2.1 — Three geologic units for comparing black-oil and compositional simulation results.

For most depletion cases, the reservoir is produced through one well on maximum withdrawal constraint (about 10% hydrocarbon pore volume per year) with minimum well bottom hole pressure of 100 bara. The producer is located in grid cell (50,10) and perforated throughout the unit. The reservoir performance is analyzed for 10 years.

For gas injection cases, the same reservoir units and layers are used as in the depletion cases. However, the location of the producer is changed from cell (50,10) to cell (50,5) and the injector is located in cell (1,5). The production constraint for the producer is reservoir volume rate (about 10% hydrocarbon pore volume per year) and minimum bottom hole pressure of 300 bara. The gas injection rate is equal to reservoir volume production rate, and maximum bottom hole injection pressure of 700 bara. The reservoir performance is compared for 15 years.

The basic reservoir properties are given in Table A-7.

The relative permeability data used in all simulation cases in this research work are given in Table B-3. The initial water saturation is 26%. The critical gas saturation is 2%. The critical oil saturation is 22.7%.

2.2 Layering

2.2.1 Introduction

A reservoir may contain many layers with different layer permeabilities and the variation may be quite frequent. In those cases, in order to simulate the reservoir

properly, it is needed to incorporate all layer properties separately, which may require large numbers of numerical layers in vertical direction in the full field reservoir simulation study. It may not be possible to include so many vertical layers, therefore it is required to reduce the number of numerical layers without loosing performance accuracy.

This section discusses the 99-layer reservoir production performance for depletion and injection cases. Methods are described to reduce the number of numerical layers. Sensitivities to number of vertical layers are also discussed for different: (1) permeability variation with depth, (2) dip angle, and (3) average reservoir permeability.

The following assumptions have been made in this study:

A. There is no variation in the porosity in different layers and the porosity has been assumed constant in all layers.
B. There is no permeability variation in the areal direction. A particular layer has constant permeability throughout the reservoir.
C. Permeability variation in the vertical direction is smooth i.e. increasing downward, decreasing downward or highest in the middle and decreasing upward and downward.
D. Reservoirs with randomly varying or high-low interspersed permeability with depth are not analyzed in this study.
E. The Dykstra-Parson coefficient has been used in this study to describe reservoir heterogeneity. The Dykstra-Parsons coefficient is calculated using permeability data from an actual North Sea reservoir.

2.2.2 Definition of Reservoir Heterogeneity

The Dykstra-Parsons coefficient of permeability variation is defined as

$$V_{DP} = \frac{k_G - k_{sd}}{k_G} \quad \text{.....(2.1)}$$

where
k_G : geometric mean permeability.
k_{sd} : permeability at one standard deviation from k_G at 84.1% cumulative probability.

It may also be defined as[5]

$$V_{DP} = \frac{D_{C=0.5} - D_{C=0.84}}{D_{C=0.5}} \quad \text{.....(2.2)}$$

where

F : flow capacity (=∑kh)
C : storage capacity (=∑øh)
D : dF/dC

The value of permeability variation coefficient is estimated as 0.75 from data taken from a model of a North Sea reservoir. Even though the Eq. 2.2 considers only two points (C = 0.5, 0.84) on the plot, it gives good description of the permeability distribution.

2.2.3 Layered Reservoir Performance

To describe the layered reservoir performance, the reservoir with 99 numerical layers, each with an equal vertical thickness of 1.51 m (total thickness 150 m) is considered. The permeability variation is described by Dykstra-Parsons coefficient of 0.75. The average permeability of the reservoir is 232 md with a maximum layer permeability of 2500 md and a minimum layer permeability of 4 md (ratio of highest to lowest k is 633). The reservoir is described by 15x5x 99 grid cells. The dip of the reservoir considered is 3.8 degrees. The 99-layer properties are given in Table B-4.

A black-oil reservoir simulator is used to study the reservoir performance. Implicit[6] formulation is used with a maximum time step of 10 days. The black-oil PVT properties are generated using the 22-component EOS model. The reservoir pressure is 495 bara at the reference depth of 4750 m. The reservoir is simulated for 10 years.

Depletion Case

The reservoir is simulated under depletion drive with one producer. The simulated performance is analyzed for two cases (a) the highest permeability at the top and (b) the highest permeability at the bottom. The reservoir is simulated for reservoir fluid with constant composition for the two permeability variations. The fluid used varies from low-GOR oil to near critical fluid to lean gas (all constant composition).

The depletion reservoir performance for the reservoir containing near critical oil is shown in **Fig. 2.2**. The oil recovery is 24.8% in the case of the highest permeability at the bottom. The oil recovery is 17.5% in the case of the highest permeability at the top.

The performance of the reservoir with a medium-rich gas condensate is shown in **Fig. 2.3**. The oil recovery is 37.2% in the case of the highest permeability at the bottom and 37.0% in the case of the highest permeability at the top.

The depletion oil recovery for different fluid systems for (a) the highest permeability at the top and (b) the highest permeability at the bottom are shown in **Fig. 2.4**. The saturation pressures for these fluid systems are shown in Fig. C-

6. For a given HCPV (for highest k at the bottom), the initial oil in-place and recoverable reserves for different fluid systems are shown in Fig. C-7.

The depletion oil recovery for lean to medium-rich gas condensate reservoir is independent on the permeability distribution. The main reason for this behavior is that practically all of the produced oil is from dissolved oil in the reservoir gas. For the low-GOR oils, the oil recovery is almost also independent on the permeability distribution. This is due to a small amount of gas liberated from the reservoir oil, because of the relatively small difference between saturation pressure and reservoir pressure at abandonment.

The oil recovery for slightly volatile oil to near critical oil is higher in the case of the highest permeability at the bottom due to the gravity segregation. The effect gravity segregation has on the production performance depends on the average permeability of the system. The oil recoveries for different average reservoirs permeabilities are given in Table B-5. The oil recoveries are 15.0, 20.0 and 23.3% for the average reservoir permeability of 10, 50 and 232 md respectively for the near critical GOC fluid.

For the cases with the high permeability at the bottom, the oil recovery increases as the GOR increases until it reaches a maximum for a volatile oil; thereafter the oil recovery decreases and has a minimum for the critical fluid. The reason for this behavior is that as the reservoir oil becomes more critical, the density difference between the reservoir oil and reservoir gas is reduced. This is due to the "rapid" decrease in oil mobility (due to shrinkage) near the saturation pressure for the near critical fluid critical.

The depletion performance of a slightly volatile oil is shown in Fig. C-8 and the oil saturation profile after 1825 days of depletion is shown in Fig. C-9. The oil saturation is more than 60% in most parts of the reservoir, in the case of the highest permeability at the top. The maximum difference (the highest permeability at the bottom and the highest permeability at the top) in oil recovery is for this fluid system (Fig. 2.4). The oil recovery is 36% in the highest permeability at the bottom case and 16% in the highest permeability at the top case.

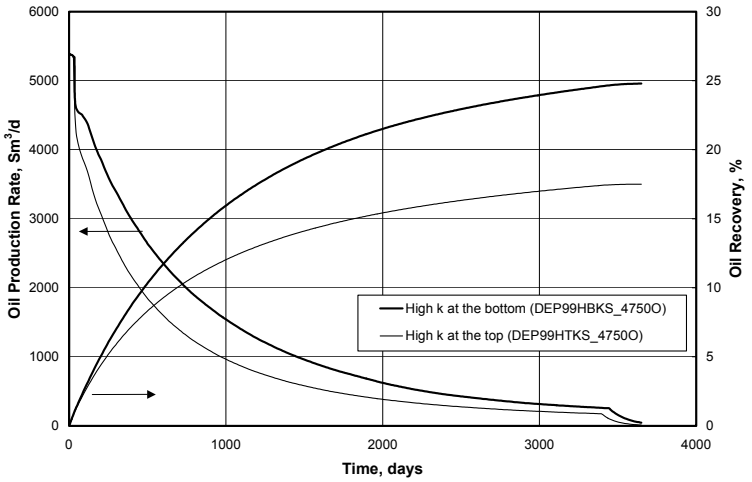

Fig. 2.2 — Depletion performance for the 99-layer reservoir with the near critical oil, constant composition.

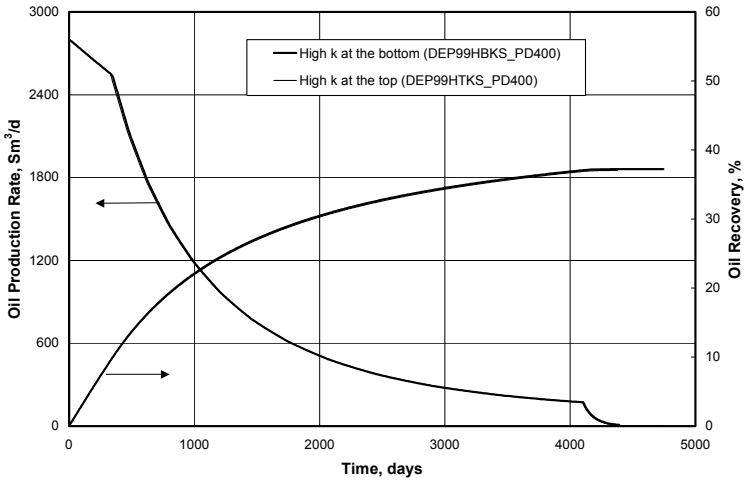

Fig. 2.3 — Depletion performance for the 99-layer reservoir with the medium-rich gas condensate, constant composition (solution GOR = 1283 Sm^3/Sm^3, dewpoint pressure = 400 bara).

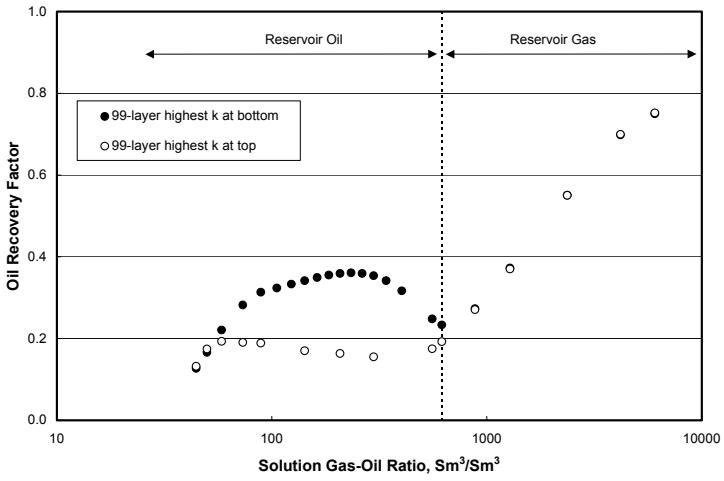

Fig. 2.4 — Depletion oil recovery for widely varying constant composition. The 99-layer case with (a) the highest permeability at the bottom and (b) the highest permeability at the top.

Gas Injection Cases[a]

The reservoir is produced on a maximum withdrawal constraint (about 10% hydrocarbon pore volume per year) with a minimum well bottom hole pressure of 300 bara. The performance prediction is analyzed for 10 years. The injection is equal to the reservoir volume production rate. The producer is located in the last cell (15,5) and the injector is placed in the first cell (1,1) and perforated through the reservoir. The black-oil reservoir simulation study has been performed. Implicit formulation is used with a maximum time step of 10 days.

The reservoir performance for the 99-layer case for (a) the high permeability at the top and (b) the high permeability at the bottom for a near critical fluid is shown in **Fig. 2.5**. The oil recovery is higher in the case of high permeability at the bottom compared to high permeability at the top. The oil recovery is 55.3% in the case of high permeability at the bottom and 40.8% in the case of high permeability at the top.

The reservoir performance for the 99-layer case for (a) the high permeability at the top and (b) the high permeability at the bottom for various fluid systems ranging from a low-GOR oil to a lean gas condensate through a near critical fluid is shown in **Fig. 2.6**. In the case of gas injection, the oil recovery reaches a maximum for the near critical fluid. As the fluid systems get leaner, the oil recovery decreases in the case of high permeability at the bottom. This is because

[a] The black-oil simulation model is used for layer performance analysis for the injection cases. However, the black-oil model cannot be used for simulating all injection cases as shown later in this chapter.

the density difference between the reservoir fluid and the injection gas decreases. For the leanest gas condensate in Fig. 2.6, the oil recovery is almost independent on the permeability distribution. The increase in oil recovery as the reservoir oil becomes more volatile is explained by the decrease in oil viscosity and the vaporization effects of the injection gas. These effects are more effective than the effect of the reduced density difference between the injection gas and the reservoir fluid. The effect that gravity has on the production performance is very dependent on average reservoir permeability as shown in **Fig. 2.7**.

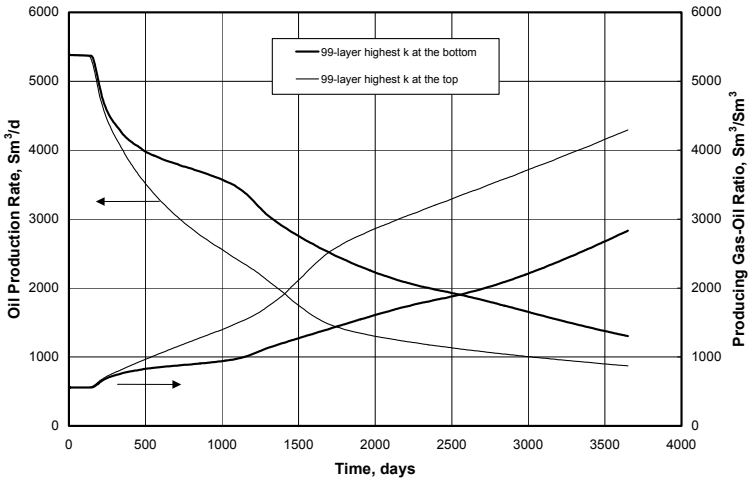

Fig. 2.5 — Gas Injection case performance for the 99-layer reservoir with the near critical fluid.

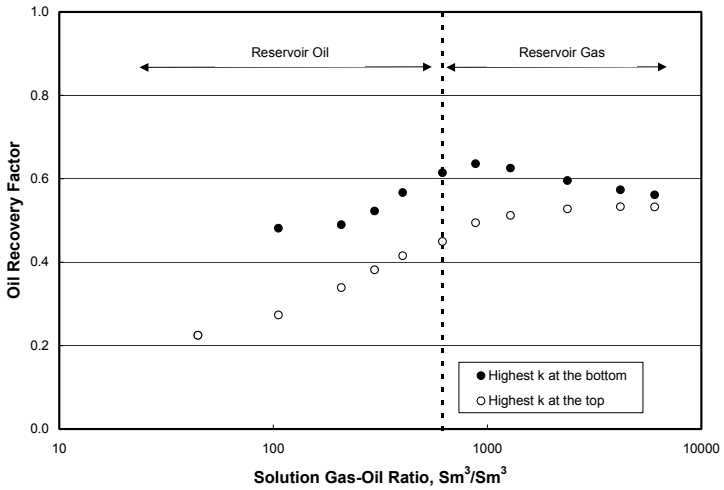

Fig. 2.6 — Gas Injection case oil recovery - 99-layer reservoir with different fluid systems (a) highest permeability at the bottom and (b) highest permeability at the top (for 10 years).

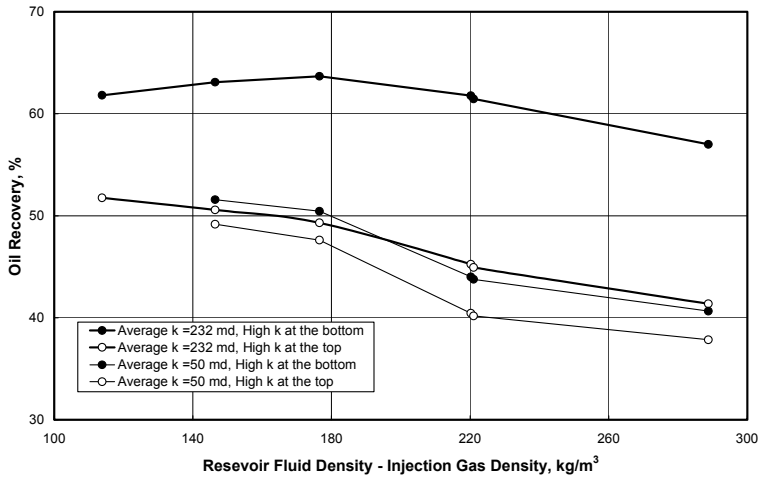

Fig. 2.7 — Effect of gravity and average reservoir permeability on oil recovery in gas injection case for the 99-layer reservoir with different fluid systems (constant composition). The injection gas density at the reservoir condition is 257 kg/m^3.

2.2.4 Layer Grouping

Since it is not practical to simulate the full-field model with large number of numerical layers (e.g. 99 layers) due to CPU time, it is required to reduce the number of numerical layers without affecting the reservoir performance. Two different methods are described for reducing the numerical layers.

- Equal flow capacity.
- Equal storage capacity.

For the purpose of layer grouping, the 99 layer reservoir is used. The whole reservoir is then grouped into model layers based on:

(a) Equal flow capacity – each model layer has the same flow capacity.
In this case, storage capacity will be different for each model layer. The model layer with the highest permeability will have the least storage capacity, but its contribution to flow is the same as all other layers (initially). The model layer with smallest permeability will have the highest storage capacity.

In this case, high permeability layer is given proper consideration in the grouping. Even if high permeability layer has less thickness, it is represented in the group.

(b) Equal storage capacity – each model layer has the same storage capacity.

In this case, flow capacity of each model layer is different, but storage capacity (layer thickness) is the same. The model layer with the highest permeability will have the highest flow capacity.

Based on the above grouping schemes, the entire reservoir thickness is divided into 10 model layers. The thickness and permeability are given in Table B-4 for each layer. In equal flow capacity case, the layer with the highest permeability has the smallest storage capacity. For 10-layer cases, layer flow and storage capacities are plotted in **Fig. 2.8**. The 99 layer is also grouped into 5 layers based on equal flow and equal storage capacity. The 5 layer properties are given in Table B-4.

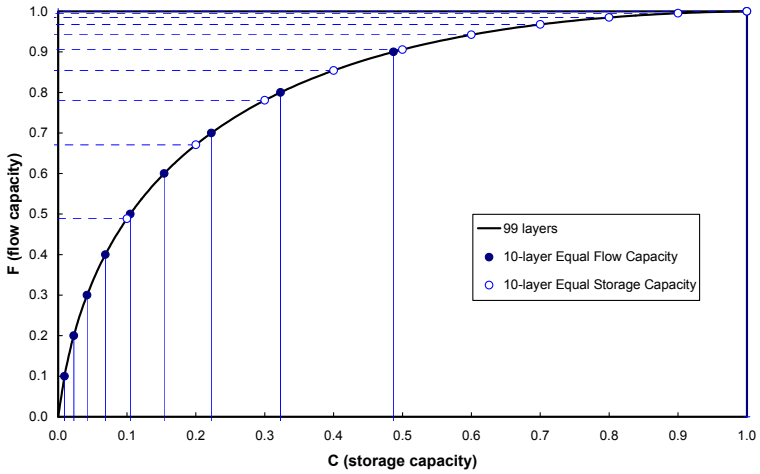

Fig. 2.8 — Layer flow and storage capacity. The 99 layers grouped to 10 layers based on (a) equal flow capacity and (b) equal storage capacity.

2.2.5 Verification of Different Grouping Methods

Depletion Case

The reservoir is produced on a maximum withdrawal constraint (about 10% hydrocarbon pore volume per year) with a minimum well bottom hole flowing pressure of 100 bara. The performance prediction is analyzed for 10 years. The only producing well is perforated throughout the reservoir in the last grid cell (15,5).

Base Case

The base case has 99 model layers of equal vertical thickness (total 150 m) and permeability variation. The arithmetic average reservoir permeability is 232 md. The reservoir fluid considered varied from lean gas condensate to near critical fluid to low-GOR oil with constant composition throughout the reservoir.

In this case, the whole reservoir is grouped into 5 model layers based on (i) equal flow capacity and (ii) equal storage capacity with the highest permeability at the bottom of the reservoir. The equal flow capacity grouping method gives better performance than the equal storage capacity grouping method as shown in **Fig. 2.9**.

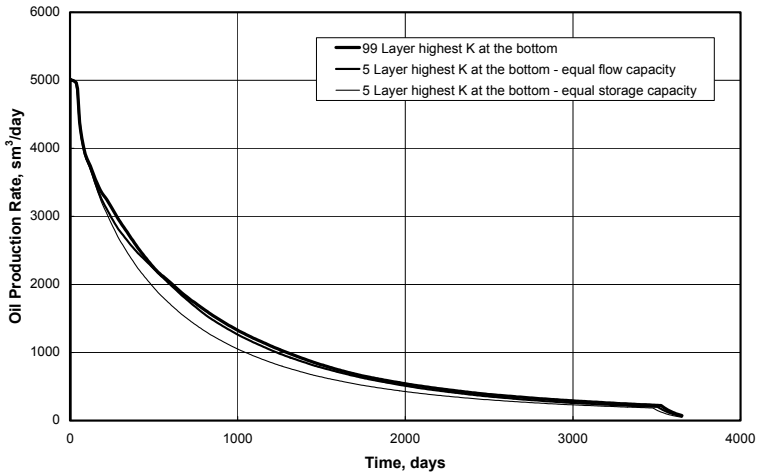

Fig. 2.9 — Reservoir depletion performance comparison of reduced layers with the 99-layer for the highest permeability at the bottom. The reduced layer performance for (a) equal flow capacity and (b) equal storage capacity.

The oil recoveries are 23.3-, 22.4-, and 20.0% for the 99-layer, 5-layer with equal flow capacity, and 5-layer with equal storage capacity respectively. There is a small difference in the 5-layer case with equal flow capacity compared to the 99-layer case.

In the case of high permeability at the top, both grouping methods give similar performance as shown in **Fig. 2.10**. The 99 layers can be grouped using either one of the two methods in the case of the highest permeability at the top for depletion case performance.

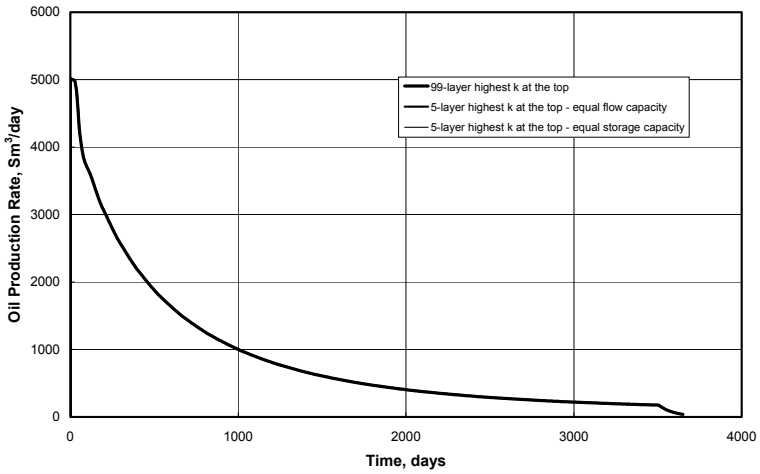

Fig. 2.10 — Reservoir depletion performance comparison of reduced layers with the 99-layer for the highest permeability at the top. Reduced layers performance for (a) equal flow capacity and (b) equal storage capacity.

Number of Numerical Layers

In order to know the minimum number of numerical layers required to represent the original (99-layered) reservoir performance closely, the whole reservoir is also grouped into 10 model layers, and performance is analyzed as shown in **Fig. 2.11**. The 10-layer equal flow capacity layering performance is close to 99-layer. There is some difference for equal storage capacity case. The reservoir layers can be grouped to 10 model layers, with equal flow capacity, to reproduce the 99-layer reservoir performance.

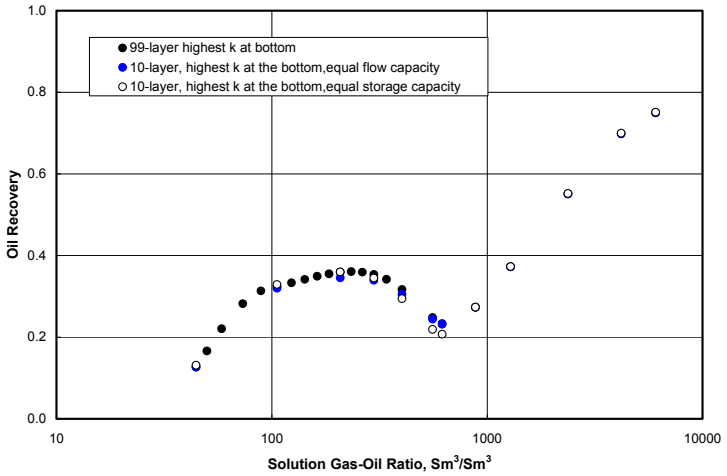

Fig. 2.11 — Depletion oil recovery - 99-layer versus 10-layer reservoir.

Gas Injection Case

The 99-layer reservoir performance is compared with the 10-layer with equal flow capacity performance and also with equal storage capacity. The reservoir performance is shown in **Fig. 2.12** for near critical fluid. The 10-layer (equal flow capacity grouping method) performance is quite similar to the 99-layer performance. The 10 layers can be used to analyze the reservoir performance of the 99-layer reservoir, even in the injection case, if layers are grouped on the basis of equal flow capacity.

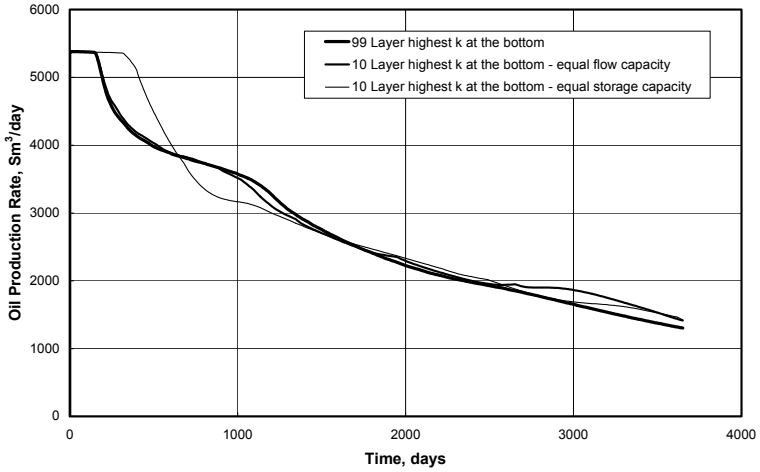

Fig. 2.12 — Reservoir performance comparison for gas injection case for reservoir containing near critical fluid - 99-layer versus 10-layer.

Selection of Number of Grid Cells

The reservoir is also simulated using different number of grid cells in x- and y directions. The performance prediction for different cases with different grid cells in x-direction is shown in **Fig. 2.13**. After 10 years of gas injection, the oil recoveries are 68.3-, 67.8-, 67.4-, and 65.4% for 1000, 100, 50, and 10 grid cells in x-directions respectively. The performance for the 1000, 100, and 50 grid cells in x-direction are quite similar. The performance for 10 grid cells in x-direction is quite different than other cases. In all these cases, 10 grid cells in y-direction and 10 layers in vertical direction are used. The 50 grid cells in x-direction are sufficient to simulate this reservoir properly. Similarly 10 grid cells in y-direction are sufficient. Based on simulation results, 50x10x10 grid cells have been used in further simulation studies for both gas injection and depletion cases.

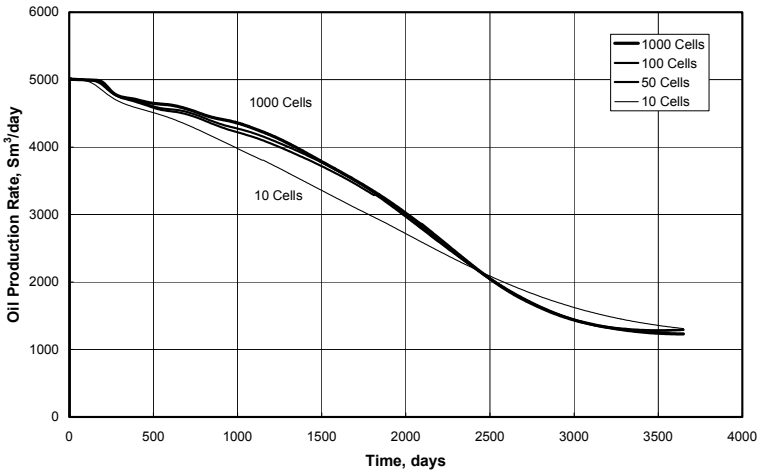

Fig. 2.13 — Reservoir performance (gas injection case) for different grid cells in x-direction for 10 grid cells in y-direction and 10 numerical layers in vertical direction. The reservoir contains near critical fluid.

2.2.6 Summary of the Layer Grouping

1. Numerical layers can be grouped (reduced) on the basis of equal flow capacity or equal storage capacity. The equal flow capacity method for grouping is in all cases better than equal storage capacity (when compared with the full 99-layer performance). Hence equal flow capacity layers have been used in all of the simulations models made for comparing black oil and compositional simulation results.

2. The 99-layered model can be grouped down to ten model layers without loosing accuracy in the production performance. In the 10-layer model, each layer has equal flow capacity. In most of the subsequent simulations models made for comparing black oil and compositional simulation results, 10 numerical layers have been used.

3. Based on the reservoir performance, 50 grid cells in x-direction, 10 grid cells in y-direction and 10 cells in z-direction are sufficient to simulate this reservoir properly. The 50x10x10 grid cells have been used in all further depletion and gas injection cases.

2.3 Depletion Cases

This section compares simulation results from a black-oil model with a compositional model for different depletion cases. Simulated production performance for the two models is compared for fluid systems ranging from a medium-rich gas condensate, to a critical fluid, to slightly volatile oils. The initial reservoir fluid composition is either constant with depth or showing a vertical compositional gradient. Scenarios with both saturated and undersaturated GOC are studied. Permeability increases downwards in most cases to maximize the effect of gravity and mixing of the reservoir fluids. Sensitivities have also been run with different permeability distributions.

The black-oil and compositional reservoir performances for different scenarios are analyzed (data file ending with an "X" indicate a data file for a compositional model run e.g. A1C1X.DATA is compositional model data file. The corresponding black-oil data file is A1C1.DATA). The nomenclature of the data files is given in Table B-8. The different depletion simulation cases are given in Table B-9.

2.3.1 Reservoirs with Constant Composition

In this case, the bottom geologic unit (average k = 200 md) is used and reservoir performances are analyzed for different fluid systems. Using the same geologic unit, the following fluid compositions are used:

GOC — Near Critical Fluid

The performance for the near critical fluid is shown in **Fig. 2.14**. The black-oil and the compositional model results are given in **Table 2.1**. After 10 years of production, the oil recoveries are almost the same in the compositional and the black-oil model (26.9% in compositional and 26.8% in black-oil model). In most part of the production life, the difference in producing GOR is less than 4% as shown in **Fig. 2.15**. The producing gas-oil ratio is 10% higher in compositional model at the end of 10 years, but at that time the oil production rate is low.

50 m above GOC — Rich Gas Condensate (RGC)

The performance for rich gas condensate fluid is shown in **Fig. 2.16**. The performance is quite similar in the black-oil and the compositional model. The oil recovery after 10 years of production is 26.3% in the compositional and 26.4% in the black-oil model. The producing GOR is similar for the first 5 years and thereafter starts deviating slowly. The producing GOR is about 5% higher in the compositional model at the end of 10 years.

50 m below GOC — Volatile Oil (VO)

Reservoir performance for volatile oil is shown in **Fig. 2.17**. The performance is similar in the black-oil and the compositional model. The oil recovery after 10

years of production is 30.9% in the compositional and 31.0% in the black-oil model. The producing GOR is also quite similar in both the compositional and the black-oil models. The producing GOR is quite high at the end of 10 years, but at that time there is almost no oil production.

Reservoir performances are also analyzed for other reservoir fluids such as medium-rich gas condensate and slightly volatile oil. The black-oil and the compositional performances are similar in all cases analyzed. A list of simulation cases with all constant composition is given in Table B-9.

Thus, the depletion performance in the black-oil and the compositional models are similar for constant composition reservoir for fluid varying from medium-rich gas condensate to near critical fluid to slightly volatile oil.

The CPU time taken for simulating the near critical fluid under depletion drive for 10 years is 16 minutes in black-oil and 86 minutes in compositional model run. The time is less by a factor of about 5 in the black-oil model compared to the compositional run and performance is similar in the black-oil and the compositional model.

Hence, the black-oil simulation models can be used for simulating the reservoir performance under depletion drive for reservoirs containing reservoir fluids with constant composition with depth.

Table 2.1 — Depletion Case - Production performance of constant composition reservoir.

		AFTER 3 YEARS			AFTER 5 YEARS			AFTER 10 YEARS		
		FOPR	FGOR	RF_o	FOPR	FGOR	RF_o	FOPR	FGOR	RF_o
		Sm3/d	Sm3/Sm3	%	Sm3/d	Sm3/Sm3	%	Sm3/d	Sm3/Sm3	%
Near Critical Fluid	EOS6	495	1674	17.9	264	2448	22.5	14	4134	26.9
	BO6	500	1657	17.6	274	2352	22.3	27	3723	26.8
Rich Gas Condensate	EOS6	328	2723	17.4	182	3844	21.5	71	5283	26.3
	BO6	329	2713	17.3	185	3772	21.5	74	5043	26.4
Volatile Oil	EOS6	670	1134	20.3	399	1471	25.4	4	4282	30.9
	BO6	678	1121	20.2	401	1459	25.3	24	1386	31.0
Medium-Rich GC	EOS6	336	2744	23.3	197	3745	30.2	80	5159	38.5
	BO6	337	2733	23.3	199	3711	30.1	83	4957	38.7
Slightly Volatile Oil	EOS6	815	806	20.0	477	1034	24.9	14	805	28.8
	BO6	810	812	19.9	472	1043	24.7	16	973	28.6

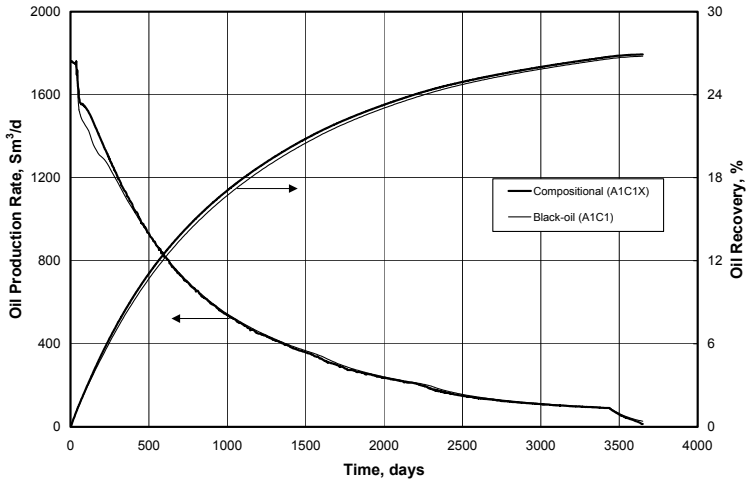

Fig. 2.14 — Depletion Case - Near critical fluid with constant composition; EOS6; (A1C1X.DATA, A1C1.DATA).

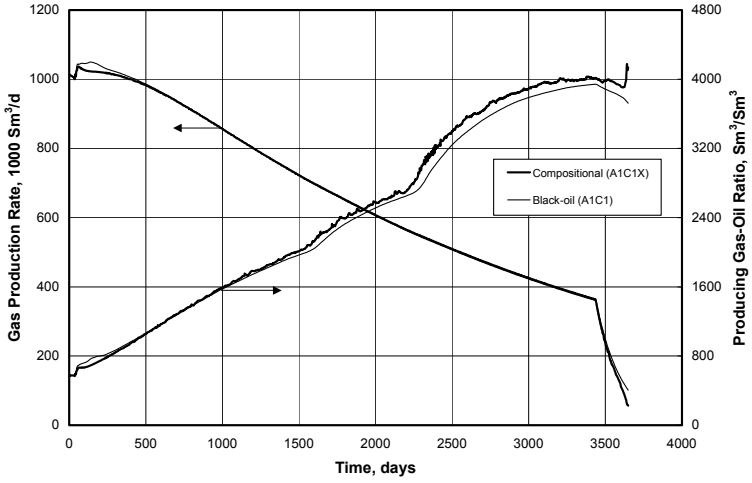

Fig. 2.15 — Depletion Case - Near critical fluid with constant composition; EOS6; (A1C1X.DATA, A1C1.DATA).

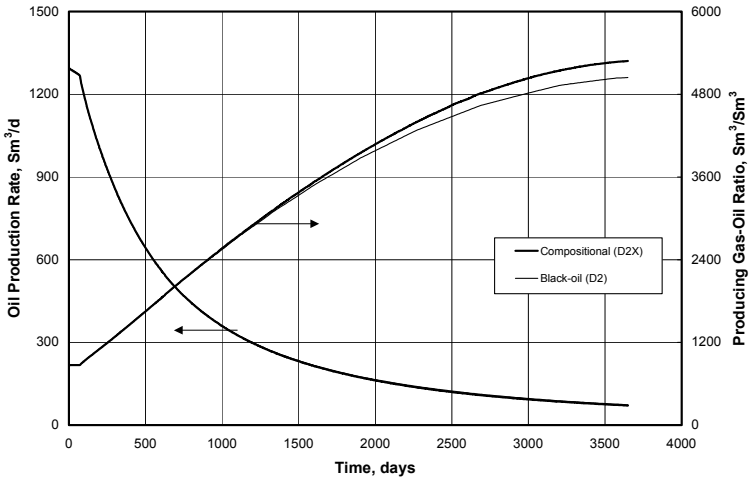

Fig. 2.16 — Depletion Case – Rich gas condensate fluid with constant composition; EOS6; (D2X.DATA, D2.DATA).

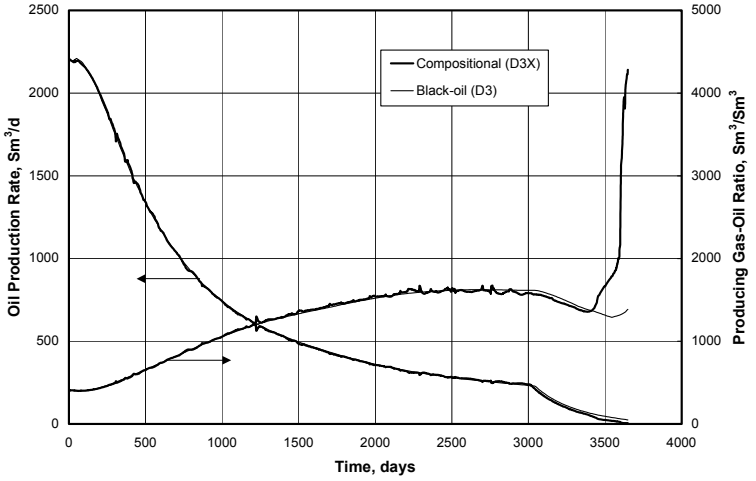

Fig. 2.17 — Depletion Case – Volatile oil reservoir with constant composition; EOS6; (D3X.DATA, D3.DATA).

2.3.2 Reservoirs with Compositional Gradient and Undersaturated GOC

The black-oil PVT tables for this undersaturated GOC case is generated by simulating a CCE experiment with the near critical GOC fluid. To simulate reservoir performance for compositionally grading reservoirs, the three geologic units are selected separately.

Bottom Geologic Unit (GU3)
This geologic unit contains oil and gas condensate with compositions varying from top to bottom. The top of the reservoir is at 4600 m and the bottom is at 4850 m with the GOC at 4750 m. The reservoir contains an undersaturated GOC — saturation (original) pressure at GOC is 473 bara, while reservoir pressure is 494.68 bara. The reservoir performance plots are shown in **Fig. 2.18**. The black-oil and compositional model results are quite similar. The oil recovery is 32.6% in the compositional model and 33.4% in the black-oil model after 10 years of production (**Table 2.2**).

Middle Geologic Unit (GU2)
This unit contains some oil, but mainly gas with compositional gradient from top to bottom. The depletion performance plots are shown in **Fig. 2.19**. The performance is quite similar in compositional and black-oil models. The oil recovery is 29.5% in the compositional model and 29.8% in the black-oil model after 10 years of depletion.

Top Geologic Unit (GU1)
This reservoir unit contains only gas condensate fluid with compositional gradient. The compositional gradient varies from medium-rich gas condensate at the top to near critical fluid at the bottom of the reservoir. The reservoir performance plots are shown in **Fig. 2.20**. In this case, there is some difference in compositional and black-oil simulation performance due to low permeability that causes condensate blockage. If the average permeability is increased then black-oil and compositional model results are quite similar (Fig. C-10). In the case of condensate blockage, special oil viscosity treatment is needed[7].

The reservoir performance for the modified oil viscosity is shown in Fig. C-11. In the case of modified oil viscosity, the saturated oil viscosities with pressures are calculated from the compositional simulation runs. The black-oil and the compositional models performances are quite similar when modified oil viscosities are used in the black-oil model.

Whole Reservoir (GU3+GU2+GU1)
In this case, all three non-communicating geologic units are considered. The compositionally grading reservoir contains medium-rich gas condensate at the top, near critical fluid at the undersaturated GOC and then slightly volatile oil at the bottom. The well is perforated through all layers. The reservoir performance is similar in the black-oil and the compositional models as shown in **Fig. 2.21**.

Table 2.2 — Depletion Case - Production performance of compositionally grading reservoir.

		AFTER 3 YEARS			AFTER 5 YEARS			AFTER 10 YEARS		
		FOPR	FGOR	RF_o	FOPR	FGOR	RF_o	FOPR	FGOR	RF_o
		Sm3/d	Sm3/Sm3	%	Sm3/d	Sm3/Sm3	%	Sm3/d	Sm3/Sm3	%
Bottom geologic unit	EOS6	432	1982	24.0	216	3123	28.2	66	4882	32.6
	BO6	438	1965	24.8	219	3097	29.1	73	4753	33.4
Middle geologic unit	EOS6	349	2558	20.3	190	3709	24.7	45	5266	29.5
	BO6	352	2550	20.6	191	3687	25.0	44	5101	29.8
Top geologic unit	EOS6	223	1900	9.3	165	2390	13.2	86	3405	19.4
	BO6	210	1835	8.9	158	2270	12.6	87	3203	18.6
Whole reservoir	EOS6	958	2844	20.1	570	3790	24.2	107	3377	27.3
	BO6	942	2894	20.3	563	3829	24.3	116	3134	27.2

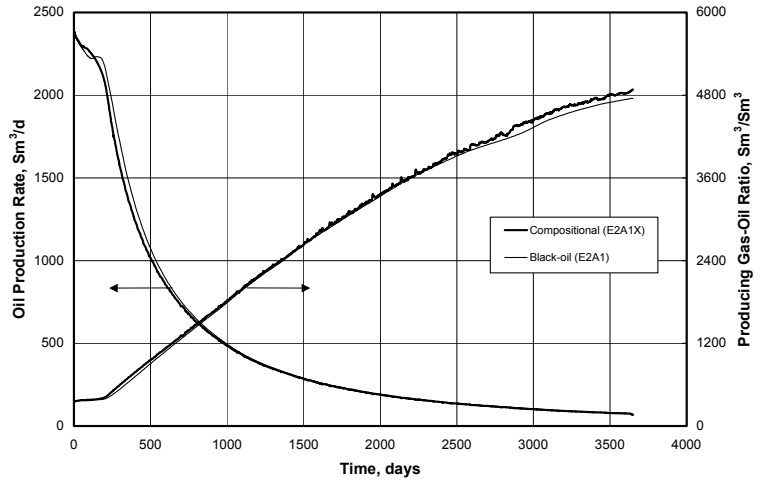

Fig. 2.18 — Depletion Case – Bottom geologic unit with compositional gradient; EOS6; (E2A1X.DATA, E2A1.DATA).

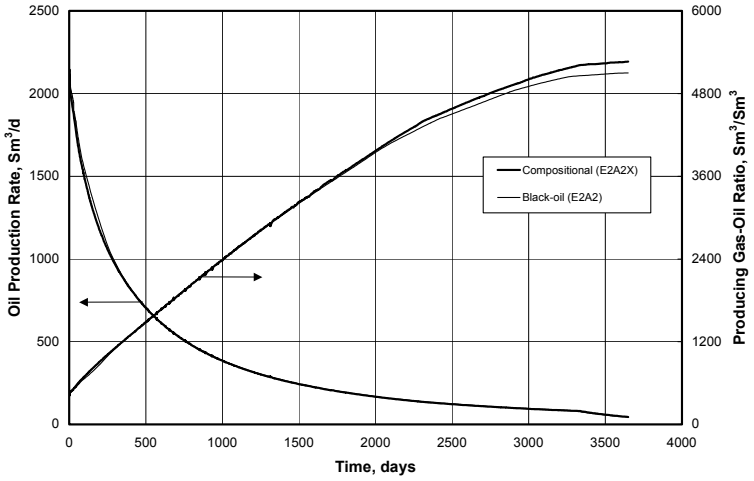

Fig. 2.19 — Depletion Case – Middle geologic unit with compositional gradient; EOS6; (E2A2X.DATA, E2A2.DATA).

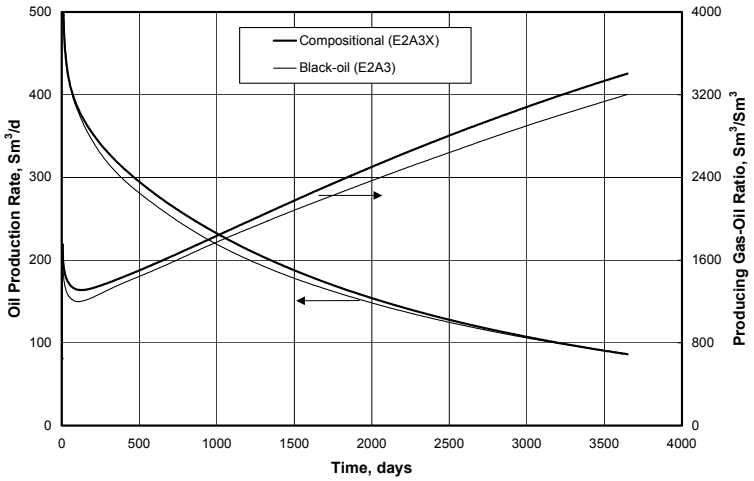

Fig. 2.20 — Depletion Case – Top geologic unit with compositional gradient; EOS6; (E2A3X.DATA, E2A3.DATA).

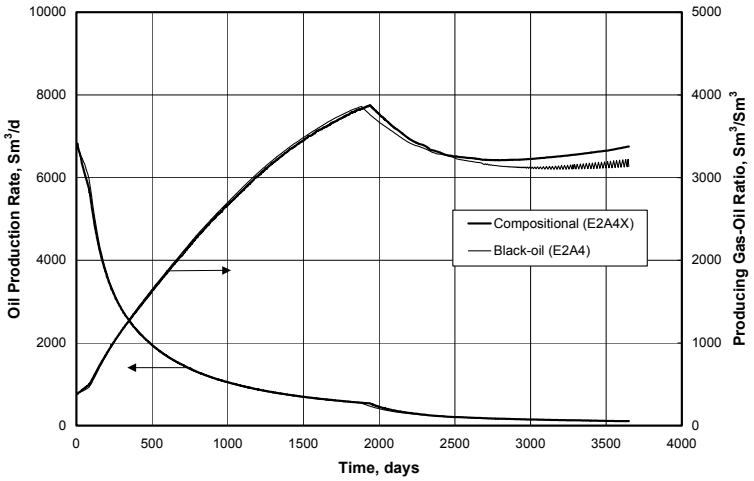

Fig. 2.21 — Depletion Case – The whole reservoir with compositional gradient and undersaturated GOC; EOS6; (E2A4X.DATA, E2A4.DATA).

2.3.3 Permeability Variations

In all of the above cases, the highest permeability is at the bottom of the reservoir. In this section, permeability distribution is changed.

Highest Permeability at the Top

The reservoir GU3 is used with constant fluid composition taken from the GOC (i.e. near critical fluid). The permeability distribution is changed such that the highest permeability is at the top of the reservoir. The reservoir performance curves are shown in **Fig. 2.22** and data are given in **Table 2.3**. The reservoir performance is quite similar in the black-oil and the compositional models.

Highest Permeability in the Middle

The reservoir GU3 is used with constant fluid composition taken from the GOC (i.e. near critical fluid). The permeability distribution is changed such that the highest permeability is in the middle of the reservoir. The reservoir performance curves are shown in **Fig. 2.23**. The reservoir performance is quite similar in the black-oil model and the compositional models.

Table 2.3 — Depletion Case - Production performance with near critical fluid and permeability variation, constant composition.

		AFTER 3 YEARS			AFTER 5 YEARS			AFTER 10 YEARS		
		FOPR	FGOR	RF_o	FOPR	FGOR	RF_o	FOPR	FGOR	RF_o
		Sm3/d	Sm3/Sm3	%	Sm3/d	Sm3/Sm3	%	Sm3/d	Sm3/Sm3	%
High k at bottom	EOS6	495	1674	17.9	264	2448	22.5	14	4134	26.9
	BO6	500	1657	17.6	274	2352	22.3	27	3723	26.8
High k at top	EOS6	294	2932	12.8	158	4152	15.4	10	5398	18.3
	BO6	289	2987	12.7	156	4184	15.4	9	5328	18.2
High k in middle	EOS6	293	2946	12.8	157	4182	15.5	10	5448	18.3
	BO6	289	2980	12.8	157	4176	15.4	9	5326	18.3

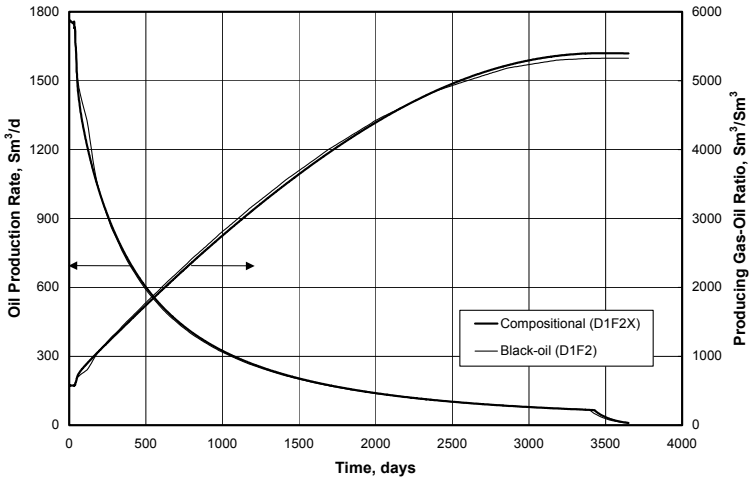

Fig. 2.22 — Depletion Case – Bottom geologic unit with near critical fluid (constant composition) and the highest permeability at the top (D1F2X.DATA, D1F2.DATA).

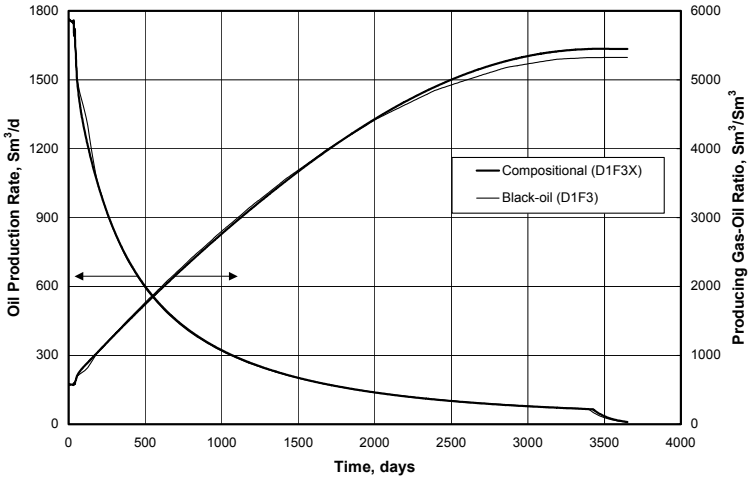

Fig. 2.23 — Depletion Case – Bottom geologic unit with near critical fluid (constant composition) and the highest permeability in the middle (D1F3X.DATA, D1F3.DATA).

2.3.4 Reservoirs with a Saturated GOC

In all of the above depletion cases, in case of reservoir containing both oil and gas, undersaturated GOC has been considered. In this case, saturated GOC is considered.

Constant Composition

The oil sample is taken from 50 m below GOC. Thereafter, equilibrium gas composition is obtained from the oil sample. The constant oil composition is used in the oil zone and the constant gas composition[a] is used in the gas zone. The GOC is considered as 4800 m and reservoir pressure at GOC is the same as saturation pressure of oil (and gas). The reservoir is simulated using the black-oil and the compositional models.

The black-oil PVT table can be generated from a simulated CCE, DLE, and CVD experiment. The black-oil and the compositional simulation producing gas-oil ratios are shown in **Fig. 2.24** and oil recoveries are shown in **Fig. 2.25 (Table 2.4)** for different black-oil PVT table generation methods. In the case of CCE, oil and gas black-oil PVT properties are generated simulating a CCE experiment using GOC oil. In the DLE case, simulated DLE experiment with GOC oil is used for generating the oil and gas black-oil PVT properties. In the case of

[a] The reservoir pressure is less than the original gas saturation pressure above the GOC, some liquid dropout may be observed above GOC in some of the compositional reservoir simulators. In those simulators, to avert liquid dropout, after simulating using constant gas composition, gas composition versus depth can be obtained. The new gas composition versus depth (above the GOC) can be used to initialize the compositional simulation model.

DLE/CVD (MIX case), the oil black-oil PVT properties are generated from simulated DLE experiment with the GOC oil and gas black-oil PVT properties are generated from simulated CVD experiment with the GOC equilibrium gas. From simulation results, the DLE/CVD combination is closer to the compositional simulation results. The black-oil PVT properties generated by simulating a DLE experiment with GOC oil and CVD experiment with GOC gas are shown in Fig. C-12.

The sensitivity study has been done for surface oil and gas densities. In CCE and DLE black-oil PVT tables, surface densities obtained from the EOS are used. In DLE/CVD combination, the surface oil density is taken from DLE and the surface gas density is taken from CVD experiment. In DLE/CVD combination, the surface oil and gas densities should be modified to match the reservoir oil and gas densities at the GOC conditions. The EOS calculated reservoir oil and gas densities with pressure are plotted against the reservoir oil and gas densities. The calculation is based on black-oil PVT tables, with surface oil density from DLE and surface gas density from CVD. There is some difference between EOS and black-oil PVT tables based calculated reservoir oil and gas densities (**Fig. 2.26**). When surface oil and gas densities are modified to match the reservoir oil and gas densities at the GOC conditions, then calculated reservoir oil and gas densities with pressure are very close to the EOS reservoir oil and gas densities (**Fig. 2.27**).

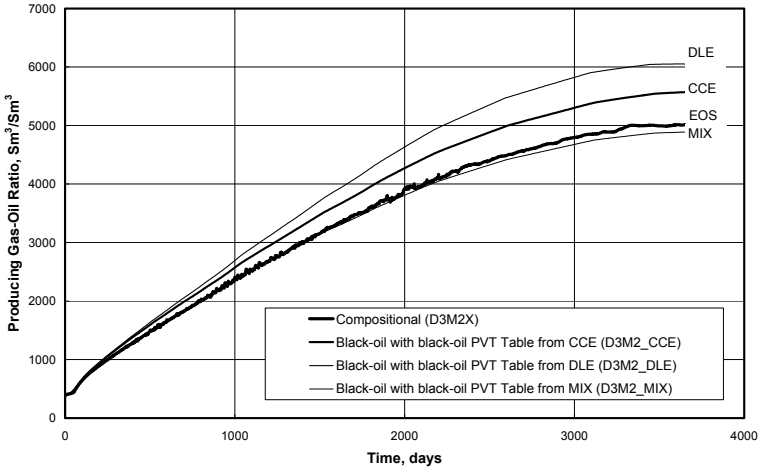

Fig. 2.24 — Depletion Case – Reservoir with constant composition in oil and gas zone with saturated GOC (D3M2X.DATA, D3M2_CCE.DATA, D3M2_DLE.DATA, D3M2_MIX.DATA).

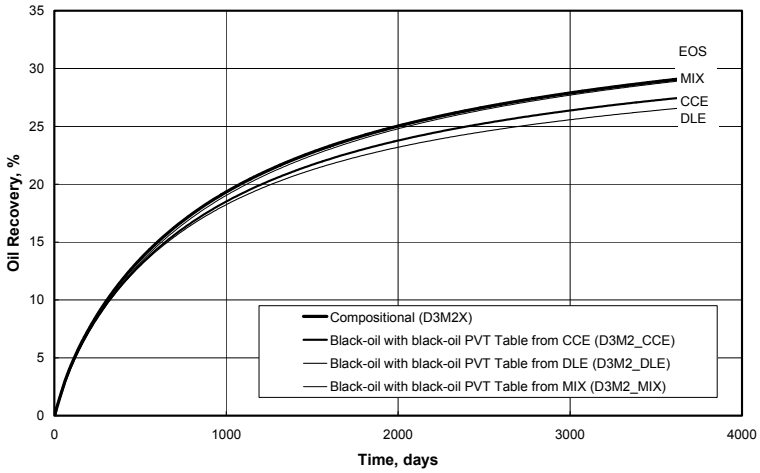

Fig. 2.25 — Depletion Case – Reservoir with constant composition in oil and gas zone with saturated GOC (D3M2X.DATA, D3M2_CCE.DATA, D3M2_DLE.DATA, D3M2_MIX.DATA).

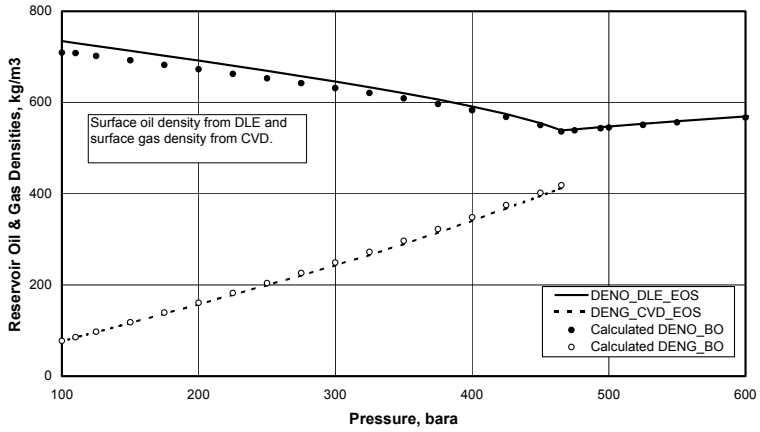

Fig. 2.26 — Reservoir saturated oil and gas densities at different pressures based on surface oil and gas densities.

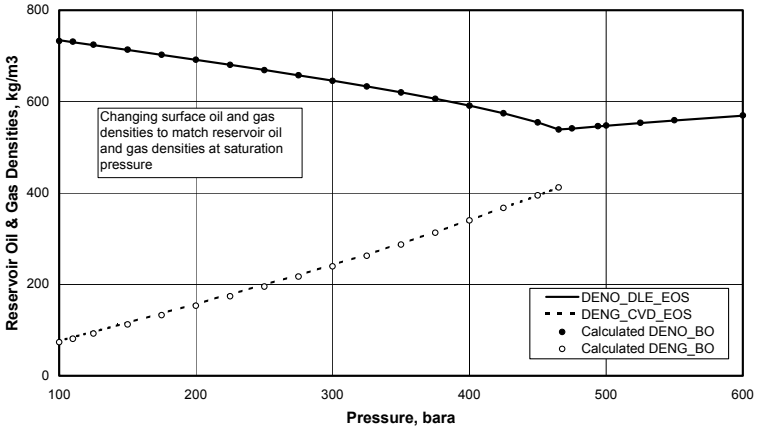

Fig. 2.27 — Reservoir saturated oil and gas densities at different pressures based on modified surface oil and gas densities.

In the case of saturated GOC, the black-oil PVT tables should be generated from a simulated DLE experiment with the GOC oil for the reservoir oil. The gas black-oil PVT table should be generated from a simulated CVD experiment with the GOC gas. When significant gravity segregation is expected, the surface gas and oil densities should be modified such that the reservoir oil and gas densities are accurate throughout depletion, as described earlier.

Compositional Gradient

In this case, compositional variation is considered. The oil and gas composition are obtained by isothermal gradient calculation from the GOC oil. The reservoir pressure at the GOC of 4800 m is equal to 465 bara.

The oil and gas composition obtained above are used for simulating in the compositional model. The solution gas-oil ratio versus depth, obtained from the compositional run, is used in the black-oil run. The reservoir performance for this compositionally gradient reservoir case is shown in **Fig. 2.28**. In this case, there is only one producer. The reservoir performance is quite similar in the black-oil and the compositional models.

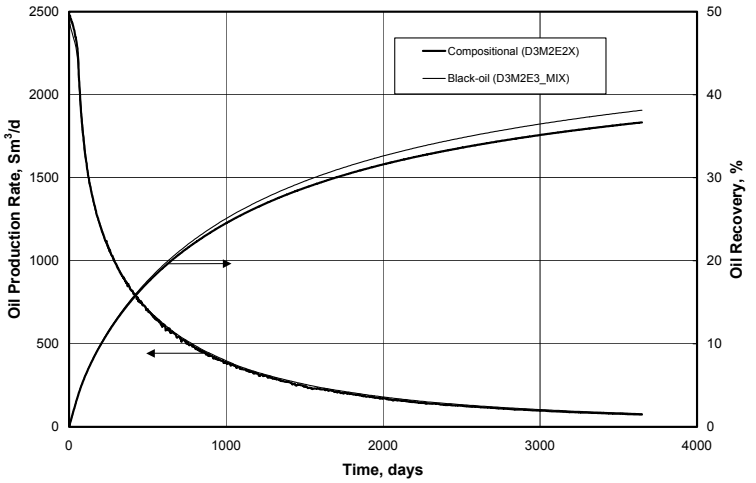

Fig. 2.28 — Depletion Case – Reservoir with compositional gradient and saturated GOC; total reservoir performance; EOS6 (D3M2E2X.DATA, D3M2E3_MIX.DATA).

Compositional Gradient with 3 Producers at Different Locations

The reservoir is also simulated using different well production scenarios. In this case, three wells are considered at three different locations (top, bottom and middle). The reservoir fluid composition varies from medium-rich gas condensate to slightly volatile oil. The black-oil PVT tables are generated from GOC oil and gas, which have the maximum saturation pressure compared to any other reservoir oil and gas. Since only one black-oil PVT table is used, this black-oil PVT table will be most representative for the GOC oil and gas. The overall field performance is plotted in **Fig. 2.29**. The overall field performance is quite similar in black-oil and composition runs.

The structurally low well performance is shown in **Fig. 2.30**. The structurally low well performance is also quite similar in black-oil and compositional simulation models.

The well performance for the structurally high well is shown in **Fig. 2.31**. The performance of the structurally high well is slightly different in black-oil and compositional runs. The gas black-oil PVT table is generated from GOC equilibrium gas at 4800 m and the structurally top well is located at 4600 m. There will be differences in gas black-oil PVT properties for the two gases. When GOC gas generated gas black-oil PVT properties are used, there will be a difference in saturation pressure for the structurally high well gas for the same oil-gas ratio (as shown in chapter 1). The difference in saturation pressure results in low GOR in the black-oil model for the structurally high well. Due to this difference in the saturation pressure, the increase in producing GOR is delayed in

the black-oil model. If the spliced gas PVT data is used, the structurally high well performance will be quite similar in the black-oil and the compositional models, but the total reservoir performance will differ in the black-oil and the compositional models, since most of the oil is near the GOC.

API Tracking Option

In some of the reservoir simulators, it is possible to use API tracking option for proper interpolation of the black-oil PVT properties between different input black-oil PVT tables. The API tracking option provides the possibility for using interpolated black-oil properties from different black-oil tables by determining the fluid API gravity along the API gravity gradient[a]. This approach minimizes the difference in initial saturation pressure and gives proper representation of the depletion properties in the black-oil model compared to the compositional model. The approach is useful, especially when large compositional gradient exists. The reservoir simulator, which is used in this study, has the limitation of using API approach only for the oil properties. Consequently, only single gas table can be used, even if API approach is used. The oil properties can be represented properly by using the API approach, but the gas properties should be used from the gas PVT table generated with the GOC fluid. Hence, API tracking option is not used in this work.

Table 2.4 — Depletion Case - Production performance for compositionally grading reservoir with saturated GOC.

		AFTER 3 YEARS			AFTER 5 YEARS			AFTER 10 YEARS		
		FOPR	FGOR	RF_o	FOPR	FGOR	RF_o	FOPR	FGOR	RF_o
		Sm3/d	Sm3/Sm3	%	Sm3/d	Sm3/Sm3	%	Sm3/d	Sm3/Sm3	%
Constant Composition	EOS6	340	2526	19.8	185	3646	24.0	72	5031	28.7
D3M2	BO6 CCE	316	2756	19.2	170	4003	23.1	65	5572	27.5
	BO6 DLE	301	2899	18.9	158	4324	22.6	57	6051	26.6
	BO6 MIX	344	2527	19.8	190	3586	24.1	74	4888	29.0
Compositional Gradient										
Field	EOS6	362	2392	22.7	203	3404	28.2	80	4809	34.5
	BO6	370	2347	23.2	208	3323	28.9	82	4660	35.4
Bottom well	EOS6	162	1726		84	2672		30	4136	
	BO6	155	1823		83	2739		31	4015	
Middle well	EOS6	102	2871		60	3875		25	5215	
	BO6	108	2706		63	3687		25	5052	
Top well	EOS6	98	2993		59	3970		25	5235	
	BO6	107	2743		63	3722		25	5061	

[a] API tracking in E100 allows different *oil* PVT properties to be defined and tracked in the oil zone; only a *single* gas PVT table, however, is allowed with this option.

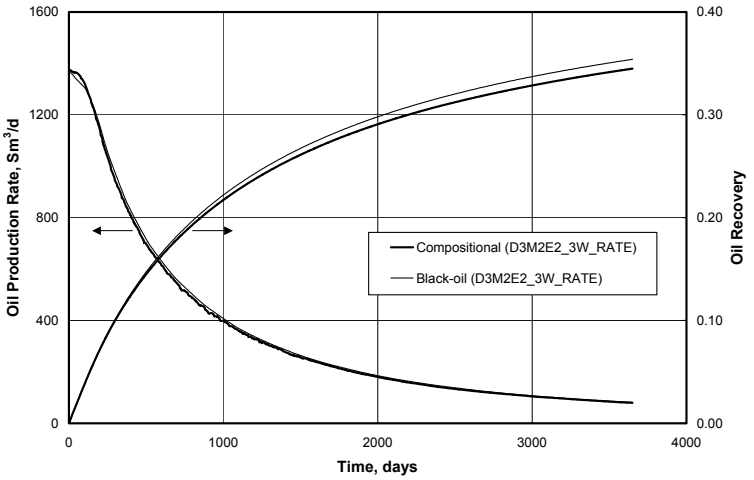

Fig. 2.29 — Depletion Case – Reservoir with compositional gradient and saturated GOC; total reservoir production with 3 wells; EOS6 (D3M2E2X_3W_RATE.DATA, D3M2E2_3W_RATE.DATA).

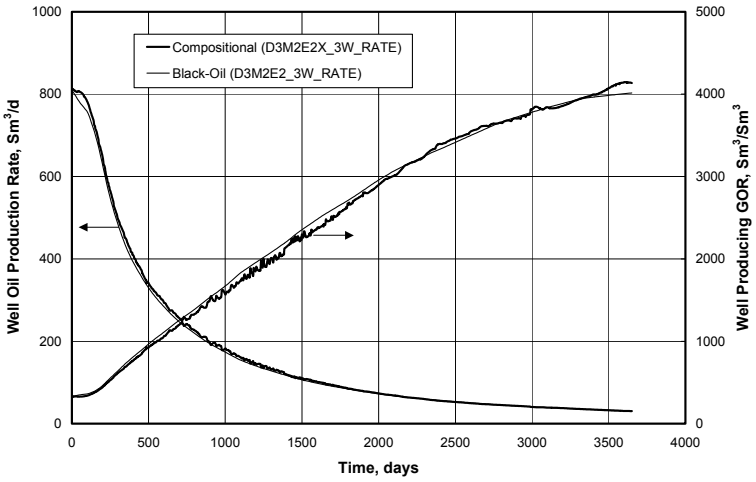

Fig. 2.30 — Depletion Case – Reservoir with compositional gradient and with saturated GOC; structurally low well; EOS6 (D3M2E2X_3W_RATE.DATA, D3M2E2_3W_RATE.DATA).

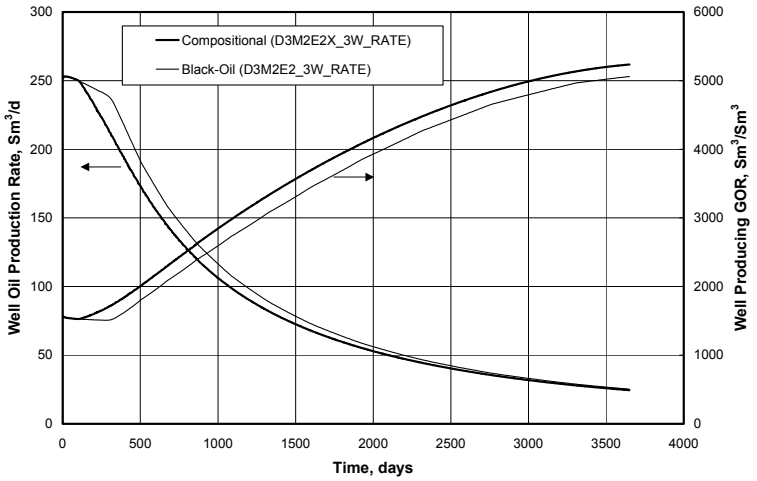

Fig. 2.31 — Depletion Case – Reservoir with compositional gradient and saturated GOC, structurally high well; EOS6 (D3M2E2X_3W_RATE.DATA, D3M2E2_3W_RATE.DATA).

2.3.5 Summary of Depletion Cases

The black-oil and the compositional model results are similar in almost all depletion simulation cases. The simulated field oil production from the black-oil model runs does not deviate more than one recovery-% from the compositional results during the ten-year production period in any case. In most cases, the deviation is less then 0.25 recovery-%. The difference in gas recovery is negligible in all of the cases. The producing GOR is generally quite accurate during most of the ten-year production period. However, in a few cases, the producing GOR starts to deviate somewhat after about five years of production. After ten years of production the GOR is up to 5% lower in the black-oil model. The cases considered are constant composition gas reservoirs, constant composition oil reservoirs, compositionally grading undersaturated GOC oil and gas reservoirs, different permeability variations, and saturated GOC oil and gas reservoirs. Hence, the black-oil simulation model can be used for simulating depletion performance.

Only one simulation case shows some difference between the black-oil and the compositional model. In that compositionally grading saturated GOC case, there are three wells completed at three different locations structurally - high, middle and low. For the structurally high wells, the well performance is slightly different in the two models. The structurally high producer has a producing GOR in the black-oil model somewhat (5-10%) too low. Even though the individual wells show some performance differences, the overall field performance is very similar.

In the case of the saturated GOC reservoir, the reservoir oil PVT data should be generated from a simulated DLE experiment with the GOC oil. The reservoir gas PVT table should be generated from a simulated CVD experiment with the GOC gas. When significant gravity segregation is expected, the surface gas and oil densities should be modified such that the reservoir oils and gas densities are accurate throughout depletion.

2.4 Gas Injection Cases

This section compares compositional and black-oil model simulation results for different gas injection cases. Both full pressure maintenance and partial pressure maintenance cases are considered. The constant composition gas condensate reservoirs, constant compositional oil reservoirs, and compositionally grading oil and gas reservoirs are considered. The reservoir permeability variation is also considered.

2.4.1 Minimum Miscibility Pressure

To calculate minimum miscibility pressure (MMP) for different fluid systems, the MMPz program developed by Zick is used. The MMP is calculated for reservoir fluid varying from the top to the bottom of the reservoir using lean injection gas (composition given in Table B-1). The calculated MMP's are shown in **Fig. 2.32**.

In the gas zone, the calculated MMP is equal to the dewpoint pressure of the reservoir gas. In the oil zone, MMP is greater than the bubblepoint pressure. The MMP is less than the reservoir pressure down to the depth of 4850 m, however, below 4850 m, MMP is higher than the reservoir pressure.

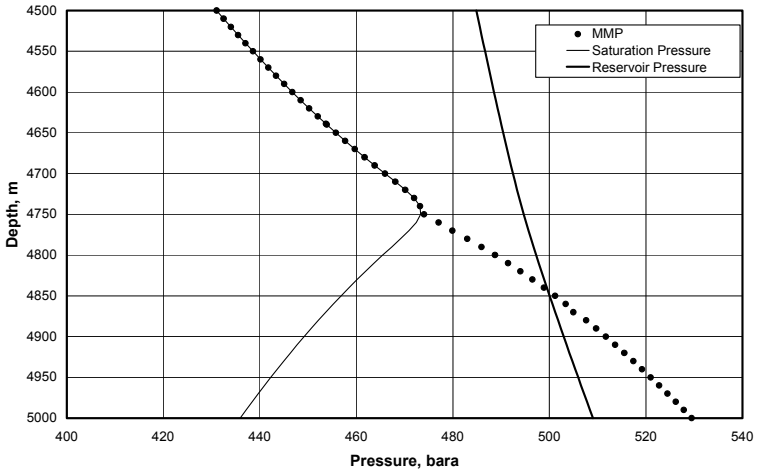

Fig. 2.32 — Minimum Miscibility Pressure – variation with depth. The lean gas is injected in the reservoir fluid taken from different depths.

2.4.2 Full Pressure Maintenance

Gas Condensate Reservoirs with Constant Composition
In order to see the effect of the composition, different reservoir fluids are selected. Using the same geologic unit (GU3, high permeability unit), the reservoir is simulated using the following fluid compositions:

250 m above GOC — Medium-rich Gas Condensate
The medium-rich gas condensate reservoir fluid is taken from 250 m above the GOC. The black-oil and compositional simulation performance is shown in **Fig. 2.33**. The performance is quite similar in the black-oil and the compositional models. The oil recovery after 15 years of gas cycling is 82.4% in the compositional model and 84.2% in the black-oil model (**Table 2.5,** Table B-10).

50 m above GOC — Rich Gas Condensate
The rich gas condensate reservoir fluid is taken from 50 m above the GOC. **Fig. 2.34** shows the reservoir performance in the black-oil and the compositional models. The oil recovery after 15 years of production is 81.8% in the compositional model and 86.8% in the black-oil model.

These cases support the conclusion by Coats[1] that reservoirs with a lean- to medium-rich gas condensate fluid produced by gas cycling above the original dewpoint can be simulated accurately with a black-oil simulator.

GOC fluid — Near Critical Fluid
The performance of the reservoir with a near critical fluid is shown in **Fig. 2.35**. The oil recovery after 15 years of production is 71.3% in the compositional model and 88.7% in the black-oil model. There is a significant difference in performance in the black-oil and the compositional models. The difference in producing GOR is also significant from the very beginning in the compositional and the black-oil models. The reservoir performance for rich injection gas in the reservoir containing near critical fluid is shown in Fig. C-13. In this case also, there is significant difference between the black-oil and the compositional model production performances.

The big difference in oil production from the two models was not expected since the reservoir pressure is higher than the minimum miscibility pressure. The calculated minimum miscibility pressure is a multi contact miscible process (vaporizing mechanism). As shown in **Fig. 2.36**, the first contact miscibility pressure is much higher than the reservoir pressure. Due to gravity effects, the 1-D multi contact miscibility process seems not to develop. Detailed analysis of the simulation results shows that injection gas is transported in the lower (high permeable) layers towards producer. Gradually (in space), less and less gas flows in the lower layer towards the producer because of gravity segregation. “Fresh” injection gas contacts “fresh” reservoir fluid. This causes condensation of oil.

Condensed oil segregates towards the bottom of the reservoir. Both oil and gas flows in the lower layers towards the producer. In order to check if the compositional simulation result is not caused by the limited amount of vertical grid cells (too few contacts), the case is rerun with the original 99-layer model. The results from this simulation are shown in **Fig. 2.37**. The oil recovery actually is lower in the 99-layer model.

Permeability Variation (Near Critical Fluid)

In all of the above gas injection cases, the highest permeability is at the bottom of the reservoir to obtain maximum gas segregation effects. In the following cases, the permeability distribution has been changed as explained below:

(a) Highest Permeability at the Top

The reservoir GU3 is used with constant fluid composition taken from GOC i.e. near critical fluid. The permeability distribution is changed such that the highest permeability is at the top of the reservoir and the lowest permeability is at the bottom of the reservoir, all layers having equal flow capacity. The black-oil and compositional models performance plots are shown in **Fig. 2.38**.

The oil recovery after 15 years of production is 50.3% in the compositional model and 56.2% in the black-oil model. The difference in oil recovery in the two models is less for high permeability at the top compared to the case with high permeability at the bottom. For the case with high permeability at the top, the producing GOR is 30% too low in the black-oil model after 15 years of production. This is expected since the displacement in this case is close to "pure" displacement.

(b) Highest Permeability in the Middle

The reservoir GU3 is used with constant fluid composition taken from GOC i.e. near critical fluid. The permeability distribution is changed such that the highest permeability is in the middle of the reservoir. The reservoir performance curves are shown in **Fig. 2.39**.

The performance from the black-oil model and the compositional model might quite different for gas injection in the reservoir containing a near critical fluid. The black-oil simulator might over predict the oil recovery significantly due to compositional effects that are not properly treated in a black-oil model. Consequently, the black-oil model may not be adequate for simulating gas injection in a reservoir with a near critical fluid.

Gravity Stable Displacement

In order to achieve gravity stable displacement, the production rate is reduced to 1% hydrocarbon pore volume per year. The reservoir performance is analyzed for the near critical fluid (**Fig. 2.40**).

In this case, the performance is almost similar in the black-oil and the compositional model. There is some difference in the late life of the reservoir (black-oil model overpredicts the reservoir performance). Hence, a black-oil model will be adequate in reservoirs, where the displacement process is gravity stable or where the effect of gravity is negligible e.g. layered no cross-flow reservoirs.

Table 2.5 — Injection Case - Production performance of constant composition gas condensate reservoir.

		AFTER 5 YEARS			AFTER 10 YEARS			AFTER 15 YEARS		
		FOPR	FGOR	RF_o	FOPR	FGOR	RF_o	FOPR	FGOR	RF_o
		Sm3/d	Sm3/Sm3	%	Sm3/d	Sm3/Sm3	%	Sm3/d	Sm3/Sm3	%
Medium-Rich GC	EOS6	493	2598	44.1	287	4568	69.1	123	10890	82.4
	BO6	501	2554	44.1	298	4412	69.7	144	9315	84.2
Rich Gas Condensate	EOS6	776	1576	43.4	446	2859	68.2	217	6014	81.8
	BO6	819	1477	44.7	494	2562	71.8	238	5535	86.8
Near Critical Fluid	EOS6	838	1437	39.2	511	2457	59.0	290	4427	71.3
	BO6	1147	983	44.2	733	1625	72.6	316	4054	88.7
Near Critical Fluid	EOS6	584	2137	30.5	305	4223	43.3	157	8327	50.3
(high k at top)	BO6	620	2005	31.7	371	3441	46.7	251	5140	56.2
Near Critical Fluid	EOS6	706	1743	35.5	203	6426	47.6	153	8536	52.7
(high k in middle)	BO6	799	1514	40.6	268	4843	54.6	155	8477	60.6
Near Critical Fluid	EOS6	176	575	5.5	175	577	10.9	174	585	16.4
(gravity stable)	BO6	175	576	5.5	174	579	10.9	172	586	16.3

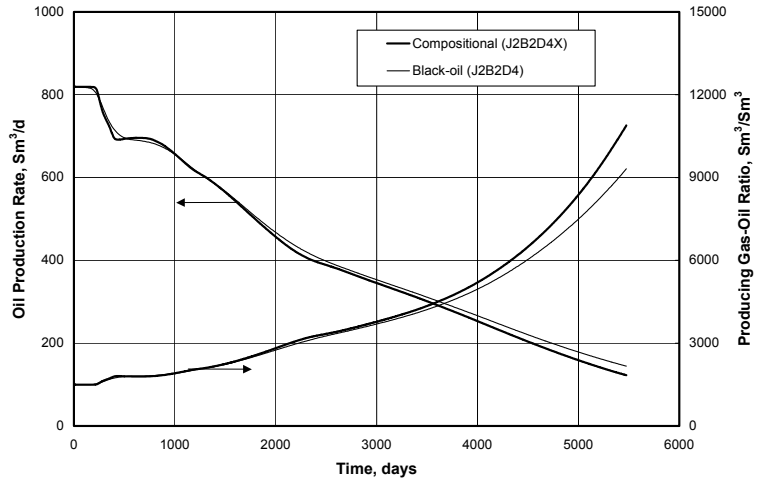

Fig. 2.33 — Injection Case – Medium-rich gas condensate with constant composition; EOS6 (J2B2D4X.DATA, J2B2D4.DATA).

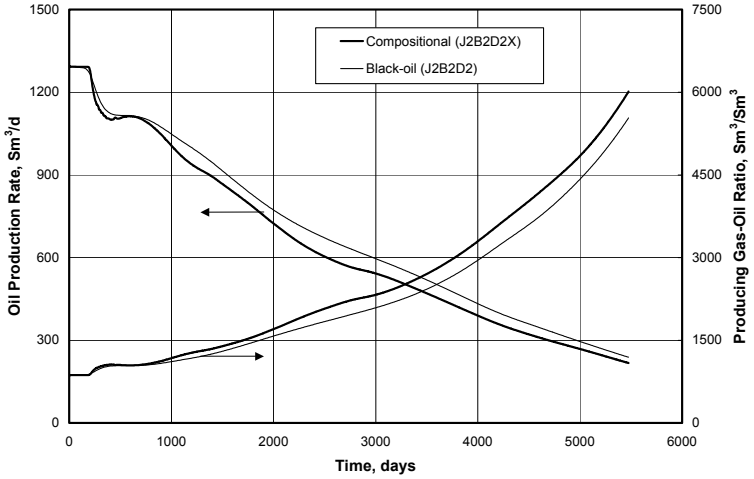

Fig. 2.34 — Injection Case – Rich gas condensate with constant composition; EOS6 (J2B2D2X.DATA, J2B2D2.DATA).

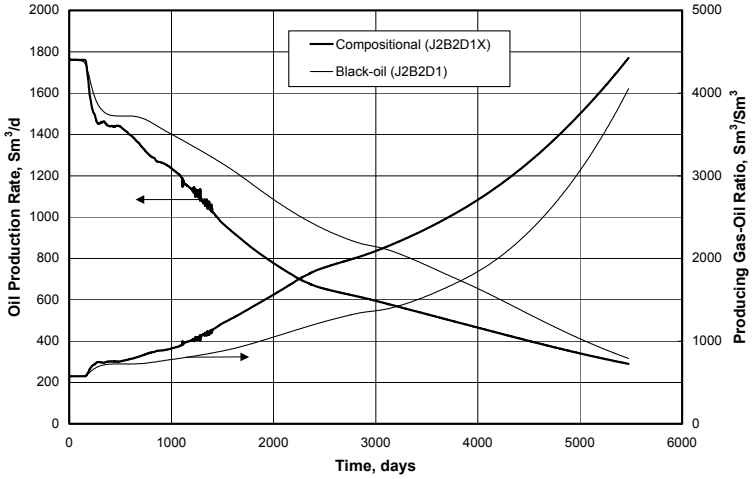

Fig. 2.35 — Injection Case – Near critical fluid with constant composition; EOS6 (J2B2D1X.DATA, J2B2D1.DATA).

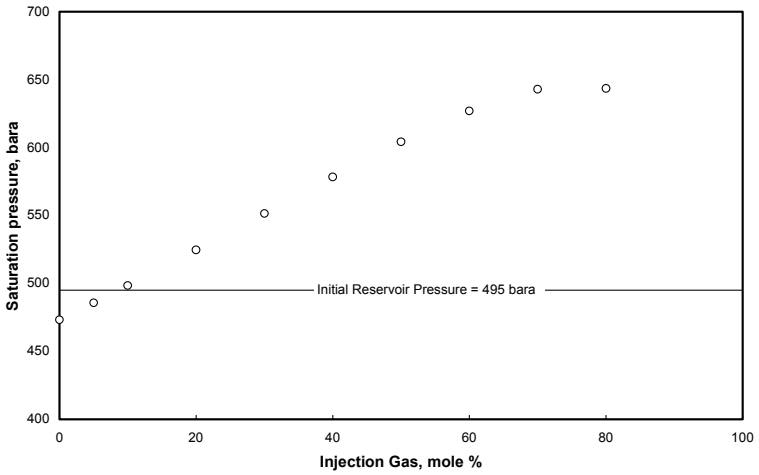

Fig. 2.36 — Injection Case – Saturation pressure variation with the amount of gas injection. The near critical fluid with lean injection gas; EOS6.

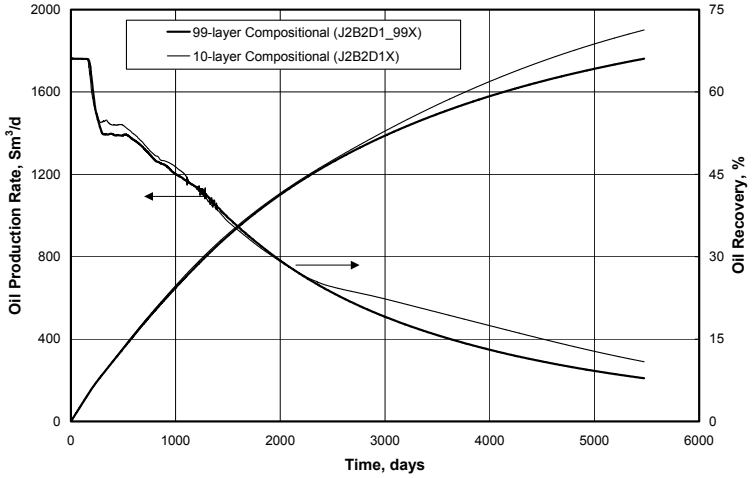

Fig. 2.37 — Injection Case – 99-layer vs. 10-layer reservoir performance for near critical fluid with constant composition; EOS6 (J2B2D1_99X.DATA, J2B2D1X.DATA).

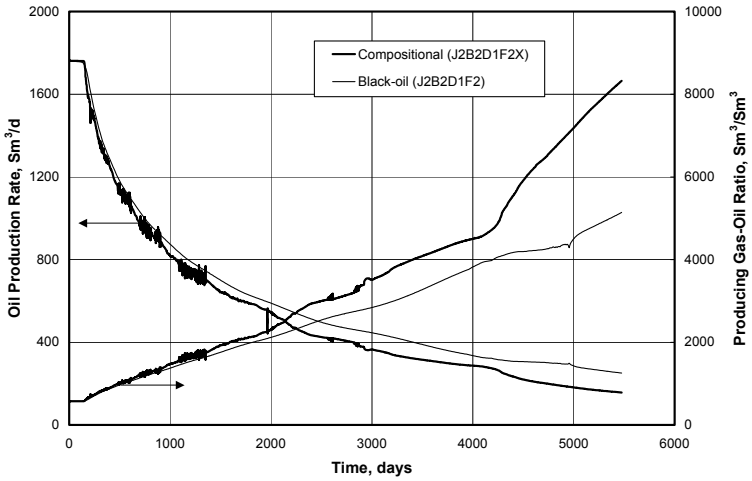

Fig. 2.38 — Injection Case – Near critical fluid with constant composition and highest permeability at the top; EOS6 (J2B2D1F2X.DATA, J2B2D1F2.DATA).

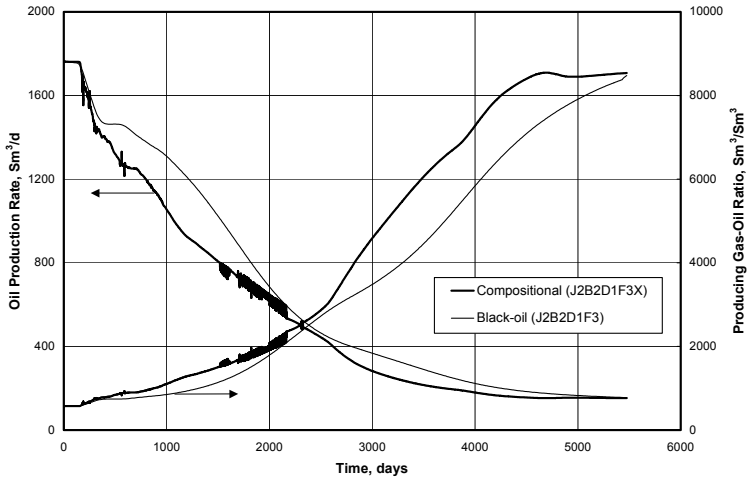

Fig. 2.39 — Injection Case – Near critical fluid with constant composition and highest permeability in the middle; EOS6 (J2B2D1F3X.DATA, J2B2D1F3.DATA).

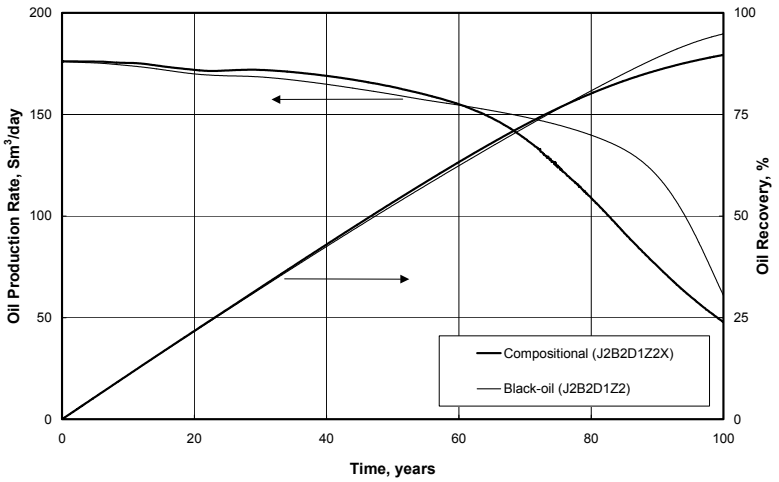

Fig. 2.40 — Injection Case – Near critical fluid with constant composition and gravity stable displacement; EOS6 (J2B2D1Z2X.DATA, J2B2D1Z2.DATA).

Oil Reservoirs with Constant Composition

Low-GOR Oil — Lean Gas Injection

The low-GOR oil sample is obtained by a simulated CCE experiment with the slightly volatile oil. The saturated oil sample is taken at 135 bara, which has a solution gas-oil ratio of 50 Sm^3/Sm^3. The swelling experiment is performed using this oil sample. The lean injection gas is injected in steps until a higher saturation pressure, equal or more than the maximum pressure expected in the reservoir (maximum BHP to the injector) is achieved. The modified black-oil PVT tables are thereafter generated using the three methods described in chapter 1. The modified oil formation volume factor is shown in **Fig. 2.41** for the different methods.

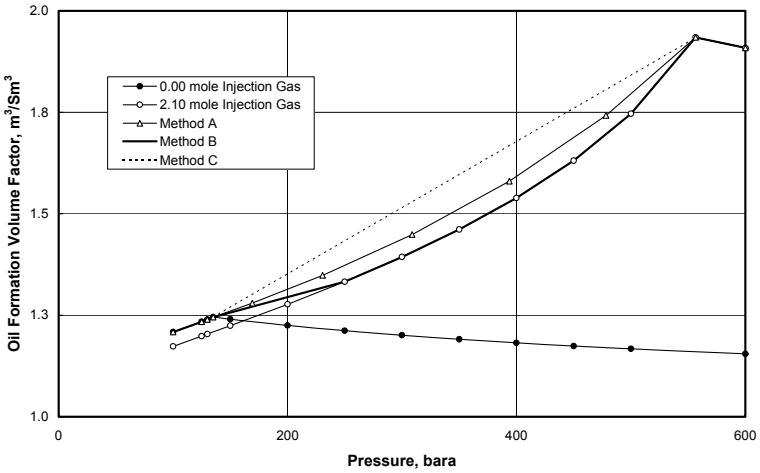

Fig. 2.41 — Modified black-oil PVT table (oil formation volume factor) for lean gas injection into low-GOR (50 Sm^3/Sm^3) oil.

Near Saturated Low-GOR Oil

The reservoir performance for the near saturated low-GOR oil is shown in **Fig. 2.42**. In this case, the reservoir pressure is 200 bara. The vaporization and swelling of the oil is treated most accurately using method B for extrapolation of black-oil PVT table in the gas injection case. The method B is conservative on swelling and initial vaporization and subsequently is closest. The difference in cumulative oil production between method B and the compositional model is 0.5 recovery-% during the simulation period of 15 years as given in **Table 2.6**. The black-oil model underpredicts the producing GOR at high producing GORs for all methods.

Highly Undersaturated Low-GOR Oil

In this case, the same low-GOR oil as in the previous case is used, but the initial reservoir pressure is increased to 500 bara from 200 bara. For highly undersaturated low-GOR oils, a black-oil model may not accurately describe the production performance as shown in **Fig. 2.43**.

In the Fig. 2.43, the performance is also shown for a case with swelling, but without vaporization, and a case with no vaporization and no swelling. The black-oil simulation case with swelling, but without vaporization has a higher oil recovery the first 15 years than the compositional model. The oil production rate during the period of 3-5 years after the start of production is up to 50% higher in the black-oil model without swelling compared to the compositional model. The reason for this is that the loss of oil recovery for "zero vaporization" is more than offset by exaggerated gravity effects caused by erroneous (too low) gas densities.

Table 2.6 — Injection Case - Production performance of Low-GOR oil reservoir (constant composition).

		AFTER 5 YEARS			AFTER 10 YEARS			AFTER 15 YEARS		
		FOPR	FGOR	RF_o	FOPR	FGOR	RF_o	FOPR	FGOR	RF_o
		Sm3/d	Sm3/Sm3	%	Sm3/d	Sm3/Sm3	%	Sm3/d	Sm3/Sm3	%
Near Saturated	**EOS6**	**2351**	**62**	**25.3**	**904**	**681**	**49.1**	**309**	**2200**	**56.2**
	Method A	**2394**	**65**	**25.9**	**1027**	**594**	**50.3**	**411**	**1661**	**59.2**
	Method B	**2210**	**79**	**25.2**	**969**	**627**	**47.9**	**424**	**1591**	**56.7**
	Method C	**2340**	**65**	**25.7**	**1063**	**521**	**51.0**	**415**	**1446**	**60.0**
Highly Undersaturated	**EOS6**	**2742**	**269**	**37.0**	**1231**	**894**	**59.4**	**461**	**2781**	**68.6**
With Swelling & vaporization	**BO6**	**2246**	**371**	**33.7**	**1202**	**920**	**55.0**	**767**	**1581**	**67.2**
With Swelling, without vaporization	**BO6**	**2489**	**307**	**40.9**	**996**	**1135**	**61.4**	**383**	**3332**	**69.7**
without swelling, without vaporization	**BO6**	**1214**	**837**	**28.2**	**604**	**1967**	**38.9**	**387**	**3238**	**45.1**

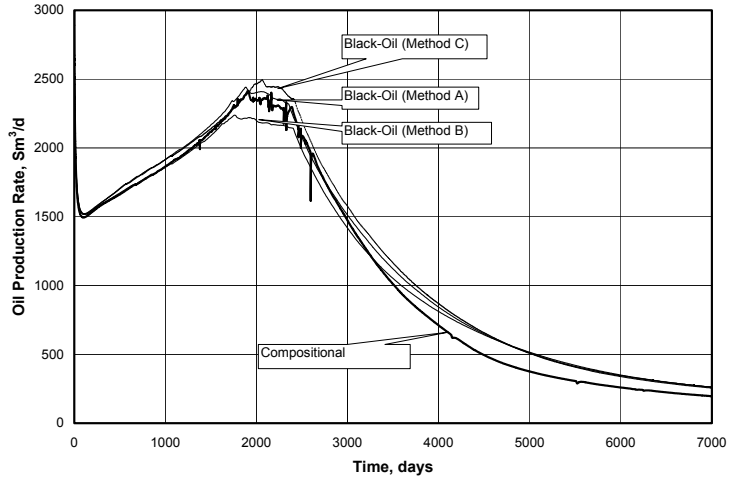

Fig. 2.42 — Injection Case – Low-GOR oil with constant composition (with and without — swelling and vaporization); EOS6 (J2B2D6T2X_200.DATA, J2B2D6T2Y2_A_200.DATA, J2B2D6T2Y2_B_200.DATA,J2B2D6T2Y2_C_200.DATA).

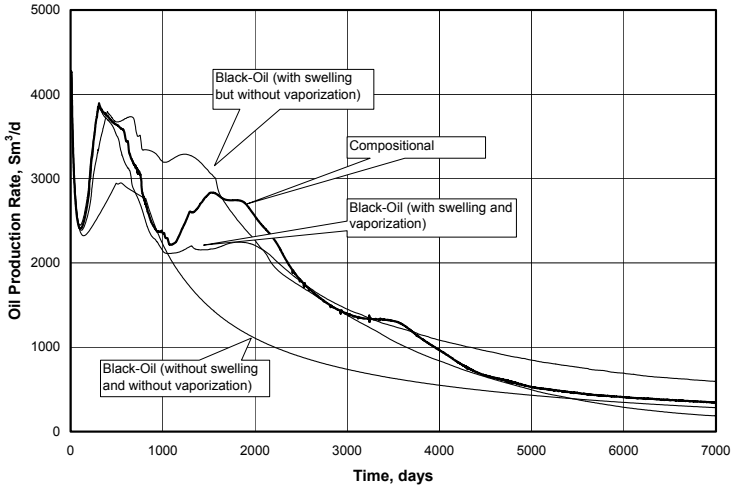

Fig. 2.43 — Injection Case – Low-GOR oil with constant composition (with and without —swelling and vaporization). Average reservoir pressure PR= 500 bara and saturation pressure Pb= 135 bara; EOS6 (J2B2D6T2X.DATA, J2B2D6T2Y2_B.DATA, J2B2D6T2Y2_B_PVDG.DATA, J2B2D6T2Y2_B_PVDG_DRSDT.DATA).

Slightly Volatile Oil (SVO) — Lean Gas Injection

The extrapolated black-oil PVT table for lean gas injection into slightly volatile oil is shown in Fig. A-31 through A-34. The production performance is shown in **Fig. 2.44** for the compositional and the black-oil models. The undersaturated oil reservoir performances are quite different in the black-oil and the compositional model (**Table 2.7**).

As shown in **Fig. 2.45**, the black-oil model performance with/without swelling but without vaporization are quite similar, but quite different from the compositional model performance. The oil plateau production period is 1.5 years in the compositional model and about 3 years in the black-oil model with no vaporization with/without swelling. The black-oil simulation run with vaporization and swelling using method (b) is quite close to the compositional model the first 5 years of production. After 5 years, the oil production is overpredicted. For this case, the results from the black-oil model (with swelling and vaporization) are about the same, independent on the different methods used to generate the modified black-oil tables.

Table 2.7 — Injection Case - Production performance of slightly volatile oil (constant composition).

		AFTER 5 YEARS			AFTER 10 YEARS			AFTER 15 YEARS		
		FOPR	FGOR	RF_o	FOPR	FGOR	RF_o	FOPR	FGOR	RF_o
		Sm3/d	Sm3/Sm3	%	Sm3/d	Sm3/Sm3	%	Sm3/d	Sm3/Sm3	%
Slightly Volatile Oil	**EOS6**	**955.2**	**1180.1**	**37.5**	**424.4**	**2891.4**	**49.6**	**276.8**	**4499**	**56.2**
	BO6	**1194.5**	**902.5**	**42.0**	**622.8**	**1888.0**	**57.5**	**509.0**	**2309**	**68.8**
J2B2D5T2X	**EOS6**	**1039**	**1107**	**37.6**	**483**	**2656**	**51.2**	**354**	**3704**	**58.9**
With Swelling & vaporization	**BO6**	**1125**	**1014**	**40.2**	**666**	**1875**	**55.8**	**552**	**2299**	**68.0**
With Swelling & without vaporization	**BO6**	**1295**	**828**	**48.2**	**252**	**5177**	**59.4**	**117**	**11471**	**62.7**
Without Swelling & without vaporization	**BO6**	**1171**	**934**	**46.9**	**253**	**5156**	**57.4**	**121**	**11052**	**60.8**

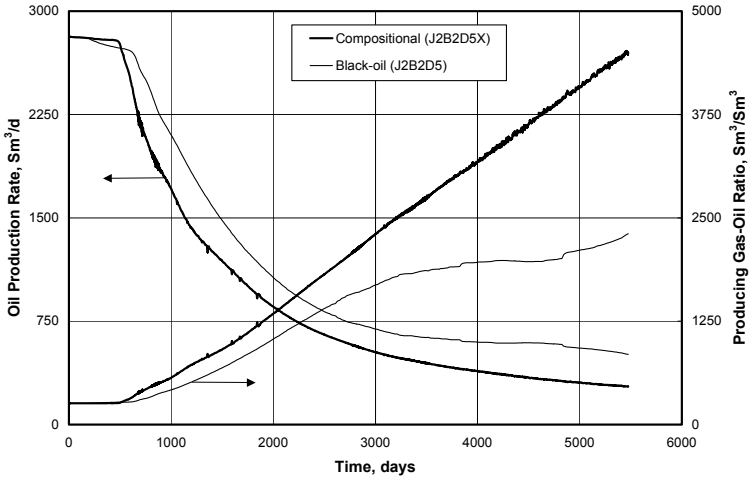

Fig. 2.44 — Injection Case – Slightly volatile oil with constant composition; EOS6 (J2B2D5X.DATA, J2B2D5.DATA).

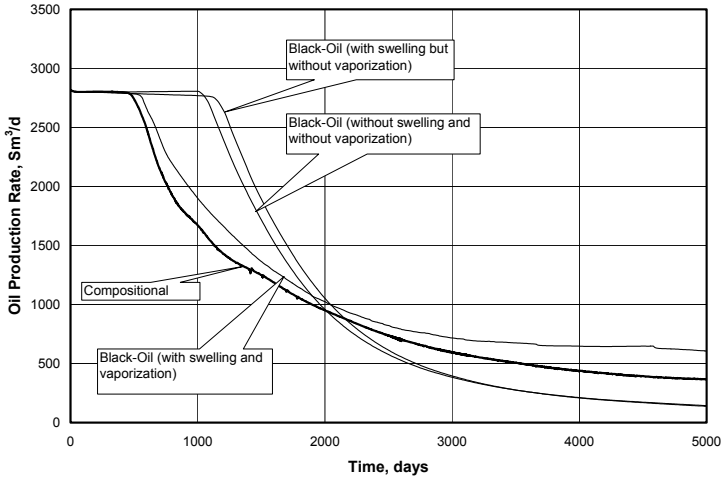

Fig. 2.45 — Injection Case – Slightly volatile oil with constant composition (with and without — swelling and vaporization); EOS6 (J2B2D5T2X.DATA, J2B2D5T2Y2_B.DATA, J2B2D5T2Y2_B_PVDG.DATA, J2B2D5T2Y2_B_PVDG_DRSDT.DATA); EOS6.

Reservoirs with Compositional Gradient and Undersaturated GOC

The reservoir performance for a compositional grading with an undersaturated GOC reservoir (GU2) is shown in **Fig. 2.46**. The oil recovery is 62.9% in the compositional model and 66.7% in the black-oil model after 15 years of gas injection.

In some cases, reservoirs with gas injection in the gas cap can be simulated with a black-oil simulator, particularly if the injectors are placed far above the original GOC. In this situation, the gas-gas displacement will be miscible. This is the case if the reservoir gas near the injector is not very rich. Furthermore, the reservoir oil will be displaced miscibly by the reservoir gas, since the GOC is undersaturated. However, in most cases, the oil production after the breakthrough of the injection gas will be too high in the black-oil model.

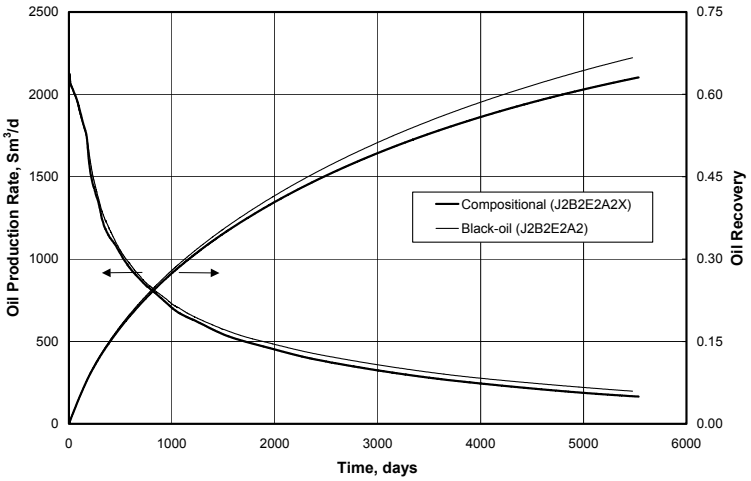

Fig. 2.46 — Injection Case – Reservoir with compositional gradient; EOS6 (J2B2E2A2X.DATA, J2B2E2A2.DATA).

2.4.3 Partial Pressure Maintenance

Undersaturated Gas Reservoir

In this case, near critical fluid is considered in the bottom geologic unit. Various amounts of produced gas is reinjected in the reservoir for partial pressure maintenance. The reservoir is simulated using the black-oil and the compositional model. The black-oil model overpredicts oil production in all cases. The performance for 100% produced gas reinjected is shown in **Fig. 2.47**. The production performance data are given in **Table 2.8**.

The comparative performance for rich gas condensate is shown in **Fig. 2.48**.

If the reservoir is produced under the depletion drive for a certain period and gas injection is started, then the difference in the black-oil and the compositional model will be even higher. The above rich gas condensate reservoir is produced for 180 days under the depletion drive followed by gas injection. The reservoir volume injection rate is equal to the reservoir volume production rate. During the first 180 days, the reservoir pressure decreases from the initial reservoir pressure of 495 bara to 435 bara. Once the gas injection is started, the reservoir pressure remains almost constant. The oil production rate for this case is shown in **Fig. 2.49**.

Table 2.8 — Injection Case - Production performance of slightly volatile oil (constant composition).

		AFTER 5 YEARS			AFTER 10 YEARS			AFTER 15 YEARS		
		FOPR	FGOR	RF_o	FOPR	FGOR	RF_o	FOPR	FGOR	RF_o
		Sm3/d	Sm3/Sm3	%	Sm3/d	Sm3/Sm3	%	Sm3/d	Sm3/Sm3	%
Near Critical Fluid	EOS6	602	1910	29.3	337	3411	43.0	246	4632	52.1
	BO6	770	1421	34.6	493	2188	53.7	331	3228	66.1
Rich Gas Condensate	EOS6	637	1830	39.7	357	3280	59.6	177	5628	72.4
	BO6	749	1509	42.8	427	2655	66.3	328	3322	83.0
Rich Gas Condensate Dep. follwed by Inj.	EOS6	641	1820	36.2	396	3019	56.9	238	5063	70.2
	BO6	782	1451	39.3	499	2350	65.1	342	3470	83.1

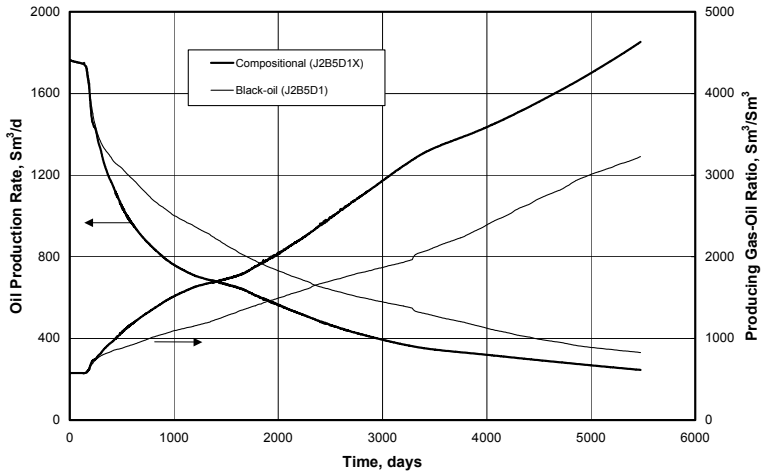

Fig. 2.47 — Injection Case – Near critical fluid with constant composition and 100% of the surface produced gas reinjected; EOS6 (J2B5D1X.DATA, J2B5D1.DATA).

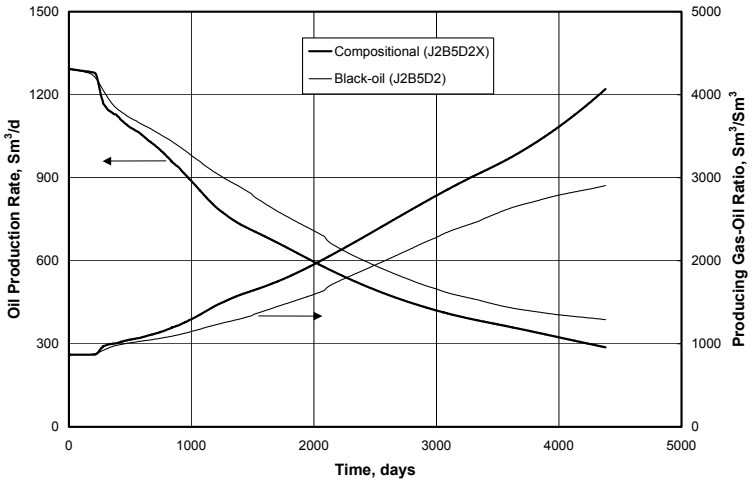

Fig. 2.48 — Injection Case – Rich gas condensate with constant composition and 100% of the surface produced gas reinjected; EOS6 (J2B5D2X.DATA, J2B5D2.DATA).

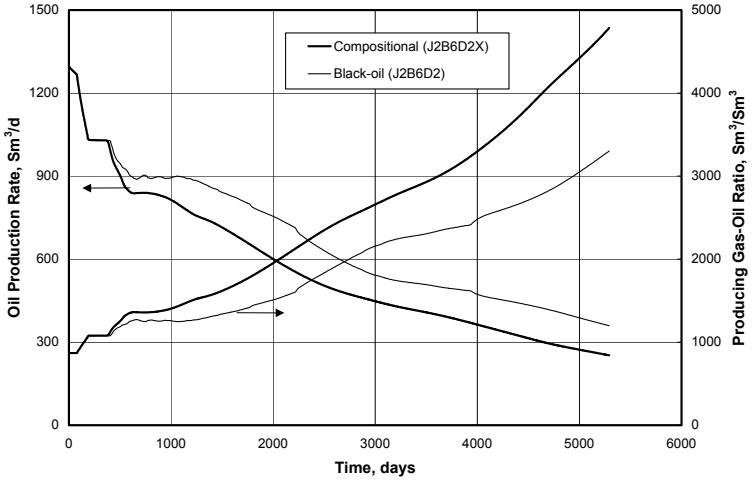

Fig. 2.49 — Injection Case – Rich gas condensate with constant composition and depletion followed by lean gas injection; EOS6 (J2B6D2X.DATA, J2B6D2.DATA).

Undersaturated Oil Reservoir

Various amounts of the produced gas have been reinjected into the top of the reservoir to simulate varying degrees of partial pressure maintenance. A volatile oil reservoir has been used for all cases. The conclusion is that the black-oil model overpredicts oil production. The performance plots for the black-oil model and the compositional model, when 100% of the surface produced gas is reinjected, are shown in **Fig. 2.50**.

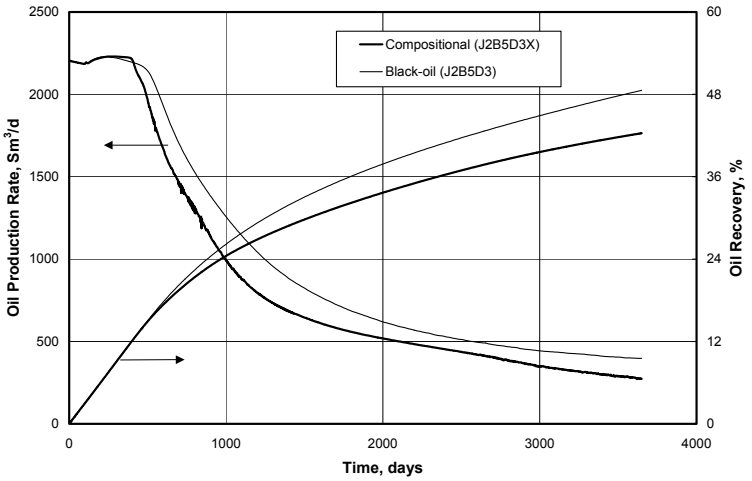

Fig. 2.50 — Injection Case – Reservoir with constant composition and 100% of the surface produced gas reinjected; EOS6 (J2B5D3X.DATA, J2B5D3.DATA).

In the case of the highest permeability at the top, the black-oil and the compositional model oil production are quite similar, but producing gas-oil ratio is too low in the black-oil model in the late production period.

Oil Reservoir with Gas Injection in the Gas Cap

The middle geologic unit (GU2) has been simulated with various amounts of produced gas being reinjected in the gas cap. The black-oil model overpredicts cumulative oil production by more than 14% (6.5 recovery-%), when 100% of the produced gas is reinjected. The performance plots are shown in **Fig. 2.51** for 80% reinjected gas case. In the case with full pressure maintenance, the displacement is miscible and the two models are much closer.

When the highest permeability is at the top, the performance for the above reservoir is as shown in **Fig. 2.52**.

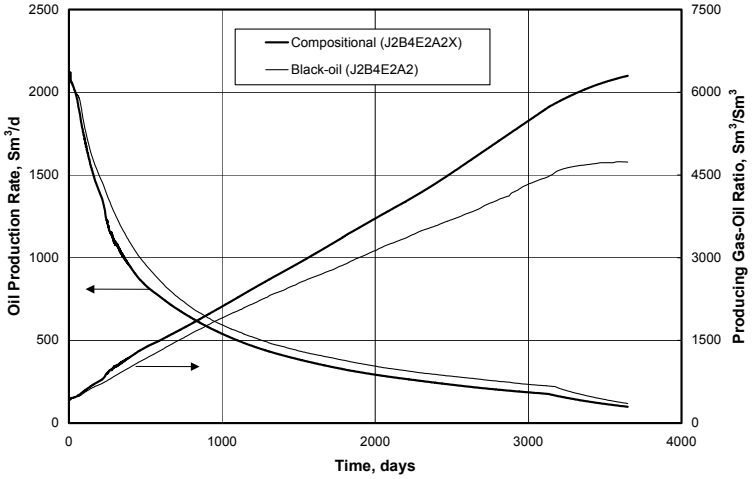

Fig. 2.51 — Injection Case – Reservoir with compositional gradient and 80% of the surface produced gas reinjected; EOS6 (J2B4E2A2X.DATA, J2B4E2A2.DATA).

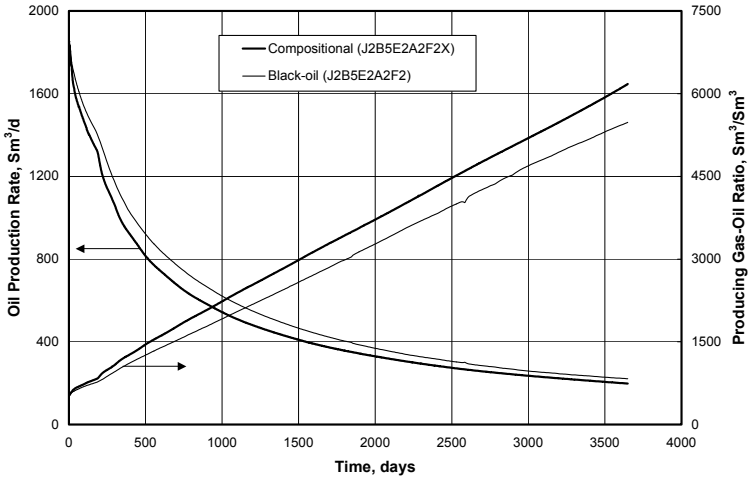

Fig. 2.52 — Injection Case – Reservoir with compositional gradient and 100% of the surface produced gas reinjected, highest permeability at the top; EOS6 (J2B5E2A2X.DATA, J2B5E2A2.DATA).

2.4.4 Summary of Gas Injection Cases

For gas cycling in gas condensate reservoirs above the dewpoint, the industry standard has been to use black-oil simulators. However, it was found in this study that in cases with a very rich gas condensate, the black-oil simulator overpredicts the oil production quite significantly due to the compositional effects, which cannot be accounted for in a black-oil model. Reservoirs with a leaner gas

condensate produced by gas cycling above dewpoint can be simulated accurately with a black-oil simulator.

For oil reservoirs, the black-oil model generally overpredicts the oil production, because the oil vaporization is overpredicted. In some cases too much vaporization causes the displacement mechanism in the reservoir to be different (usually less gravity dominated), which may lead to too low oil production.

In reservoirs where the displacement process is gravity stable, a black-oil simulator might be good enough if the oil production or producing GOR after breakthrough of injection gas is not important.

Lean gas injection in near saturated slightly volatile oil reservoirs (i.e. reservoirs with some swelling, but with minor vaporization effects) can in most cases be simulated with a black-oil simulator if the black-oil PVT tables are generated using the suggested guidelines.

Reservoirs with gas injection in the gas cap can in some cases be simulated with a black-oil simulator, especially if the injectors are placed far above the original GOC. The oil production after breakthrough of injection gas will in most cases be too high in black-oil model.

There are special options in some of the black-oil reservoir simulators to account for overprediction of vaporization and swelling. Those options require simulation results from the compositional simulators to tune the parameters needed in vaporization and swelling options. Those options have not been investigated in this study.

2.5 Conclusions

1. For numerical modeling of reservoir geologic units showing continuous permeability variation with depth (high-to-low, low-to-high, low-to-high-to-low, etc), it was found that defining "average model layers" was most accurate using equal flow capacity per layer instead of equal storage capacity (e.g. equal layer thickness).

2. A black-oil model is always adequate for simulating depletion performance of petroleum reservoirs if (a) solution GOR and solution OGR are used to initialize fluids in-place, and (b) the PVT data are generated properly, according to recommended procedures in chapter 1.

3. A compositional simulation model is generally recommended for gas injection studies.

4. For gas injection, a black-oil model can only be used in (a) oil reservoirs when there is minimal component mass transfer (e.g. insignificant vaporization) and (b) lean to medium-rich gas condensate reservoirs undergoing cycling above the dewpoint.

5. Whether a black-oil model can be used to describe a gas injection process may be strongly influenced by reservoir heterogeneities and resulting gravity-dominated flow (even in gas condensate cycling with gas-gas displacement).

6. For rich, near critical gas condensate reservoirs, with high permeability in the lowermost layers, black-oil and EOS modeling give significantly different oil recovery performances even with full-pressure maintenance gas cycling. Lean injection gas percolating upwards results in important phase behavior changes which are modeled very differently with the black-oil (miscible displacement) and EOS (severe condensation without revaporization) models.

2.6 References

1. Coats, K. H.: "Simulation of Gas Condensate Reservoir Performance," JPT (Oct. 1985) 1870.
2. Coats, K. H., Thomas, L. K., and Pierson, R. G.: "Compositional and Black-oil Reservoir Simulation," paper SPE 29111 presented at the 13th SPE Symposium on Reservoir Simulation held in San Antonio, TXD, USA, 12-15 February 1995.
3. El-Banbi, A.H., Forrest, J.K., Fan, L., and McCain, Jr., W.D.: "Producing Rich-Gas-Condensate Reservoirs — Case History and Comparison Between Compositional and Modified Black-Oil Approaches," paper SPE 58988 presented at the 2000 SPE International Petroleum Conference and Exhibition, Feb. 1-3.
4. Fevang, Ø., Singh, K., and Whitson, C.H.: "Guidelines for Choosing Compositional and Black-oil Models for Volatile Oil and Gas-Condensate Reservoirs," paper SPE 63087 presented at the 2000 Annual Technical Conference and Exhibition, Dallas, Texas, 1-4 October 2000.
5. Lake L. W.: *Enhanced Oil Recovery*, Prentice Hall, Englewood Cliffs, New Jersy 07632.
6. Mattax, C.C and Dalton, R.L.: *Reservoir Simulation*, Monograph Series, SPE, Richardson, TX (1990).
7. Fevang, Ø. and Whitson, C. H. : "Modeling Gas Condensate Well Deliverability," SPE Reservoir Engineering, (Nov. 1996) 221.

Nomenclature

B_{gd}	=	dry-gas FVF, m^3/Sm^3
B_o	=	oil FVF, m^3/Sm^3
BO	=	black-oil
EOS	=	equation of state
C_{og}	=	conversion from stock-tank condensate to equivalent surface gas
FVF	=	formation volume factor
FGOR	=	reservoir producing gas-oil ratio
FOPR	=	reservoir oil production rate
GOR	=	gas-oil ratio, Sm^3/Sm^3
h	=	thickness, m
HCPV	=	hydrocarbon pore volume, m^3
HBKF	=	highest k at the bottom (layers with equal flow capacity)
HBKS	=	highest k at the bottom (layers with equal storage capacity)
HTKF	=	highest k at the top (layers with equal flow capacity)
HTKS	=	highest k at the top (layers with equal storage capacity)
IFIP	=	initial fluid in-place, Sm^3
IGIP	=	initial gas in-place, Sm^3
IOIP	=	initial oil in-place, Sm^3
k	=	permeability, md
k_{ij}	=	binary interaction parameters between i & j
k_{rg}	=	gas relative permeability
k_{ro}	=	oil relative permeability
k_{rw}	=	water relative permeability
M	=	molecular weight
M_o	=	oil molecular weight
OGR	=	oil-gas ratio, Sm^3/Sm^3
p_b	=	bubblepoint pressure, bara
p_c	=	critical pressure, bara
p_{cow}	=	oil-water capillary pressure, bara
p_{cgo}	=	gas-oil capillary pressure, bara
p_d	=	dewpoint pressure, bara
p_R	=	reservoir pressure, bara
P	=	parachor
PV	=	pore volume, m^3
P_{sc}	=	standard condition pressure, bara or Pa
r_s	=	solution oil-gas ratio, Sm^3/Sm^3
R	=	universal gas constant
R_s	=	solution gas-oil ratio, Sm^3/Sm^3
R_v	=	solution oil-gas ratio, Sm^3/Sm^3
RF_g	=	surface gas recovery
RF_o	=	surface oil recovery

s	=	volume shift
S_L	=	liquid saturation
S_w	=	water saturation
T_c	=	critical temperature, K
T_b	=	boiling temperature at standard pressure, K
T_{sc}	=	standard condition temperature, C or K
V_c	=	critical volume
y_{7+}	=	mole fraction of C_{7+} in gas phase
z	=	compressibility or "deviation," factor
ρ_{gR}	=	reservoir gas density, kg/m^3
ρ_{gs}	=	surface gas density, kg/m^3
ρ_o	=	oil density, kg/m^3
ρ_{oR}	=	reservoir oil density, kg/m^3
ρ_{os}	=	surface oil density, kg/m^3
μ_g	=	gas viscosity, cp
μ_o	=	oil viscosity, cp
ω	=	acentric factor
ϕ	=	porosity

Appendix A

Guidelines for Choosing Compositional and Black-oil Models for Volatile Oil and Gas-Condensate Reservoirs (SPE 63087)

SPE 63087

Guidelines for Choosing Compositional and Black-Oil Models for Volatile Oil and Gas-Condensate Reservoirs

Øivind Fevang, SPE, PERA, Kameshwar Singh, SPE, NTNU, and Curtis H. Whitson, SPE, NTNU/PERA

This paper was prepared for presentation at the 2000 SPE Annual Technical Conference and Exhibition held in Dallas, Texas, 1–4 October 2000.

Abstract

This paper provides specific guidelines for choosing the PVT model, black-oil or equation of state (EOS), for full-field reservoir simulation of volatile/near-critical oil and gas condensate fluid systems produced by depletion and/or gas injection.

In the paper we have used a "generic" reservoir from the North Sea containing a fluid system with compositional grading from a medium-rich gas condensate upstructure, through an undersaturated critical mixture at the gas-oil contact, to a volatile oil downstructure.

A component pseudoization procedure is described which involves a stepwise automated regression from the original 22-component EOS. We found that a six-component pseudoized EOS model described the reservoir fluid system with good accuracy and, for the most part, this EOS model was used in the study.

Methods are proposed for generating consistent black-oil PVT tables for this complex fluid system. The methods are based on consistent initialization and accurate in-place surface gas and surface oil volumes when compared with initialization with an EOS model. We also discuss the trade-off between accurate initialization and accurate depletion performance (oil and gas recoveries).

Each "reservoir" is simulated using black-oil and compositional models for various depletion and gas injection cases. The simulated performance for the two PVT models is compared for fluid systems ranging from a medium rich gas condensate to a critical fluid, to slightly volatile oils. The initial reservoir fluid composition is either constant with depth or exhibits a vertical compositional gradient. Scenarios both with saturated and undersaturated GOC are considered. The reservoir performance for the two PVT models is also compared for different permeability distributions.

Reservoir simulation results show that the black-oil model can be used for *all* depletion cases if the black-oil PVT data are generated properly. In most gas injection cases, the black-oil model is not recommended — with only a few exceptions.

We also show that black-oil simulations using solution oil/gas ratio equal to zero (r_s=0) does not always define a *conservative* ("P10") sensitivity for gas injection processes. If gravity segregation is strong, the incremental loss of oil recovery due to "zero vaporization" is more than offset by exaggerated density differences caused by erroneous gas densities.

Introduction

Reservoir simulation is a versatile tool for reservoir engineering. Usually CPU-time is the limiting factor when the simulation model is made. The objective of this paper is to provide guidelines for choosing black-oil or compositional reservoir simulators. The paper also recommends procedures for generation of black-oil PVT tables and for initialization of black-oil and pseudoized EOS simulation models. Furthermore, a stepwise component pseudoization procedure in order to minimize the number of component when a compositional simulator is required.

Simulated production performance both for injection and depletion from black-oil and compositional are compared for a variety of reservoir fluids ranging a medium rich gas condensate to a critical fluid, to slightly volatile. Both reservoirs with constant composition and compositional grading reservoir with depth have been simulated.

Selection of Reservoir Fluid System

A fluid sample was selected from a North Sea field. The reservoir is slightly undersaturated with an initial reservoir pressure of 490 bara at the "reference" depth of 4640 m MSL. The selected reference sample contains 8.6 mol-% C_{7+}, it has a two-stage GOR of 1100 Sm^3/Sm^3 and a dewpoint of 452 bara at 163 ^oC. **Table 1** gives the reference fluid composition **(Fig. 1)**.

22-Component SRK EOS Model

The Pedersen et al. SRK[1] EOS characterization method was used to generate the "base" EOS model. Decanes-plus was split into 9 fractions using the EOS simulation program PVTsim.

The Pedersen et al[2]. viscosity correlation is known to be more accurate in viscosity predictions than the LBC[3] correlation, particularly for oils. We therefore used the Pedersen predicted viscosities as "data" to tune the LBC correlation[4] (i.e. the critical volumes of C_{7+} fractions). To cover a range of viscosities that might be expected during a gas injection project, we also generated viscosity "data" using mixtures of the reference fluid and methane, flashing the mixtures at pressures in the range 100 to 300 bara. This resulted in oil viscosities up to 7 cp, considerably higher than reservoir oil "depletion" viscosities from the reference fluid (maximum 0.5 cp).

For gas viscosities, the difference between the tuned LBC correlation and Pedersen viscosities ranged from -5 to -12%. For oil viscosities, the tuned LBC correlation predicts oil viscosities about ±15% compared with Pedersen viscosities.

The final 22-component EOS/LBC model is given in **Table 2**.

Isothermal Gradient Calculation

Based on isothermal gradient calculations[5] using the "base" 22-component SRK EOS model the reservoir fluids vary from medium rich gas condensate to highly-volatile oil in the depth interval from 4500 to 5000 m MSL, with GORs ranging from 1515 to 244 Sm^3/Sm^3, C_{7+} content ranging from 6.9 to 22 mol-%, dewpoints ranging from 428 to 473 (maximum), and bubblepoints pressure ranging from 473 to 435 bara (**Table 3**). The reservoir pressure varies from 485 bara at the top to 509 bara at the bottom. At the GOC, reservoir pressure is 495 bara and (critical) saturation pressure is 473 bara — i.e. the reservoir is undersaturated by 22 bar at the GOC. Variations in C_{7+} and saturation pressure are shown in **Fig. 2**.

Selection of Different Fluid Samples

In this study we used different fluid systems for a given "reservoir", all originating from the compositional gradient calculation using the 22-component EOS model. The fluid systems are:

1. Compositional gradient throughout the entire reservoir, from undersaturated gas-condensate at the top to a lower-GOR volatile oil at the bottom; middle geologic unit.
2. Only the grading gas condensate fluids above the GOC (i.e. remove the underlying oil); top geologic unit.
3. Only the grading oil below the GOC (i.e. remove the overlying gas); bottom geologic unit.
4. A gas condensate, initially undersaturated, is taken from a specified depth in the reservoir. This gas condensate fluid is assumed to have constant composition with depth.
5. A relatively-low GOR volatile oil taken at a specified depth in the reservoir. This oil is assumed to have constant composition with depth.
6. A low-GOR oil was "constructed" from the oil at 250 m below the GOC, where this oil was further flashed to a pressure of 135 bara with a resulting GOR of 50 Sm^3/Sm^3.

For fluid systems (4) and (5) above, several fluids were selected at depths 250, 50 and 10 m above and below the GOC, as well as the GOC composition. In this way, seven "samples" were used from the single compositional gradient calculation (Fig. 2).

Pseudoization – Reducing Number of Components

Because it is impractical to conduct full-field and large-sector model simulations using the 22-component EOS model (due to CPU and memory limitations), several "pseudoized" or reduced-component EOS models were developed – EOS models with 19-, 12-, 10-, 9-, 6-, 4-, and 3 components.

The pseudoization procedure is summarized below:

1. Using the original (22-component) EOS model, simulate a set of PVT experiments which cover a wide range of pressures and compositions expected in the recovery processes used to produce a reservoir.
2. PVT experiments included constant composition tests, depletion-type experiments (differential liberation and constant volume depletion), separator tests, and multicontact gas injection (swelling) tests. Two quite-different injection gases (**Table 4**) were used for the swelling test simulations.
3. The simulated PVT properties were used as "data" for the step-wise pseudoizations.
4. At each step in pseudoization, new pseudocomponents were formed from existing components. Regression was used to fine tune the newly-formed pseudo-component EOS parameters and a select number of BIPs.
5. Step 4 was repeated a number of times, trying (manually) to select the best grouping at each stage in the pseudoization process.

The procedure allows the determination of which components are best to group, and at what point during pseudoization that the quality of EOS predictions deteriorate beyond what is acceptable for engineering calculations.

Generating the 22-Component EOS PVT "Data"

The 22-component EOS model was first used to generate a large set of PVT data. A total of eight feeds (one reference sample and seven generated from the compositional gradient calculation; four gas samples, one near-critical sample, and three oil samples) were used for generating PVT data. Depletion-type PVT tests and separator tests were used, together with swelling-type tests for several injection gases. All calculated PVT results using these feeds were treated as "data" for pseudoization.

A total of 8 CCE-, 8 SEP-, 5 CVD-, 8 DLE- and 8 MCV experiments were used for generating the "data" for pseudoization.

Stepwise Pseudoization

First, a 19-component EOS model was obtained after grouping C_1+N_2, i-C_4+n-C_4, and i-C_5+n-C_5.

The regression parameters for PVT fits were EOS constants A and B of the newly-formed pseudo-components and (collectively) the binary interaction parameters between C_1 and C_{7+}. All simulated tests were used for the PVT fit. For viscosity fits (at each stage in the pseudoization process), only DLE and MCV viscosity data were used in regression. Viscosity regression parameters were the critical volumes of the newly-formed pseudocomponents.

PVT properties of the 19-component EOS model matched the 22-component EOS model almost exactly.

The 12-component EOS model was obtained by grouping the original eleven C_{7+} fractions into 5 fractions on the basis of (more-or-less) equal mass fraction of the C_{7+} fractions. The heaviest component was kept as the original fraction and other C_{7+} components were grouped into 4 pseudo-components. Regression was performed again, where we found that the 12-component EOS model predicts PVT properties very similar to the 22-component EOS model.

The 10-component EOS Model was obtained after reducing C_{7+} fractions from 5 to 3 fractions based on equal mass fraction of the C_{7+} fractions. Regression was performed and the 10-component EOS model predicts PVT properties which are comparable with the 22-component EOS model.

In the 9-component EOS model, C_2 and CO_2 were grouped together. There is little change from the 10-component EOS.

Further grouping was done in steps. In each step, one component was grouped with another suitable component and properties were compared with the 22-component EOS model (after regression). From the 9-component EOS model we grouped to 8-, 7-, and finally 6 components. Based on our previous experience, it has been found that it is usually necessary to have 3 C_{7+} fractions. Our final 6-component EOS model contained 3 C_{7+} components and 3 C_{6-} components: (N_2,C_1), (CO_2,C_2), (C_3-C_6), (C_7-F2), (F3-8), F9, given in **Table 5**.

From the 6-component EOS model, another series of grouping was conducted. The 4-component EOS model contained only 2 C_{7+} fractions, where a reasonable match was obtained for most PVT properties. However, from the 4-component model to the 3-component model, PVT properties deteriorated significantly. The deviation in most of the PVT properties was large using the 3-component EOS.

The 22-component EOS model versus the 6-component EOS model PVT properties are shown in **Figs. 3** and **4.**

As an independent check on the validity of the pseudoized EOS models, we used depletion recovery factors calculated from CVD tests as a verification of how accurate the pseudoized models maintained surface oil and surface gas recoveries when compared with the original EOS22 model. CVD data are used to compute surface oil and gas recoveries[6] at different pressures (based on simplified surface flash). The difference in oil recoveries is shown in **Figs. 5** and **6**. When deviation in condensate *recovery* is used for comparison (Fig.5) the leanest upstructure gas at 4500 m shows the largest difference between EOS6 and EOS22. However, in terms of *reserves*, Fig. 6 shows that the largest error is in the richest downstructure gas at 4750 m, where a "typical" North Sea HCPV has been used to convert recovery factors to reserves.

Black-Oil PVT Properties

In the black-oil model, the PVT system consists of two reservoir phases – oil (o) and gas (g) – and two surface components – surface oil ($\bar{o}$) and surface gas ($\bar{g}$). The equilibrium calculations in a black-oil model are made using the solution gas-oil and solution oil-gas ratios R_s and r_s, respectively, where surface "component K-values" can be readily expressed in terms of R_s and r_s.

Black-oil PVT properties have been generated in this study with an EOS model using the Whitson-Torp procedure[7]. In this approach, a depletion-type experiment is simulated – either a CCE, CVD, or DLE test. At each step in the depletion test, the equilibrium oil and equilibrium gas are taken separately through a surface separation process. The surface oil and surface gas products from the reservoir oil phase are used to define the oil FVF B_o and the solution GOR R_s. The surface oil and surface gas products from the reservoir gas phase are used to define the "dry" gas FVF B_{gd} and the solution OGR r_s.

It is also necessary to choose a single set of *constant* surface gas and surface oil densities used to calculate reservoir densities (together with pressure-dependent properties R_s, B_o, r_s, and B_{gd}). Proper selection of surface "component" densities can ensure improved accuracy in black-oil reservoir density calculations.

For saturated reservoirs initially containing both reservoir oil and reservoir gas, the black-oil PVT properties may differ in the "gas cap" and "oil zone" regions. Consistent treatment of this problem may be important. The best approach is to perform a depletion test on the initial reservoir gas alone, retaining only the r_s, μ_g, and B_{gd} properties, and separately performing a depletion test on the initial reservoir oil alone, retaining only the R_s, μ_o, and B_o properties.

A special problem involves generating black-oil PVT properties for gas injection studies in an undersaturated oil reservoir. This involves extrapolation of the saturated oil PVT properties, sometimes far beyond the initial bubblepoint pressure. Several methods can be used for generating the extrapolated saturated BO PVT tables, but we have found one which seems consistently better.

Reservoir Simulation – Initialization

To obtain correct and consistent initial fluids in place (IFIP) for black-oil and compositional models it is important to initialize the models properly. This involves proper treatment

of (1) fluid contacts and phase definitions, (2) PVT models, (3) compositional (solution-GOR) gradients, and (4) the relative importance of IFIP versus ultimate recoveries for the relevant recovery mechanisms.

Initializing EOS Models

The reservoir was initialized with the 6-component EOS model[8] and initial fluids in place were compared with that of the 22-component EOS model. Three different initialization methods with the 6-component EOS model were used:

1. Method A – starting with the reference feed, the 6-component EOS model was used to make an isothermal gradient calculation, providing a compositional gradient based on the 6-component EOS model. In this method, the calculated GOC was somewhat different than with the 22-component EOS model.
2. Method B – starting with the reference feed, use the 6-component EOS model for isothermal gradient calculation and adjust the reservoir pressure at the reference depth such that the calculated GOC equaled the GOC from the 22-component model. The resulting compositional gradient using the 6-component EOS model was then used in the reservoir simulation model, but with the correct reservoir pressure at reference depth.
3. Method C - use the 22-component EOS model for the gradient calculation, and then manually pseudoize to obtain the 6-component compositional gradient.

The C_{7+} compositional variation with depth for the above three methods is shown in **Fig. 7**. Method C gives the most correct reservoir fluid compositional gradient (when compared with the 22-component initialization). The initial fluids in place calculated with the different methods are given in **Table 6**.

Method C is recommended *in general* for initializing pseudoized EOS models. This assumes, however, that the saturation pressure gradient and key PVT properties are similar for the full-EOS and pseudoized-EOS models; differences in saturation pressures (**Fig. 8**) and PVT properties will potentially have an impact on recoveries. With our pseudoization procedure these differences were minimized and make method C the recommended procedure.

Initializing Black-Oil Models

For obtaining accurate initial fluids in place and description of reservoir recovery processes, black-oil PVT tables and "compositional gradients" must be selected carefully.

The compositional gradient in a black-oil model is given by the depth variation of solution GOR (R_s) in the oil zone and the solution OGR (r_s) in the gas zone. The use of solution GOR and OGR versus depth – *instead of saturation pressure versus depth* – is important for minimizing "errors" in initial fluids in place.

The choice of how to generate a *proper* black-oil PVT table includes the following issues:

1. Whether the purpose is (a) to describe accurately the actual reservoir PVT behavior or (b) for the purpose of comparing black-oil with compositional simulation results.
2. Treatment of compositional gradients, and whether the reservoir has a saturated gas-oil contact or an undersaturated "critical" gas-oil contact.
3. Extrapolation of saturated PVT properties to pressures higher than the maximum saturation pressure found initially in the reservoir.
4. Choice of the surface gas and surface oil densities to minimize the "errors" in reservoir gas and reservoir oil densities calculated from the black-oil PVT tables — used to compute the vertical flow potential for (a) static initialization and (b) dynamic flow calculations.

In this study a single reference fluid had been obtained by sampling in the gas cap. This sample, based on the isothermal gradient calculation with the EOS22 and EOS6 models, indicated a fluid system with compositional grading through a critical (undersaturated) gas-oil contact.

It was necessary to extrapolate the black-oil PVT properties at least to the maximum saturation pressure of the critical mixture at the gas-oil contact. Three methods of extrapolation were studied, all based on the EOS6 model:

1. Adding incipient (oil) phase composition to the reference sample until the saturation pressure reached the GOC saturation pressure.
2. Adding the GOC composition from the gradient calculation to the reference sample until the saturation pressure reached the GOC maximum value.
3. Using the GOC composition itself.

For each method, a composition with a saturation pressure equal to the GOC critical fluid saturation pressure was obtained. This composition was then used to generate the black-oil PVT tables using a constant composition expansion experiment (with separator tests conducted separately for each equilibrium phase during the depletion).

To initialize the black-oil model[9], we first chose a solution GOR&OGR versus depth relation. From the discussions in the previous section, Methods A, B, and C were used for generating compositional variation with depth for the 6-component EOS model. From the compositional gradient with depth, each of the three methods also generated a solution GOR&OGR versus depth relation. When comparing black-oil initialization using the three methods A, B, and C combined with the three methods for generating black-oil PVT properties (1, 2, and 3 above), we found that Method C always gave more accurate and consistent initial fluids in place; by consistent we mean that the method provided a more accurate estimation of the 22-component EOS initialization. The most accurate and consistent IFIP in the black-oil model was achieved using Method C for solution GOR versus depth together with Method 3 for generating the black-oil PVT tables.

The comparative (EOS22 vs. EOS6 and EOS6 vs. BO6) initial fluids in place are given in Table 6.

The most important aspect of initializing a black-oil model for a reservoir with compositional gradients is the proper use of solution OGR and solution GOR versus depth. These two black-oil PVT properties represent in fact *composition* and should, accordingly, be used to initialize the reservoir model. It would not make sense, for example, to initialize a compositional simulator with saturation pressure versus depth, and it is equally "illogical" in a black-oil model – with the added disadvantage that the resulting initial fluids in place can be very wrong.

Because a single PVT table is often used in a black-oil model, and particularly for reservoirs with an undersaturated critical GOC, we know that the resulting PVT pressure dependence of fluids throughout the column are not represented exactly. Fluid at each depth has its "own" set of black-oil PVT tables — i.e. the pressure dependence of PVT properties is somewhat different for fluids at different depths. This is shown in **Figs. 9** and **10**. Initializing with solution GOR versus depth is accurate because the variation in oil formation volume factor with solution gas-oil ratio is similar for the different fluids, as shown in **Fig. 11**.

Despite an initialization of composition with depth in a black-oil model, where solution OGR and solution GOR are taken directly from the compositional EOS model, we know that the saturation pressure versus depth will not be represented properly in the black-oil model. This "error" in saturation pressure versus depth has practically no effect on initial fluids in place, but it does have a potential effect on depletion recoveries. Figs. 9 and 10 show the magnitude of error in saturation pressure found in the black-oil model initialized based on correct solution OGR and solution GOR versus depth.

Our experience shows that the error in saturation pressure versus depth usually has little impact on production performance and ultimate recoveries. It may have a short-lived effect on recovery (rates) versus time as the reservoir depletes below the initial saturation pressures; ultimate recoveries are not usually affected noticeably.

Reservoir Simulation Examples

Basic Reservoir and Model Data. The basic reservoir and fluid properties are given in **Table 7**. The relative permeabilities are shown in **Fig. 12**.

The generic reservoir simulation model contains three geological units. The thickness of each unit is 50 meters. Each geological unit generally has ten numerical layers and each layer has a constant permeability. The heterogeneity of each geological unit is described by a Dykstra-Parsons coefficient of 0.75. The average permeability in each geological unit is 5, 50, and 200 md (top, middle and bottom). The reservoir has a dip of 3.8 degrees.

The base numerical model for one geological unit has 50x10x10 grid cells. The base case has a vertical producer, which is located downdip in cell (50,10) and is perforated in all layers. The producer is controlled by a reservoir volume rate of 10% hydrocarbon pore volume per year.

Nomenclature and a short description of all the simulation cases discussed in this paper are given in **Table 8** and **9.**

Full EOS versus Pseudoized EOS

Simulation cases with depletion and with gas injection were simulated with the full 22-component and the 6-component fluid characterization to verify that the 6-component characterization accurately describes production performance. The near-critical fluid with constant composition was selected for depletion performance. The depletion performance of the two EOS models are very similar as shown in **Figs. 13** and **14**. We selected the near-critical fluid with lean gas injection for the injection case. The production performance was very close, as shown in **Figs**. **15** and **16.** We have used 6-component EOS model for all subsequent simulation cases.

BOvsEOS Reservoir Simulation — Depletion

This section compares simulation results from a black-oil model with a compositional model[10-13] for different depletion cases. Simulated production performance for the two models are compared for fluid systems ranging from a medium rich gas condensate, to a critical fluid, to slightly volatile oils. The initial reservoir fluid composition is either constant with depth or shows a vertical compositional gradient. Scenarios both with saturated and undersaturated GOC are studied. Permeability increases downwards in most cases to maximize the effect of gravity and mixing of the reservoir fluids. Sensitivities have also been run with different permeability distributions.

Table 8 gives a summary of the performance of all the depletion cases we ran in this study. Only a few of the simulation cases are discussed here (marked in bold). Data sets for all cases are available upon request.

The simulated field oil production from black-oil model runs did not deviate more than one recovery-% from the compositional results during the ten-year production period in any case. In most cases the deviation was less then 0.25 recovery-%. The difference in gas recovery was negligible in all cases. The producing GOR is generally quite accurate during most of the ten-year production period. However, in a few cases, the producing GOR started to deviate somewhat after about five years of production and after ten years of production the GOR was up to 10% lower in the black-oil model. It should be noted that in the case of a reservoir with a large compositional gradient, the producers high on the structure will generally have a producing GOR in the black-oil model somewhat (5-10%) too low. However, if the main part of the oil production comes from downdip wells then the overall field oil production will be accurately predicted by the black-oil model.

Reservoirs with an Undersaturated GOC. The black-oil PVT tables should be generated by simulating a CCE experiment using the critical GOC fluid. In Eclipse 100, the black-oil PVT table needs to be manually extrapolated to a

saturation pressure higher than the initial reservoir pressure at GOC.

Black-oil PVT data for fluids with a saturation pressure 30-50 bar from the critical point may cause convergence problems. This is due to the highly non-linear PVT behavior near the critical point. Fortunately, these near-critical data can be deleted from the black-oil PVT tables without changing the production performance.

In this paper we show the production performance for three different cases:

1. A near-critical fluid with constant composition (**Figs. 17** and **18)**.
2. A near-critical fluid with compositional gradient (**Figs. 19** and **20)**.
3. Volatile oil with constant composition with highest permeability at the top **(Figs. 21** and **22)**.

Reservoirs with a Saturated GOC. In the following cases the black-oil PVT tables have been generated from a simulated DLE experiment with the GOC oil for the reservoir oil. The reservoir gas PVT table has been generated from a simulated CVD experiment with the GOC gas. When significant gravity segregation is expected, the surface-gas and surface-oil densities should be modified such that the reservoir-oil and reservoir-gas densities are accurate throughout depletion.

The simulated field production performance was very similar for both models for all the cases shown in Table 8.

Only one simulation case showed some difference between the black-oil and the compositional model. In this case, there were three wells completed at different locations structurally - high, middle and low. All the wells were completed throughout the reservoir (i.e. 10 numerical layers). For the structurally high wells the performance was different in the two models (**Figs**. **23** and **24**). The structurally-high well produced with a too-low GOR below the "saturation pressure" in the black-oil simulation compared to the compositional model. The difference in producing GOR is due to an error in saturation pressures in the black-oil simulation as discussed earlier and demonstrated in Fig. 9. Even though the individual wells showed some performance differences, the overall 3-well total performance is very similar as shown in **Figs. 25** and **26**.

BOvsEOS Reservoir Simulation — Gas Injection

This section compares simulation results between an EOS simulator and a black-oil simulator for many cases with gas injection. We have tried to examine if any general guidelines can be found when a black-oil model can be used to simulate gas injection. We found it difficult to come up with general rules, though some guidelines are given. Summaries with "key" production data for all of the simulation runs are reported in **Table 9**. A few cases are discussed below.

Full Pressure Maintenance

Gas Condensate Reservoirs with Constant Composition. For gas cycling in gas condensate reservoirs above the dew point, Coats[10] showed that black-oil simulators can be used. **Figs. 27** and **28** show the performance of a reservoir with a medium rich gas condensate with constant composition. The oil recovery after 15 years of production is 82.4% in the compositional model and 84.2% in black-oil model. Note the effect of gravity in this case is small.

Most of our simulation results support the conclusion by Coats[10] that gas condensate reservoirs produced by gas cycling above the original dewpoint can be simulated accurately with a black-oil simulator.

However, we found in some cases with (1) a rich gas condensate and (2) increasing permeability downwards, that a black-oil simulator significantly overpredicts oil recovery due to compositional effects that are not properly treated in a black-oil model. This is shown in **Figs. 29** and **30**, where oil recovery after 15 years is 71.3% in the compositional model and 88.7% in the black-oil model; the difference in oil recovery is less for high permeability at the top (50% versus 56% oil recovery).

A black-oil simulator may be adequate in reservoirs where the displacement process is gravity stable or where the effect of gravity is negligible.

Oil Reservoir with Constant Composition. A black-oil model may over-predict oil production for high-pressure gas injection because oil vaporization is over-estimated. Lean gas injection in reservoirs with some swelling but with minor vaporization effects can in most cases be simulated with a black-oil simulator if the black-oil PVT tables are generated using the guidelines outlined below.

Black-oil PVT tables used in injection processes are made by splicing the black-oil PVT tables for the original reservoir oil and the swollen oil. Black-oil PVT data for the swollen oil is generated using a multi-contact swelling experiment. The injection gas is added to the original oil sample in steps until the saturation pressure of the swollen oil is somewhat higher than the maximum (injection) pressure.

The modified black-oil PVT tables (both oil and gas) used in the simulation model can be generated using three different approaches:

A. Original BO PVT table + incremental swollen oil properties from the original bubblepoint to the highest pressure.
B. Original PVT table + depletion of the fully-swollen oil to the saturation pressure of the original oil.
C. Original PVT table + one additional data at the fully-swollen saturation point.

The modified black-oil PVT data for the different approaches are shown in **Figs. 31** through **34** for lean gas injection into a slightly volatile oil.

The reservoir performance for a near-saturated low-pressure reservoir (P_R= 200 bara and P_b= 135 bara) with low-GOR oil is shown in **Figs. 35** and **36**. The difference in cumulative oil production between method B and the compositional model is less than 2 recovery-% during

simulation period (20 years). However the black-oil model under predicts the producing GOR at high producing GORs for all methods. The difference between the three methods are generally small as shown in this case. However, based on experience method B seems to be consistently better.

For highly-undersaturated low-GOR oils a black-oil model does not accurately describe the production performance as shown in **Figs. 37** and **38.** In this case the same low-GOR oil as in the previous case was used but the initial reservoir pressure was increased to 500 bara.

In Figs. 37 and 38, the performance is also shown for a case with swelling but without vaporization, and a case with no vaporization and no swelling. The black-oil simulation case with swelling but without vaporization has a higher oil recovery the first 15 years than the compositional model. The oil production rate in the period 3-5 years after start of production is up to 50% higher in the black-oil model without swelling compared to the compositional model. The reason for this is that the loss of oil recovery for "zero vaporization" is more than offset by exaggerated gravity effects caused by too-low gas densities; $\Delta\rho_{og}$ is too high.

The production performance is also compared for black-oil and compositional simulations for a slightly volatile oil. The black-oil PVT properties for the slightly volatile oil are shown in Figs. 31 through 34. The simulated production performance curves are shown in **Figs. 39** and **40.** In this case the black-oil simulation run with swelling but with no vaporization and the black-oil simulation with no swelling and with no vaporization are quite similar, but quite different from the compositional model. The oil plateau production period is 1.5 years in the compositional model and about 3 years in the black-oil models with no vaporization with/without swelling. The black-oil simulation run with vaporization and swelling using method B is quite close to the compositional model the first 5 years of production. After 5 years the oil production is over predicted. For this case the results from the black-oil model (with swelling and vaporization) were about the same, independent on the different methods used to generate the modified black-oil tables (Table 9).

Reservoirs with Compositional Gradient and Undersaturated GOC. In some cases, reservoirs with gas injection in the gas cap can be simulated with a black-oil simulator, particularly if the injectors are placed far above the original GOC. An example is the reservoir performance for a reservoir with compositional grading and an undersaturated GOC is shown in **Figs. 41** and **42**. In this situation, the gas-gas displacement will be miscible (if the reservoir gas near the injector is not very rich). Furthermore, the reservoir oil will be displaced miscibly by the reservoir gas since the GOC is undersaturated. However, in most cases, oil production after gas breakthrough will be too high in the black-oil model.

Partial Pressure Maintenance

Undersaturated Oil Reservoir. Various amounts of the produced gas have been reinjected into the top of the reservoir to simulate varying degrees of partial pressure maintenance (Table 9). A volatile oil reservoir has been used for all cases. The conclusion is that the black-oil model consistently over predicts oil production due to excess vaporization.

Oil Reservoir with Gas Injection in the Gas Cap. The reservoir with compositional grading has been simulated with various amounts of produced gas being reinjected (Table 9) in the gas cap. The black-oil simulator over-predicts cumulative oil production by more than 14% (6.5 recovery-%) when 100% of the produced gas is reinjected. The performance plots are shown in **Figs. 43** and **44**. Note that for full pressure maintenance, the displacement is miscible and the two simulators are much closer (Figs. 41 and 42).

Recommended Procedures

Black-Oil PVT Properties — Depletion

Independent of the type of reservoir fluid, we have found that it is important to include undersaturated properties for fluids with different saturation pressures – not only the fluid with the highest saturation pressure.

Whether the black-oil PVT tables should be calculated using the full- or the pseudoized EOS depends on the purpose of the black-oil simulation. When the purpose is to compare black-oil with compositional simulation results we recommend generating the black-oil PVT tables with the same EOS model used for the compositional simulations. If accuracy in PVT is desired, black-oil properties should be generated with the full EOS. If the procedures outlined in this paper are used to pseudoize, the difference in inplace volumes between the full- and the pseudoized EOS should be small (<1% of IFIP).

Undersaturated Oil Reservoirs. For undersaturated oil reservoirs, the black-oil PVT tables are made by simulating a CCE experiment using the fluid with the highest solution GOR. Make sure undersaturated PVT properties are calculated up to maximum initial reservoir pressure; at least for Eclipse 100.

Undersaturated Gas Reservoirs. For undersaturated gas reservoirs, the black-oil PVT tables are made by simulating a CCE experiment using the fluid with the highest solution OGR. Make sure undersaturated PVT properties are calculated up to maximum initial reservoir pressure.

Saturated GOC. For reservoirs with a saturated GOC, the black-oil gas PVT table is made simulating a CVD experiment with the GOC equilibrium gas. The oil PVT table is made by simulating a DLE experiment with the GOC equilibrium oil. It is also necessary to choose a single set of constant surface gas and surface oil densities used to calculate reservoir densities (together with R_s, B_o, r_s, and B_{gd}). We recommend using surface oil and surface gas densities which give correct reservoir oil and reservoir gas densities at the GOC. The equations to calculate surface oil and gas densities are:

$$\rho_{os} = \frac{\rho_{oR} B_o - R_s \rho_{gR} B_{gd}}{1 - r_s R_s} \quad \text{.....(1)}$$

$$\rho_{gs} = \frac{\rho_{gR} B_{gd} - r_s \rho_{oR} B_o}{1 - r_s R_s} \quad \text{.....(2)}$$

Undersaturated GOC. For reservoirs with an undersaturated GOC the black-oil PVT tables are made by simulating a CCE experiment with the GOC critical fluid. Some of the nearest-to-critical-pressure data may need to be omitted if $|d(R_s)/dp|$ or $|d(r_s)/dp|$ is too large.

For reservoir simulators that do not support an undersaturated GOC, a "fictitious" saturated GOC has to be introduced. This requires using a "fictitious" saturation pressure for the critical fluid that is slightly higher than the initial reservoir pressure at the undersaturated GOC. Changing the saturation pressure of the fluids near the undersaturated GOC the second pressure point with saturated properties should be at a pressure just slightly (0.1-1.0 bar) lower than the saturation pressure of the critical fluid.

Black-Oil PVT Properties — Gas-Injection. For undersaturated oil reservoirs undergoing gas injection the injection pressure will be higher than the saturation pressure of the highest-bubblepoint oil in the reservoir. In such cases the black-oil PVT table has to be extended to include saturated oil and gas properties up to maximum pressure in the reservoir during gas injection (usually this is the maximum injection pressure). The black-oil PVT data for the swollen oil and equilibrium gas should be generated using a single-point swelling experiment. The injection gas is added to the highest-original-bubblepoint reservoir oil sample until the saturation pressure is somewhat higher than the maximum injection/reservoir pressure. The fully-swollen oil is depleted in several steps using a CCE test down to the highest-original-bubblepoint. The black-oil PVT properties from the swollen oil are then "spliced" to the PVT tables from the original oil. This procedure has always been the most accurate.

Initializing EOS Models. In most cases a full-field reservoir model uses an EOS with a reduced number of components compared to the EOS model used to develop the initial fluid characterization. The most accurate method to initialize a reservoir in such a case is to manually pseudoize the gradient calculated with the full EOS to obtain the component compositional gradient for the reduced EOS. This assumes, however, that the saturation pressure gradient and key PVT properties are similar for the full-EOS and pseudoized-EOS models.

Initializing Black-Oil Models. The compositional gradient in a black-oil model is given by variation of solution GOR (R_s) in the oil zone and the solution OGR (r_s) in the gas zone. This will lead to consistent inplace oil and gas volumes, but may result in an error in the saturation pressure versus depth. Whether the gradient should be calculated using the full or reduced EOS depends on the purpose of the black-oil simulation.

Conclusions

1. A black-oil model is always adequate for simulating depletion performance of petroleum reservoirs if (a) solution GOR and solution OGR are initialized properly, and (b) the PVT data are generated properly.
2. A compositional simulation model is generally recommended for gas injection studies. For gas injection, a black-oil model can only be used in (a) oil reservoirs when there is minimal vaporization and (b) lean to medium-rich gas condensate reservoirs undergoing cycling above the dewpoint for gas condensate fluids.
3. Initial fluids in place can be calculated accurately for pseudoized-EOS and black-oil models by initializing with the correct compositional gradient. In a compositional model, compositional gradient should be calculated from the original EOS model – i.e. the EOS model prior to pseudoization. In a black-oil model, the solution GORs and OGRs versus depth should be used. Black-oil PVT data should be generated from a properly-selected fluid with sufficiently-high saturation pressure.
4. For developing an EOS model for a reservoir fluid, C_{7+} (or C_{10+}) fraction should be split into 3-5 fractions initially. Usually, however, the EOS can be pseudoized down to as few as 6 to 8 components. When pseudoizing, key component properties are adjusted to minimize the difference between the pseudoized EOS and the original EOS for a wide range of PVT conditions and compositions.

Nomenclature

B_{gd} = dry-gas FVF, m^3/Sm^3
B_o = oil FVF, m^3/Sm^3
GOR = gas-oil ratio, Sm^3/Sm^3
OGR = oil-gas ratio, Sm^3/Sm^3
P_b = bubblepoint pressure, bara
P_d = dewpoint pressure, bara
P_R = reservoir pressure, bara
R_s = solution gas-oil ratio, Sm^3/Sm^3
r_s = solution oil-gas ratio, Sm^3/Sm^3
ρ_{gR} = reservoir gas density, kg/m^3
ρ_{gs} = surface gas density , kg/m^3
ρ_{oR} = reservoir oil density , kg/m^3
ρ_{os} = surface oil density, kg/m^3
μ_o = oil viscosity, cp
μ_g = gas viscosity, cp

Acknowledgements

We want to thank the participants of the "Guidelines for Choosing Compositional and Black-Oil Models for Volatile Oil and Gas-Condensate Reservoirs" project – Den norske stats oljeselskap a.s, Elf Petroleum Norge A/S, Mobil Exploration Norway Inc., Neste Petroleum A/S, Norsk Hydro Produksjon a.s, Norske Conoco AS, and Norwegian Petroleum Directorate (NPD) – for financial and technical support during this work.

References

1. Soave, G.: "Equilibrium Constants for a Modified Redlich-Kwong Equation of State," Chem. Eng. Sci.(1972), 27, 1197-1203.
2. Pedersen, K. S. and Fredenslund, A.: "An Improved Corresponding States Model for the Prediction of Oil and Gas Viscosities and Thermal Conductivities," Chem. Eng. Sci., 42, (1987), 182.
3. Lohrenz, J., Bray, B. G., and Clark, C. R.: "Calculating Viscosities of Reservoir Fluids From Their Compositions," J. Pet. Tech. (Oct. 1964) 1171-1176; Trans., AIME, 231.
4. Whitson C.H : "PVTx : An Equation-of-State Based Program for Simulating & Matching PVT Experiments with Multiparameter Nonlinear Regression," Version 98.
5. Whitson, C. H. and Belery, P.: "Compositional Gradients in Petroleum Reservoirs," paper SPE 28000 presented at the University of Tulsa/SPE Centennial Petroleum Engineering Symposium held in Tulsa, OK August 29-31, 1994.
6. Whitson, C.H., Fevang, Ø., and Yang, T.: "Gas Condensate PVT – What's Really Important and Why?," paper presented at the IBC Conference "Optimization of Gas Condensate Fields", London, 28-29 January 1999
7. Whitson, C. H. and Torp, S. B.: "Evaluating Constant Volume Depletion Data," JPT (March, 1983) 610; Trans AIME, 275.
8. Eclipse 300, 1998a Release
9. Eclipse 100, 1998a Release
10. Coats, K. H.: "Simulation of Gas Condensate Reservoir Performance," JPT (Oct. 1985) 1870.
11. Coats, K. H., Thomas, L. K., and Pierson, R. G.: "Compositional and Black-oil Reservoir Simulation," paper SPE 29111 presented at the 13th SPE Symposium on Reservoir Simulation held in San Antonio, TXD, USA, 12-15 February 1995.
12. Fevang, Ø. and Whitson, C. H.: "Modeling Gas Condensate Well Deliverability," SPE Reservoir Engineering, (Nov. 1996) 221.
13. El-Banbi, A.H., Forrest, J.K., Fan, L., and McCain, Jr., W.D.: "Producing Rich-Gas-Condensate Reservoirs — Case History and Comparison Between Compositional and Modified Black-Oil Approaches," paper SPE 58955 presented at the 2000 SPE International Petroleum Conference and Exhibition, Feb. 1-3.

Table 1 — Reference Fluid Composition, 4640 m MSL

Component	Mol-%	Molecular Weight	Specific Gravity
N_2	0.20		
CO_2	6.02		
C_1	67.24		
C_2	9.58		
C_3	4.39		
i-C_4	0.75		
n-C_4	1.41		
i-C_5	0.50		
n-C_5	0.55		
C_6	0.78		
C_7	1.42	90.73	0.7440
C_8	1.63	102.66	0.7740
C_9	1.00	116.79	0.7960
C_{10+}	4.53	245.96	0.8520
C_{7+}	8.58	178.00	0.8330

Table 2 — Parameters for the 22-Component SRK EOS

Component	MW	Critical Temperature	Critical Pressure	Acentric Factor	Critical Volume	Boiling Point
	M	T_C	P_C	ω	V_C	T_b
		K	bara		m^3/kmol	K
N_2	28.0	126.2	33.9	0.04	0.0898	77.4
CO_2	44.0	304.2	73.8	0.23	0.0940	194.7
C_1	16.0	190.6	46.0	0.01	0.0990	111.6
C_2	30.1	305.4	48.8	0.10	0.1480	184.6
C_3	44.1	369.8	42.5	0.15	0.2030	231.1
i-C_4	58.1	408.1	36.5	0.18	0.2630	261.4
n-C_4	58.1	425.2	38.0	0.19	0.2550	272.7
i-C_5	72.2	460.4	33.8	0.23	0.3060	301.0
n-C_5	72.2	469.6	33.7	0.25	0.3040	309.2
C_6	86.2	507.4	29.7	0.30	0.3700	341.9
C_7	90.7	528.0	34.9	0.45	0.4455	365.1
C_8	102.7	551.1	32.1	0.49	0.4576	389.9
C_9	116.8	574.2	28.9	0.53	0.4925	415.4
F1	140.1	604.7	24.1	0.59	0.5855	449.6
F2	167.6	636.3	20.7	0.67	0.6966	490.8
F3	197.5	666.9	18.4	0.75	0.8240	529.1
F4	235.5	702.1	16.4	0.84	0.9925	571.1
F5	268.6	730.2	15.4	0.92	1.1389	604.3
F6	309.3	762.9	14.4	1.01	1.3292	640.6
F7	364.4	803.8	13.6	1.11	1.5892	685.2
F8	442.4	858.4	12.8	1.23	1.9747	735.6
F9	621.6	979.3	12.1	1.32	2.9611	829.6

Component	Specific Gravity	Volume Shift	BIPS	BIPS	Parachor
	γ	s	k_{N2-i}	k_{CO2-i}	P
N_2	0.4700	-0.008			41
CO_2	0.5072	0.083	0.000		70
C_1	0.3300	0.023	0.020	0.120	77
C_2	0.4500	0.060	0.060	0.120	108
C_3	0.5077	0.082	0.080	0.120	150
i-C_4	0.5631	0.083	0.080	0.120	182
n-C_4	0.5844	0.097	0.080	0.120	192
i-C_5	0.6247	0.102	0.080	0.120	225
n-C_5	0.6310	0.121	0.080	0.120	233
C_6	0.6643	0.147	0.080	0.120	271
C_7	0.7440	0.044	0.080	0.100	313
C_8	0.7740	0.075	0.080	0.100	352
C_9	0.7960	0.106	0.080	0.100	392
F1	0.8071	0.150	0.080	0.100	421
F2	0.8198	0.171	0.080	0.100	491
F3	0.8306	0.174	0.080	0.100	564
F4	0.8421	0.162	0.080	0.100	650
F5	0.8522	0.142	0.080	0.100	720
F6	0.8623	0.114	0.080	0.100	800
F7	0.8743	0.069	0.080	0.100	896
F8	0.8883	0.005	0.080	0.100	1010
F9	0.9136	-0.134	0.080	0.100	1169

Table 3 — Molar Compositions from Different Depths Based on Isothermal Gradient Calculation

Component	Depth (m MSL) 4500	4640	4700	4740	4750	4760	4800	5000
N_2	0.21	0.20	0.19	0.18	0.17	0.17	0.16	0.14
CO_2	6.03	6.02	5.98	5.90	5.86	5.82	5.72	5.52
C_1	69.36	67.24	65.42	62.86	61.94	61.06	58.71	53.94
C_2	9.53	9.58	9.59	9.56	9.54	9.51	9.40	9.06
C_3	4.26	4.39	4.48	4.56	4.59	4.60	4.62	4.57
$i\text{-}C_4$	0.72	0.75	0.77	0.80	0.81	0.81	0.82	0.82
$n\text{-}C_4$	1.33	1.41	1.47	1.53	1.55	1.56	1.59	1.62
$i\text{-}C_5$	0.46	0.50	0.53	0.56	0.57	0.57	0.59	0.61
$n\text{-}C_5$	0.51	0.55	0.58	0.62	0.63	0.64	0.66	0.68
C_6	0.71	0.78	0.84	0.90	0.92	0.94	0.98	1.03
C_7	1.26	1.42	1.55	1.72	1.77	1.82	1.95	2.15
C_8	1.42	1.63	1.80	2.03	2.10	2.17	2.34	2.62
C_9	0.86	1.00	1.12	1.28	1.33	1.38	1.50	1.71
C_{10+}	3.35	4.53	5.69	7.52	8.23	8.94	10.95	15.54
C_{7+}	6.89	8.58	10.16	12.54	13.44	14.32	16.75	22.02
GOR_s Sm^3/Sm^3	1515	1101	857	621	557	504	391	244
P_s, bara	428.2	452.5	465.5	473.3	473.4	472.5	465.2	434.7

Table 4 — Composition of Injection Gas, mol-%

Component	MW	Rich gas	Lean gas
N_2	28.01	0.22048	0.49000
CO_2	44.01	6.74831	0.70000
C_1	16.04	76.09282	84.11000
C_2	30.07	10.19108	8.95000
C_3	44.10	3.99573	3.66000
$i\text{-}C_4$	58.12	0.57026	0.53000
$n\text{-}C_4$	58.12	0.96544	0.85000
$i\text{-}C_5$	72.15	0.25467	0.21000
$n\text{-}C_5$	72.15	0.25128	0.19000
C_6	86.18	0.22000	0.13000
C_{7+}	90.73	0.48993	0.18000

Table 5 — Parameters for the 6-Component SRK EOS

Component	MW	Critical Temperature	Critical Pressure	Acentric Factor	Critical Volume	Boiling Point
	M	T_C K	P_C bara	ω	V_C m^3/kmol	T_b K
C_1N_2	16.1	190.3	45.9	0.01	0.0990	111.4
CO_2C_2	35.4	304.8	60.8	0.16	0.1208	189.4
$C_{3\text{-}6}$	55.1	418.9	37.8	0.20	0.2601	269.6
$C_{7\text{-}9}$F1-2	116.9	577.4	28.4	0.54	0.5117	420.4
F3-8	281.0	753.3	15.2	0.97	1.1163	626.7
F9	621.6	979.3	12.1	1.32	2.5673	829.6

Component	Specific Gravity	Volume Shift	BIPS	BIPS	OmegaA	OmegaB	Parachor
	γ	s	$k_{C1N2\text{-}I}$	$k_{CO2C2\text{-}I}$	Ω_a	Ω_b	P
C_1N_2	0.3305	0.023			0.4269	0.09	77
CO_2C_2	0.4757	0.067	0.05735		0.4440	0.0915	93
$C_{3\text{-}6}$	0.5630	0.099	0.00041	0.05749	0.4208	0.0837	181
$C_{7\text{-}9}$F1-2	0.7864	0.109	0.00027	0.04791	0.4225	0.0894	379
F3-8	0.8576	0.118	0.00027	0.04791	0.4141	0.0827	732
F9	0.9136	-0.134	0.00027	0.04791	0.4275	0.0866	1169

Table 6 — Reservoir Initialization Procedures Summary

Compositional Model				
CASE	IOIP (10^6 Sm^3)	IGIP (10^9 Sm^3)	ΔIOIP[a] (%)	ΔIGIP[a] (%)
EOS22	13.22	11.02	-	-
EOS6, Method A	13.34	11.03	0.94	0.07
EOS6, Method B	12.96	11.13	-1.98	1.00
EOS6, Method C	13.10	11.08	-0.88	0.56
Black-Oil Model				
CASE	IOIP (10^6 Sm^3)	IGIP (10^9 Sm^3)	ΔIOIP[b] (%)	ΔIGIP[b] (%)
BO6, Method 1	12.96	11.17	-1.07	0.81
BO6, Method 2	12.89	11.17	-1.60	0.81
BO6, Method 3	13.02	11.13	-0.61	0.45

(a) Deviations relation to EOS22 values
(b) Deviation relation to EOS6, Method C values

Table 7 — Reservoir and Rock Properties

Absolute Horizontal permeability, md	5 - 200
Top geologic unit, md	5
Middle geologic unit, md	50
Bottom geologic unit, md	200
Vertical/Horizontal permeability ratio	0.1
Dykstra-Parsons coefficient	0.75
Porosity, %	15
Reservoir Height, m (3 units, 50 m each)	150
Rock Compressibility, bar^{-1}	4.00E-5
Irreducible Water Saturation, %	26
Initial Reservoir Pressure, bara at 4750 m	494.68
Initial Reservoir Temperature, °C	163
Initial Gas-Oil Contact, m	4750
Critical Gas Saturation, %	2.0
Critical Oil Saturation, %	22.7
Residual Oil Saturation, %	21.5

Table 8 — Simulation Cases and Performance — Depletion

Case Name	File Name	Case Description	Model	Reservoir Performance								
				AFTER 3 YEARS			AFTER 5 YEARS			AFTER 10 YEARS		
				FOPR Sm^3/d	FGOR Sm^3/Sm^3	RF_r %	FOPR Sm^3/d	FGOR Sm^3/Sm^3	RF_r %	FOPR Sm^3/d	FGOR Sm^3/Sm^3	RF_r %
EOS Models												
D1	A1C1X	Near Critical Fluid ($V_{ro\,max}$=55%), EOS 6	EOS6	495	1674	17.9	264	2448	22.5	14	4134	26.9
	A1C3X	Near Critical Fluid ($V_{ro\,max}$=55%), EOS 22	EOS22	505	1626	17.8	284	2243	22.5	8	5514	26.9
D2	A1C4X	Near Critical Fluid ($V_{ro\,max}$=55%), EOS 3	EOS3	343	2646	16.3	161	4362	19.3	43	7450	22.1
Initial Fluid, Constant												
D3	A1C1X	Near Critical Fluid ($V_{ro\,max}$=55%)	EOS6	495	1674	17.9	264	2448	22.5	14	4134	26.9
	A1C1		BO6	500	1657	17.6	274	2352	22.3	27	3723	26.8
D4	D2	Rich Gas Condensate ($V_{ro\,max}$ = 28% and r_s = 0.00115 Sm^3/Sm^3)	EOS6	328	2723	17.4	182	3844	21.5	71	5283	26.3
	D2X		BO6	329	2713	17.3	185	3772	21.5	74	5043	26.4
D5	D3X	Volatile Oil (B_{ob} = 2.3 and R_S = 407 Sm^3/Sm^3)	EOS6	670	1134	20.3	399	1471	25.4	4	4282	30.9
	D3		BO6	678	1121	20.2	401	1459	25.3	24	1386	31.0
D6	D4X	Medium Rich Gas Condensate ($V_{ro\,Max}$ = 12% and r_s = 0.00066 Sm^3/Sm^3)	EOS6	336	2744	23.3	197	3745	30.2	80	5159	38.5
	D4		BO6	337	2733	23.3	199	3711	30.1	83	4957	38.7
D7	D5X	Slightly Volatile Oil (B_{ob} = 1.8 and R_S = 256 Sm^3/Sm^3)	EOS6	815	806	20.0	477	1034	24.9	14	805	28.8
	D5		BO6	810	812	19.9	472	1043	24.7	16	973	28.6
Initial Fluid, Variable												
D8	E2A1X	Mainly Oil and some GC with fluid gradient as in bottom layer	EOS6	432	1982	24.0	216	3123	28.2	66	4882	32.6
	E2A1		BO6	438	1965	24.8	219	3097	29.1	73	4753	33.4
D9	E2A2X	Gas Condensate and Oil with fluid gradient as in middle layer	EOS6	349	2558	20.3	190	3709	24.7	45	5266	29.5
	E2A2		BO6	352	2550	20.6	191	3687	25.0	44	5101	29.8
D10	E2A3X	Only Gas Condensate fluid gradient as in top layer.	EOS6	223	1900	9.3	165	2390	13.2	86	3405	19.4
	E2A3		BO6	210	1835	8.9	158	2270	12.6	87	3203	18.6
D11	E2A3_10X	Only Gas Condensate fluid gradient as in top layer (k=50 md)	EOS6	329	2766	20.4	186	3870	25.5	61	5310	31.4
	E2A3_10		BO6	330	2765	20.8	187	3862	25.9	57	5271	31.8
Permeability Variations												
D12	D3F2X	Volatile Oil, Permeability High-Top	EOS6	256	3187	10.7	134	4470	12.5	0	5397	14.2
	D3F2		BO6	245	3324	10.5	128	4631	12.3	0	5243	13.8
D13	D3F3X	Volatile Oil, Permeability High-Middle	EOS6	255	3205	12.4	133	4514	14.2	0	5452	15.9
	D3F3		BO6	247	3302	12.4	130	4617	14.1	0	5807	15.7
Saturated GOC												
D14	D3M2X	Volatile Oil, constant oil and gas composition	EOS6	340	2526	19.8	185	3646	24.0	72	5031	28.7
	D3M2_CCE		BO6	316	2756	19.2	170	4003	23.1	65	5572	27.5
	D3M2_DLE		BO6	301	2899	18.9	158	4324	22.6	57	6051	26.6
	D3M2_MIX		BO6	344	2527	19.8	190	3586	24.1	74	4888	29.0
D15	D3M2E2X	Oil and Gas gradient	EOS6	352	2482	25.5	196	3545	30.7	74	5180	36.7
	D3M2E2_CCE		BO6	332	2651	24.8	182	3844	29.7	69	5518	35.3
	D3M2E2_DLE		BO6	317	2783	24.4	169	4142	29.1	63	6016	34.2
	D3M2E2_MIX		BO6	360	2436	25.6	202	3451	31.1	79	4845	37.4
D16	D3M2E2X_3W_RATE	Oil and Gas gradient (3 wells- top, middle & bottom)	EOS6	362	2392	22.7	203	3404	28.2	80	4809	34.5
			BO6	370	2347	23.2	208	3323	28.9	82	4660	35.4
		Structurally bottom well (P5010)	EOS6	162	1726	-	84	2672	-	30	4136	-
			BO6	155	1823	-	83	2739	-	31	4015	-
		Structurally middle well (P2505)	EOS6	102	2871	-	60	3875	-	25	5215	-
			BO6	108	2706	-	63	3687	-	25	5052	-
		Structurally top well (P0101)	EOS6	98	2993	-	59	3970	-	25	5235	-
			BO6	107	2743	-	63	3722	-	25	5061	-

Table 9— Simulation Cases and Performance — Injection

Case Name	File Name	Case Description	Model	Reservoir Performance								
				AFTER 5 YEARS			AFTER 10 YEARS			AFTER 15 YEARS		
				FOPR Sm^3/d	FGOR Sm^3/Sm^3	RF, %	FOPR Sm^3/d	FGOR Sm^3/Sm^3	RF, %	FOPR Sm^3/d	FGOR Sm^3/Sm^3	RF, %
EOS Models												
I1	J2B2D1C3X	Near Critical Fluid, Lean Gas Injection	EOS22	863	1386	39.5	513	2443	59.5	264	4871	71.1
	J2B2D1X		EOS6	838	1437	39.2	511	2457	59.0	290	4427	71.3
Full Pressure Maintenance												
Gas Condensate Reservoirs with Constant												
I2	J2B2D1X	Near Critical Fluid, Lean Gas Injection	EOS6	838	1437	39.2	511	2457	59.0	290	4427	71.3
	J2B2D1		BO6	1147	983	44.2	733	1625	72.6	316	4054	88.7
I3	J2B2D2X	Rich Gas Condensate, Lean Gas Injection	EOS6	776	1576	43.4	446	2859	68.2	217	6014	81.8
	J2B2D2		BO6	819	1477	44.7	494	2562	71.8	238	5535	86.8
I4	J2B2D4X	Medium Rich Gas Condensate, Lean Gas Injection	EOS6	493	2598	44.1	287	4568	69.1	123	10890	82.4
	J2B2D4		BO6	501	2554	44.1	298	4412	69.7	144	9315	84.2
I5	J2B2D1Z2X	Near Critical Fluid, Lean Gas Injection, gravity stable	EOS6	176	575	5.5	175	577	10.9	174	585	16.4
	J2B2D1Z2		BO6	175	576	5.5	174	579	10.9	172	586	16.3
I6	J2B2D2Z2X	Rich Gas Condensate, Lean Gas Injection, gravity stable	EOS6	129	870	5.5	129	874	10.9	128	880	16.4
	J2B2D2Z2		BO6	129	870	5.5	128	874	10.9	127	881	16.3
Oil Reservoirs with Constant Composition												
I7	J2B2D5X	Slightly Volatile oil (SVO), Lean Gas Injection	EOS6	955	1180	37.5	424	2891	49.6	277	4499	56.2
	J2B2D5	SVO, Lean Gas Injection, black-oil extrapolation by Ecl	BO6	1195	902	42.0	623	1888	57.5	509	2309	68.8
	J2B2D5Y2_A	SVO, Lean Gas Injection, black-oil extrapolation by method A	BO6	1181	910	40.9	631	1846	56.6	513	2272	67.7
	J2B2D5Y2_B	SVO, Lean Gas Injection, black-oil extrapolation by method B	BO6	1141	950	40.8	619	1889	56.0	519	2244	67.2
	J2B2D5Y2_C	SVO, Lean Gas Injection, black-oil extrapolation by method C	BO6	1172	908	40.9	606	1912	56.2	499	2313	66.9
I8	J2B2D5T2X	SVO, Lean Gas Injection	EOS6	1039	1107	37.6	483	2656	51.2	354	3704	58.9
	J2B2D5T2Y2_B	SVO, (with vaporization and swelling)	BO6	1125	1014	40.2	666	1875	55.8	552	2299	68.0
	J2B2D5T2Y2_B_PVDG	SVO (no vaporization)	BO6	1295	828	48.2	252	5177	59.4	117	11471	62.7
	J2B2D5T2Y2_B_PVDG_DRSDT	SVO, (no vaporization and no swelling)	BO6	1171	934	46.9	253	5156	57.4	121	11052	60.8
I9	J2B2D6T2X	Low GOR oil, Lean Gas Injection	EOS6	2742	269	37.0	1231	894	59.4	461	2781	68.6
	J2B2D6T2Y2_A	Low-GOR oil, LG injection, black-oil extrapolation by method A	BO6	2171	394	33.2	1239	888	55.1	809	1489	67.9
	J2B2D6T2Y2_B	Low-GOR oil, LG injection, black-oil extrapolation by method B	BO6	2246	371	33.7	1202	920	55.0	767	1581	67.2
	J2B2D6T2Y2_C	Low-GOR oil, LG injection, black-oil extrapolation by method C	BO6	2227	386	33.0	1256	847	55.5	818	1405	68.3
I10	J2B2D6T2X_200	Low GOR oil, Lean Gas Injection (Initial Pr = 200 bara)	EOS6	2351	62	25.3	904	681	49.1	309	2200	56.2
	J2B2D6T2Y2_A_200	Low-GOR oil, LG injection, black-oil extrapolation by method A	BO6	2394	65	25.9	1027	594	50.3	411	1661	59.2
	J2B2D6T2Y2_B_200	Low-GOR oil, LG injection, black-oil extrapolation by method B	BO6	2210	79	25.2	969	627	47.9	424	1591	56.7
	J2B2D6T2Y2_C_200	Low-GOR oil, LG injection, black-oil extrapolation by method C	BO6	2340	65	25.7	1063	521	51.0	415	1446	60.0
I11	J2B2D6T2X	Low-GOR oil, Lean Gas, Injection	EOS6	2742	269	37.0	1231	894	59.4	461	2781	68.6
	J2B2D6T2Y2_B	Low-GOR oil (with vaporization and swelling)	BO6	2246	371	33.7	1202	920	55.0	767	1581	67.2
	J2B2D6T2Y2_B_PVDG	Low-GOR oil (no vaporization)	BO6	2489	307	40.9	996	1135	61.4	383	3332	69.7
	J2B2D6T2Y2_B_PVDG_DRSDT	Low-GOR oil (no vaporization and no swelling)	BO6	1214	837	28.2	604	1967	38.9	387	3238	45.1
I12	J4B2D5X	SVO, Injection C1N2	EOS6	872	1312	34.8	436	2807	46.4	436	2807	46.4
	J4B2D5Y2_B	SVO, Injection C1N2, black-oil extrapolation by method B	BO6	1138	940	40.8	587	1950	55.7	587	1950	55.7
	J4B2D5Y2_C	SVO, Injection C1N2, black-oil extrapolation by method C	BO6	1155	916	40.7	577	1973	55.6	577	1973	55.6
Compositional Gradient (Reservoirs with Undersaturated GOC)												
I13	J2B2E2A2X	Fluid gradient as in middle layer, Injection of LG	EOS6	480	2648	38.5	268	4850	53.8	168	7834	62.9
	J2B2E2A2		BO6	509	2489	39.5	301	4317	56.2	198	6628	66.7
Permeability Variation (Near Critical Fluid)												
I14	J2B2D1F2X	Near Critical Fluid, High Perm at Top, Injection Lean Gas	EOS6	584	2137	30.5	305	4223	43.3	157	8327	50.3
	J2B2D1F2		BO6	620	2005	31.7	371	3441	46.7	251	5140	56.2
I15	J2B2D1F3X	Near Critical Fluid ,High Perm at Middle, Injection Lean Gas	EOS6	706	1743	35.5	203	6426	47.6	153	8536	52.7
	J2B2D1F3		BO6	799	1514	40.6	268	4843	54.6	155	8477	60.6
Partial Pressure Maintenance												
Undersaturated Oil Reservoirs												
I16	J2B3D3X	Volatile Oil, Inject (lean gas) 50% of produced gas	EOS6	740	916	24.9	5	2336	26.8	0	0	26.8
	J2B3D3		BO6	728	770	25.1	23	798	27.2	0	0	27.2
I17	J2B4D3X	Volatile Oil, Inject (lean gas) 80% of produced gas	EOS6	885	1108	25.8	453	2142	31.9	1	2944	35.4
	J2B4D3		BO6	1097	853	27.1	589	1594	35.0	0	0	37.9
I18	J2B5D3X	Volatile Oil, Inject (lean Gas) all produced gas	EOS6	883	1190	25.7	553	1949	32.4	273	3968	42.3
	J2B5D3		BO6	1149	860	27.7	676	1532	36.3	397	2594	48.6
Oil Reservoir with Gas Injection in Gas Cap												
I19	J2B3E2A2X	Layer 2 gradient, Inject (lean gas) 50% of produced gas	EOS6	447	2333	23.1	120	2979	27.6	3	2498	29.1
	J2B3E2A2		BO6	488	2137	24.7	128	2599	29.8	0	0	31.1
I20	J2B4E2A2X	Layer 2 gradient, Inject (lean gas) 80% of produced gas	EOS6	502	2268	24.4	319	3434	31.2	98	6300	40.1
	J2B4E2A2		BO6	557	2025	26.6	374	2912	34.3	118	4732	45.1
I21	J2B5E2A2X	Layer 2 gradient, Inject (lean Gas) all produced gas	EOS6	553	2174	25.5	393	3080	33.3	231	5225	45.9
	J2B5E2A2		BO6	647	1822	28.3	462	2575	37.5	270	4394	52.4
Permeability Variation												
I22	J2B5E2A2F2X	Layer 2 gradient, Inject all produced gas (LG), highest k at top	EOS6	511	2382	22.8	354	3464	30.0	198	6177	41.1
	J2B5E2A2F2		BO6	584	2042	25.1	400	3014	33.2	221	5480	45.6
I23	J2B5D3F2X	Volatile Oil, Inject all produced gas (LG), highest K at top	EOS6	558	2078	16.6	396	2940	21.2	238	4848	28.7
	J2B5D3F2		BO6	605	1912	17.0	441	2622	22.1	269	4231	30.6

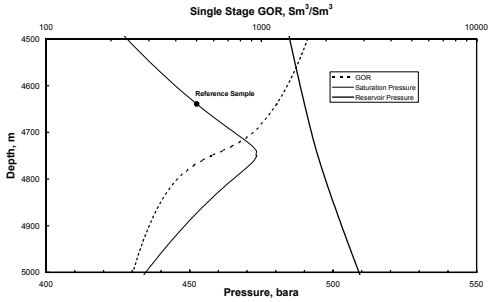

Fig. 1 — GOR, reservoir and saturation pressure variation with depth.

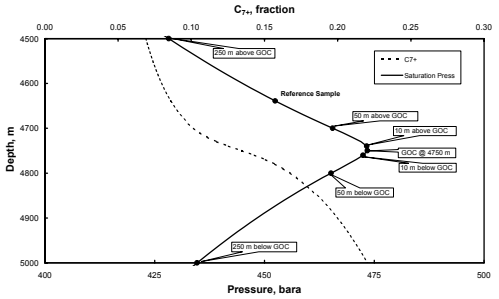

Fig. 2 — C_{7+} variation with depth and different feed locations.

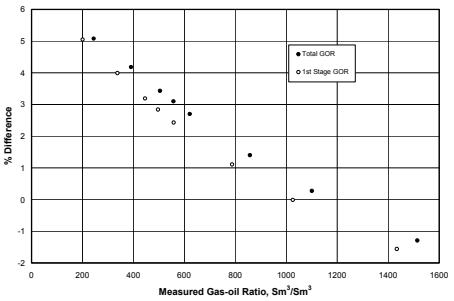

Fig. 3 — Difference in separator gas-oil ratio - EOS22 vs. EOS6 (separator experiment).

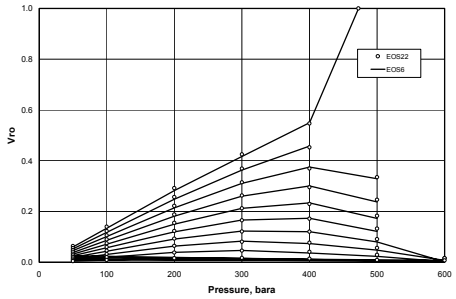

Fig. 4 — Relative oil volume comparison - EOS22 vs. EOS6 : rich gas injection in oil sample (multicontact swelling experiment).

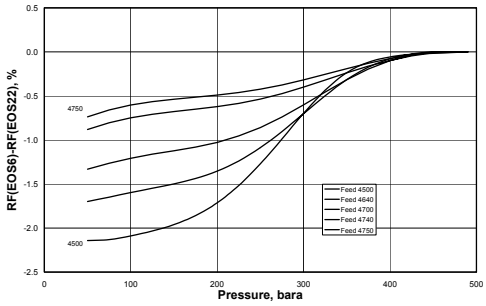

Fig. 5 — Difference in oil recovery - EOS22 vs. EOS6 based on CVD data.

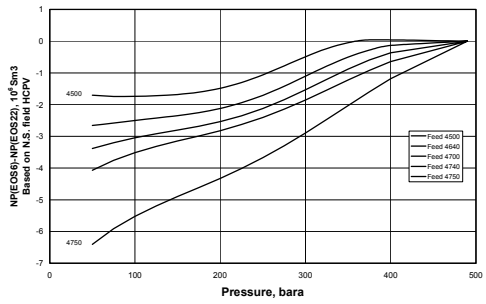

Fig. 6 — Difference in total oil production - EOS22 vs. EOS6 based on CVD data.

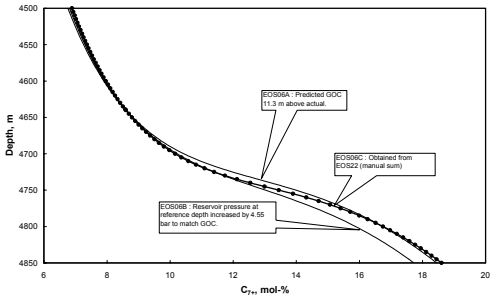

Fig. 7 — C_{7+} composition variation with depth under different initialization methods.

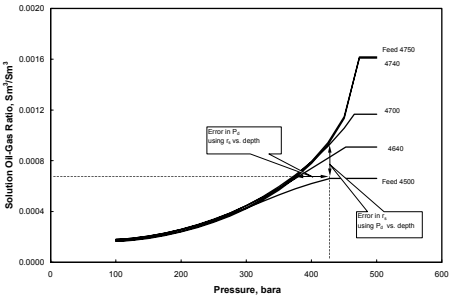

Fig. 10 — Initializing black-oil model — (a) solution OGR vs. depth (b) saturation pressure vs. depth

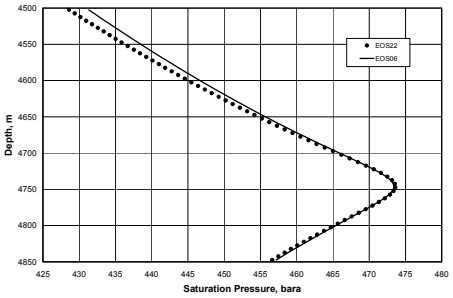

Fig. 8 — Saturation pressure with depth (EOS22 vs. EOS6).

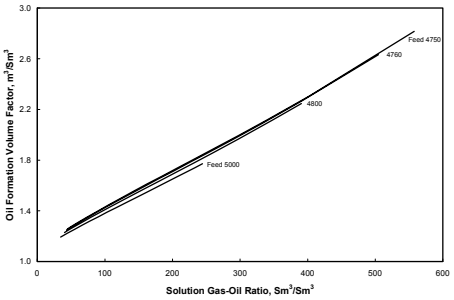

Fig. 11 — Oil formation volume factor versus solution gas-oil ratio for fluids from different locations.

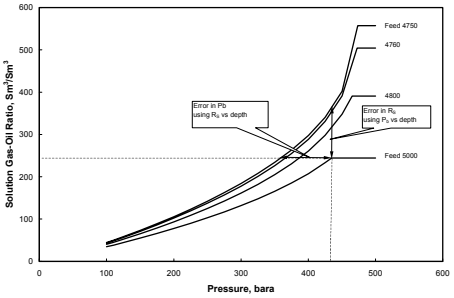

Fig. 9 — Initializing black-oil model — (a) solution GOR vs. depth (b) saturation pressure vs. depth

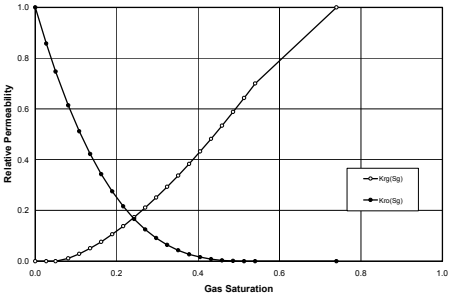

Fig. 12 — Oil and gas relative permeabilities.

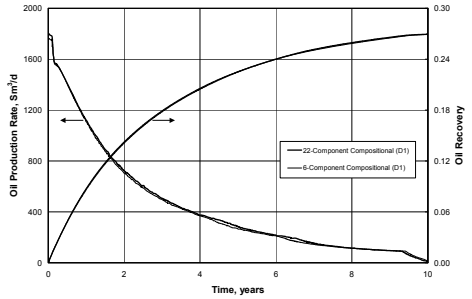

Fig. 13 — Depletion Case - EOS22 vs. EOS6 (near critical fluid with constant composition).

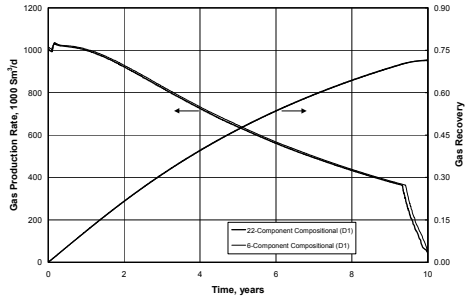

Fig. 14 — Depletion Case - EOS22 vs. EOS6 (near critical fluid with constant composition).

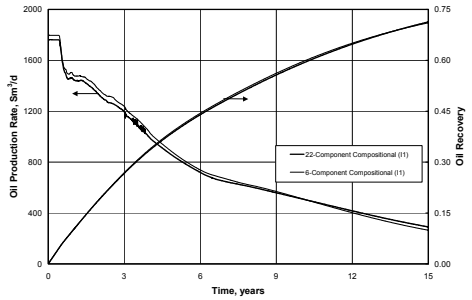

Fig. 15 — Injection Case - EOS22 vs. EOS6 (near critical fluid with constant composition).

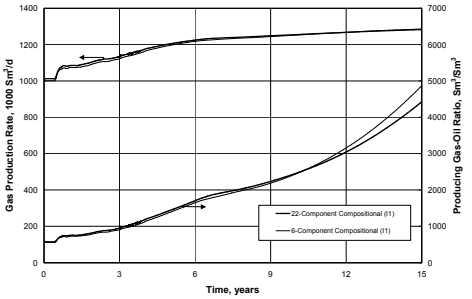

Fig. 16 — Injection Case - EOS22 vs. EOS6 (near critical fluid with constant composition).

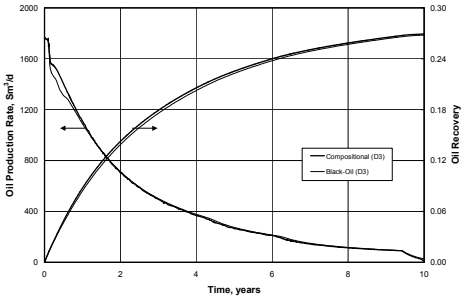

Fig. 17 — Depletion Case - Near critical fluid with constant composition; EOS6.

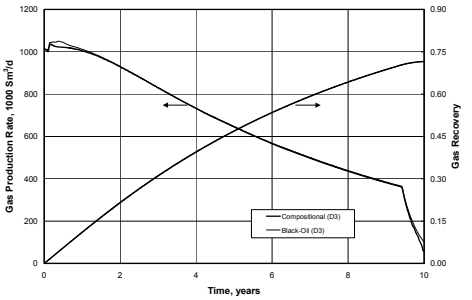

Fig. 18 — Depletion Case - Near critical fluid with constant composition; EOS6.

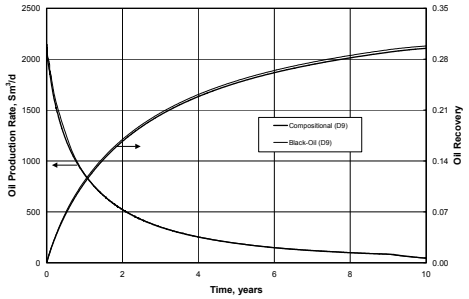

Fig. 19 — Depletion Case - Reservoir with Compositional Gradient; EOS6.

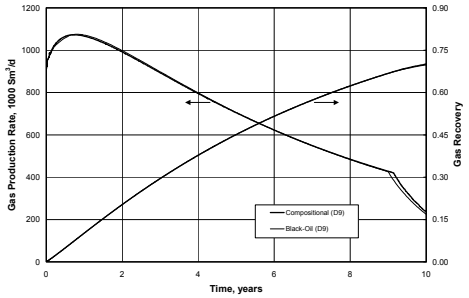

Fig. 20 — Depletion Case - Reservoir with compositional gradient; EOS6.

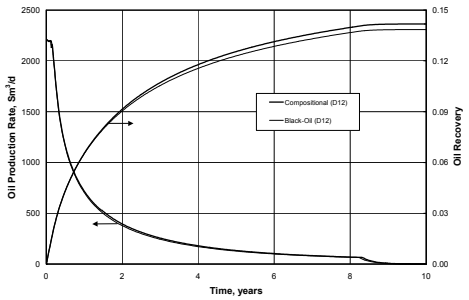

Fig. 21 — Depletion Case - Volatile oil reservoir with constant composition and highest permeability at the top; EOS6.

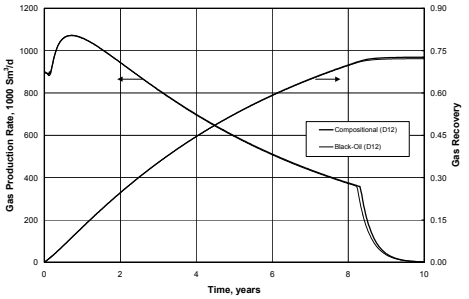

Fig. 22 — Depletion Case - Volatile oil reservoir with constant composition and highest permeability at the top; EOS6.

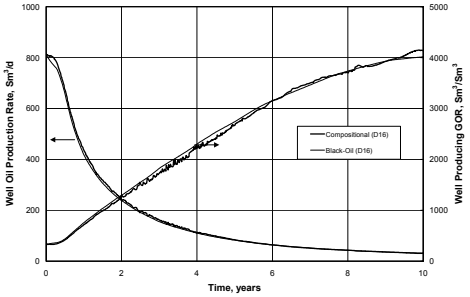

Fig. 23 — Depletion Case - Reservoir with compositional gradient with saturated GOC (structurally low well); EOS6.

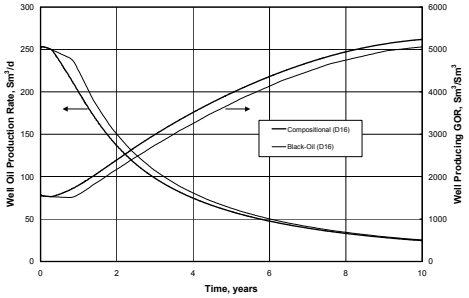

Fig. 24 — Depletion Case - reservoir with compositional gradient with saturated GOC (structurally high well); EOS6.

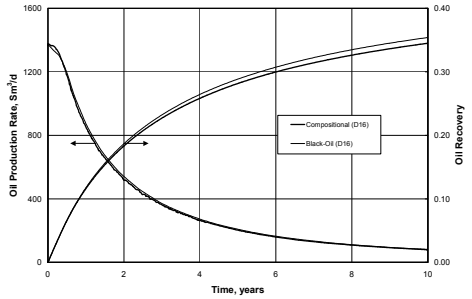

Fig. 25 — Depletion Case - Reservoir with compositional gradient with saturated GOC (total field – all three wells); EOS6.

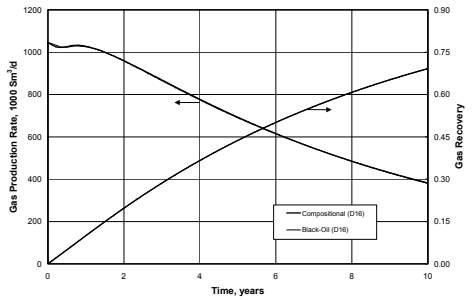

Fig. 26 — Depletion Case - reservoir with compositional gradient with saturated GOC (total field – all three wells); EOS6.

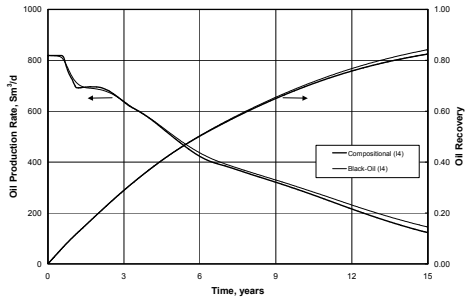

Fig. 27 — Injection Case - Medium rich gas condensate with constant composition; EOS6.

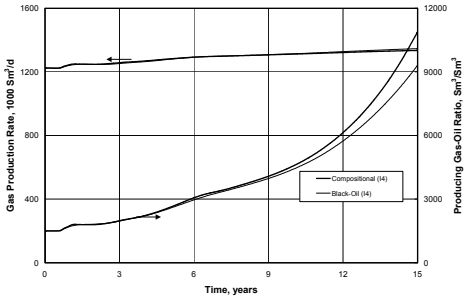

Fig. 28 — Injection Case - Medium rich gas condensate with constant composition; EOS6.

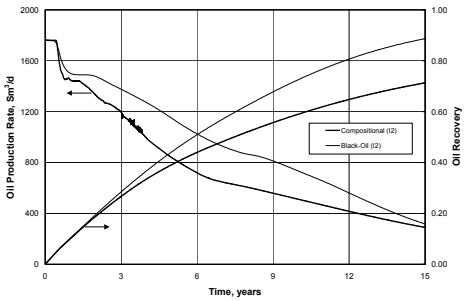

Fig. 29 — Injection Case - Near critical fluid with constant composition; EOS6.

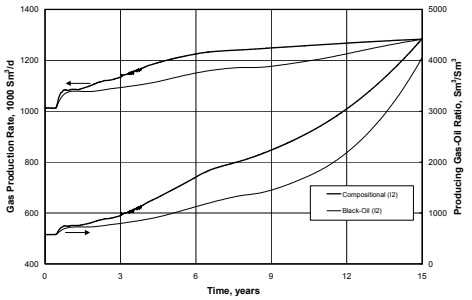

Fig. 30 — Injection Case - Near critical fluid with constant composition; EOS6.

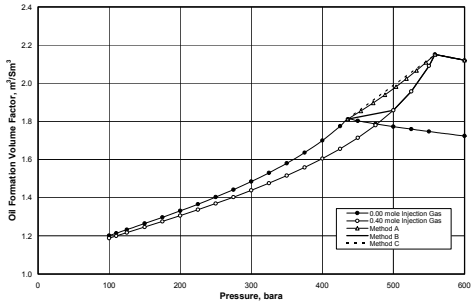

Fig. 31 — Modified BO PVT table (oil formation volume factor) for lean gas injection in slightly volatile oil.

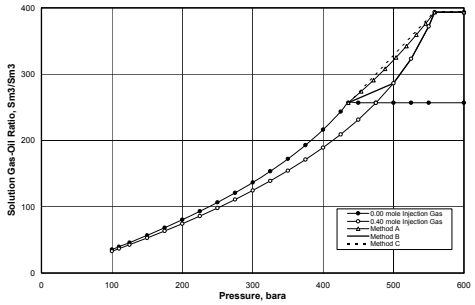

Fig. 32 — Modified BO PVT table (solution gas-oil ratio) for lean gas injection in slightly volatile oil.

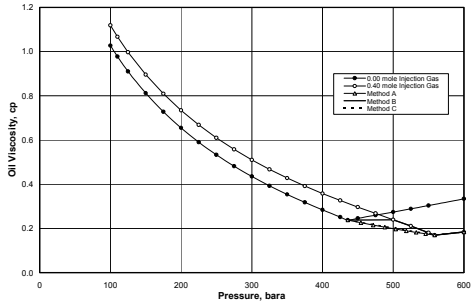

Fig. 33 — Modified BO PVT table (oil viscosity) for lean gas injection in slightly volatile oil.

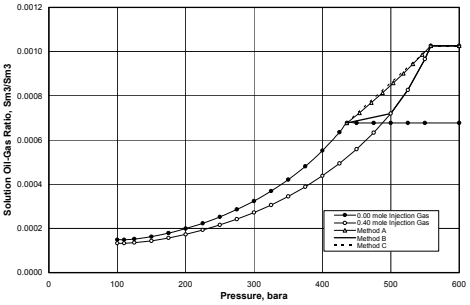

Fig. 34 — Modified BO PVT table (oil-gas ratio) for lean gas injection in slightly volatile oil.

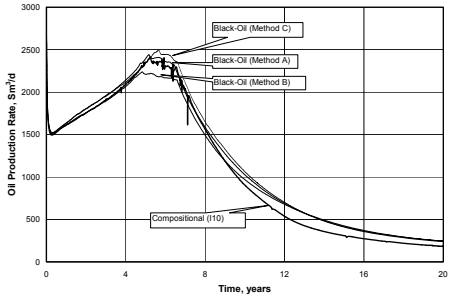

Fig. 35 — Injection Case - Low GOR (50 Sm^3/Sm^3) oil with constant composition. Average reservoir pressure P_R= 200 bara and saturation pressure P_b= 135 bara; EOS6.

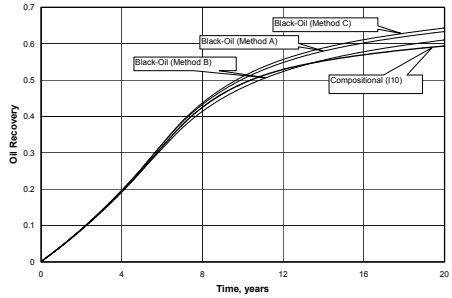

Fig. 36 — Injection Case - Low GOR (50 Sm^3/Sm^3) oil with constant composition. Average reservoir pressure P_R= 200 bara and saturation pressure P_b= 135 bara; EOS6.

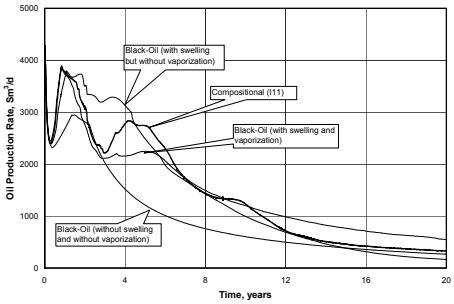

Fig. 37 — Injection Case - Low GOR oil with constant composition (with and without —swelling and vaporization). Average reservoir pressure P_R= 500 bara and saturation pressure P_b= 135 bara; EOS6.

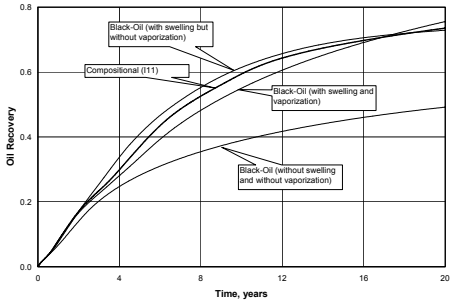

Fig. 38 — Injection Case - Low GOR Oil with constant composition (with and without —swelling and vaporization). Average reservoir pressure P_R= 500 bara and saturation pressure P_b= 135 bara; EOS6.

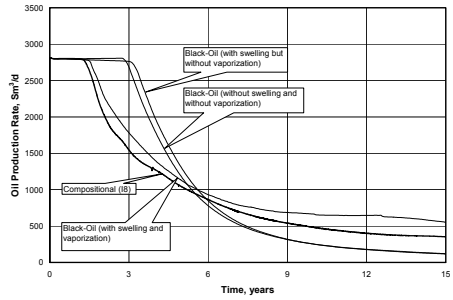

Fig. 39 — Injection Case - Slightly volatile oil with constant composition (with and without —swelling and vaporization); EOS6.

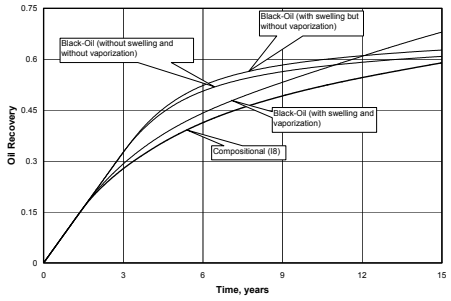

Fig. 40 — Injection Case - Slightly volatile oil with constant composition (with and without —swelling and vaporization) ; EOS6.

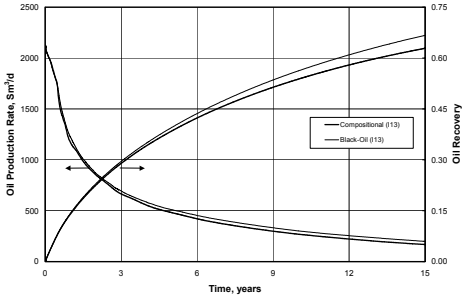

Fig. 41 — Injection Case - Reservoir with compositional gradient; EOS6.

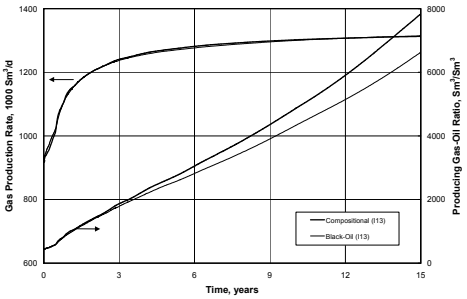

Fig. 42 — Injection Case - Reservoir with compositional gradient; EOS6.

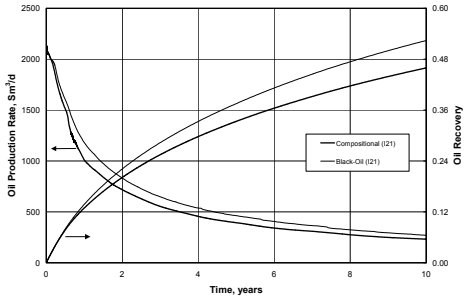

Fig. 43 — Injection Case - Reservoir with compositional gradient and 100% of the surface produced gas reinjected; EOS6.

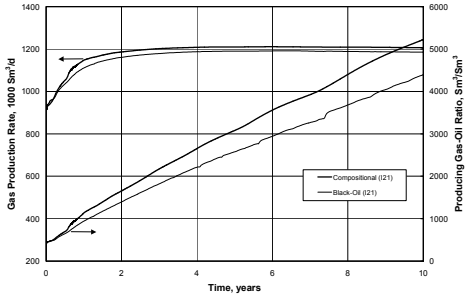

Fig. 44 — Injection Case - Reservoir with compositional gradient and 100% of the surface produced gas reinjected; EOS6.

Appendix B

Table B-1— Fluid composition at different depths and injection gas composition.

Molar compositions from different depths based on isothermal gradient calculation and injection gases										
Component	Depth (m MSL)								Injection Gas	
	4500	4640	4700	4740	4750	4760	4800	5000	RG	LG
EOS22										
N_2	0.0021	0.0020	0.0019	0.0018	0.0017	0.0017	0.0016	0.0014	0.0022	0.0049
CO_2	0.0603	0.0602	0.0598	0.0590	0.0586	0.0582	0.0572	0.0552	0.0675	0.0070
C_1	0.6936	0.6724	0.6542	0.6286	0.6194	0.6106	0.5871	0.5394	0.7609	0.8411
C_2	0.0953	0.0958	0.0959	0.0956	0.0954	0.0951	0.0940	0.0906	0.1019	0.0895
C_3	0.0426	0.0439	0.0448	0.0456	0.0459	0.0460	0.0462	0.0457	0.0400	0.0366
i-C_4	0.0072	0.0075	0.0077	0.0080	0.0081	0.0081	0.0082	0.0082	0.0057	0.0053
n-C_4	0.0133	0.0141	0.0147	0.0153	0.0155	0.0156	0.0159	0.0162	0.0097	0.0085
i-C_5	0.0046	0.0050	0.0053	0.0056	0.0057	0.0057	0.0059	0.0061	0.0025	0.0021
n-C_5	0.0051	0.0055	0.0058	0.0062	0.0063	0.0064	0.0066	0.0068	0.0025	0.0019
C_6	0.0071	0.0078	0.0084	0.0090	0.0092	0.0094	0.0098	0.0103	0.0022	0.0013
C_7	0.0126	0.0142	0.0155	0.0172	0.0177	0.0182	0.0195	0.0215	0.0023	0.0011
C_8	0.0142	0.0163	0.0180	0.0203	0.0210	0.0217	0.0234	0.0262	0.0017	0.0006
C_9	0.0086	0.0100	0.0112	0.0128	0.0133	0.0138	0.0150	0.0171	0.0006	0.0001
F1	0.0080	0.0096	0.0109	0.0127	0.0133	0.0139	0.0152	0.0174	0.0002	0.0000
F2	0.0061	0.0076	0.0088	0.0104	0.0110	0.0115	0.0128	0.0149	0.0001	0.0000
F3	0.0047	0.0060	0.0071	0.0086	0.0092	0.0096	0.0109	0.0128	0.0000	0.0000
F4	0.0050	0.0067	0.0082	0.0103	0.0111	0.0117	0.0135	0.0165	0.0000	0.0000
F5	0.0024	0.0033	0.0042	0.0054	0.0059	0.0063	0.0074	0.0094	0.0000	0.0000
F6	0.0032	0.0046	0.0061	0.0083	0.0092	0.0100	0.0121	0.0161	0.0000	0.0000
F7	0.0018	0.0029	0.0040	0.0058	0.0066	0.0073	0.0093	0.0134	0.0000	0.0000
F8	0.0016	0.0029	0.0044	0.0071	0.0082	0.0094	0.0128	0.0211	0.0000	0.0000
F9	0.0008	0.0018	0.0032	0.0065	0.0080	0.0097	0.0156	0.0338	0.0000	0.0000
EOS6										
C_1N_2	0.6957	0.6744	0.6561	0.6304	0.6211	0.6123	0.5887	0.5408	0.7631	0.8460
CO_2C_2	0.1555	0.1560	0.1557	0.1546	0.1539	0.1533	0.1512	0.1458	0.1694	0.0965
$C_{3\text{-}6}$	0.0799	0.0838	0.0866	0.0897	0.0905	0.0912	0.0926	0.0932	0.0626	0.0557
$C_{7\text{-}9}$F1-2	0.0495	0.0576	0.0644	0.0734	0.0764	0.0791	0.0860	0.0970	0.0049	0.0018
F3-8	0.0186	0.0263	0.0339	0.0456	0.0500	0.0543	0.0659	0.0893	0.0000	0.0000
F9	0.0008	0.0018	0.0032	0.0065	0.0080	0.0097	0.0156	0.0338	0.0000	0.0000
C_{7+}	0.0689	0.0858	0.1016	0.1254	0.1344	0.1432	0.1675	0.2202		
GOR, Sm3/Sm3	1101	1515	857	621	557	504	391	244.00		
p_s, bara	428.2	452.5	465.5	473.3	473.4	472.5	465.2	434.7		

Notes:
1. Reference depth is 4640 m MSL.
2. GOR is based on 2-stage separator (EOS22).
3. Saturation pressure p_s at 163 ^{o}C.

Table B-2 — Primary stage separator gas composition from different reservoir fluid systems.

Components	Primary stage separator gas composition from different feeds, mol %							
	4500	4640	4700	4740	4750	4760	4800	5000
N_2	0.23814	0.23277	0.22824	0.22237	0.22048	0.21882	0.21505	0.21095
CO_2	6.44972	6.56650	6.64098	6.72244	6.74831	6.77231	6.83790	7.00037
C_1	76.48633	76.24716	76.13445	76.08544	76.09282	76.11007	76.19894	76.52612
C_2	9.82048	9.96661	10.06559	10.16587	10.19108	10.20983	10.23539	10.17776
C_3	3.94459	3.99529	4.01367	4.00653	3.99573	3.98185	3.92852	3.75905
i-C_4	0.58739	0.58942	0.58608	0.57542	0.57026	0.56481	0.54801	0.50677
n-C_4	1.01704	1.01350	1.00208	0.97662	0.96544	0.95403	0.92023	0.84180
i-C_5	0.28522	0.27915	0.27178	0.25944	0.25467	0.25003	0.23725	0.21081
n-C_5	0.28733	0.27917	0.27036	0.25649	0.25128	0.24627	0.23270	0.20530
C_6	0.26782	0.25453	0.24259	0.22588	0.22000	0.21450	0.20013	0.17284
C_{7+}	0.61591	0.57589	0.54416	0.50350	0.48993	0.47749	0.44588	0.38825

Table B-3 — Relative permeability data used in the simulation studies.

Oil-Water Relative Permeability				Oil-Gas Relative Permeability			
S_W	k_{rw}	k_{row}	p_{cow}	S_L	k_{rg}	k_{rog}	p_{cgo}
0.260	0.0000	1.0000	0	0.260	1.0000	0.0000	0
0.288	0.0060	0.9430	0	0.460	0.7000	0.0000	0
0.315	0.0160	0.8100	0	0.487	0.6430	0.0000	0
0.343	0.0290	0.6720	0	0.514	0.5880	0.0010	0
0.371	0.0450	0.5360	0	0.541	0.5340	0.0030	0
0.398	0.0630	0.4220	0	0.568	0.4820	0.0080	0
0.426	0.0820	0.3430	0	0.595	0.4320	0.0160	0
0.454	0.1040	0.2750	0	0.622	0.3830	0.0270	0
0.481	0.1260	0.2160	0	0.649	0.3370	0.0430	0
0.537	0.1770	0.1250	0	0.676	0.2930	0.0640	0
0.592	0.2320	0.0640	0	0.703	0.2510	0.0910	0
0.647	0.2930	0.0270	0	0.730	0.2110	0.1250	0
0.703	0.3580	0.0080	0	0.757	0.1730	0.1660	0
0.758	0.4270	0.0010	0	0.784	0.1380	0.2160	0
0.785	0.4630	0.0000	0	0.811	0.1060	0.2750	0
0.813	0.5000	0.0000	0	0.838	0.0760	0.3430	0
1.000	1.0000	0.0000	0	0.865	0.0535	0.4220	0
				0.892	0.0350	0.5120	0
				0.925	0.0172	0.6386	0
				0.950	0.0071	0.7473	0
				0.960	0.0040	0.7940	0
				0.967	0.0022	0.8277	0
				0.980	0.0000	0.8929	0
				1.000	0.0000	1.0000	0

Table B-4 — Reservoir Layering - 99-layer, 10-layer, and 5-layer thickness and permeabilities.

Layer	k, md	Thickness, m	Flow capacity, fraction	Storage capacity, fraction	Fn	Cn
99 Layers						
1	2517	1.515	0.1096	0.01	0.1096	0.01
2	1725	1.515	0.0751	0.01	0.1847	0.02
3	1357	1.515	0.0591	0.01	0.2438	0.03
4	1133	1.515	0.0493	0.01	0.2931	0.04
5	978	1.515	0.0426	0.01	0.3357	0.05
6	864	1.515	0.0376	0.01	0.3733	0.06
7	774	1.515	0.0337	0.01	0.4070	0.07
8	702	1.515	0.0305	0.01	0.4375	0.08
9	642	1.515	0.0279	0.01	0.4655	0.09
10	591	1.515	0.0257	0.01	0.4912	0.10
11	548	1.515	0.0238	0.01	0.5151	0.11
12	510	1.515	0.0222	0.01	0.5373	0.12
13	477	1.515	0.0208	0.01	0.5580	0.13
14	447	1.515	0.0195	0.01	0.5775	0.14
15	421	1.515	0.0183	0.01	0.5958	0.15
16	397	1.515	0.0173	0.01	0.6131	0.16
17	375	1.515	0.0163	0.01	0.6294	0.17
18	356	1.515	0.0155	0.01	0.6449	0.18
19	338	1.515	0.0147	0.01	0.6596	0.19
20	321	1.515	0.0140	0.01	0.6736	0.20
21	306	1.515	0.0133	0.01	0.6869	0.21
22	292	1.515	0.0127	0.01	0.6996	0.22
23	278	1.515	0.0121	0.01	0.7117	0.23
24	266	1.515	0.0116	0.01	0.7233	0.24
25	255	1.515	0.0111	0.01	0.7344	0.25
26	244	1.515	0.0106	0.01	0.7450	0.26
27	234	1.515	0.0102	0.01	0.7552	0.27
28	224	1.515	0.0098	0.01	0.7649	0.28
29	215	1.515	0.0094	0.01	0.7743	0.29
30	207	1.515	0.0090	0.01	0.7833	0.30
31	199	1.515	0.0087	0.01	0.7920	0.31
32	191	1.515	0.0083	0.01	0.8003	0.32
33	184	1.515	0.0080	0.01	0.8083	0.33
34	177	1.515	0.0077	0.01	0.8160	0.34
35	170	1.515	0.0074	0.01	0.8234	0.35
36	164	1.515	0.0072	0.01	0.8306	0.36
37	158	1.515	0.0069	0.01	0.8375	0.37
38	153	1.515	0.0066	0.01	0.8441	0.38
39	147	1.515	0.0064	0.01	0.8505	0.39
40	142	1.515	0.0062	0.01	0.8567	0.40
41	137	1.515	0.0060	0.01	0.8627	0.41
42	132	1.515	0.0058	0.01	0.8684	0.42
43	128	1.515	0.0056	0.01	0.8740	0.43
44	123	1.515	0.0054	0.01	0.8794	0.44
45	119	1.515	0.0052	0.01	0.8845	0.45
46	115	1.515	0.0050	0.01	0.8895	0.46
47	111	1.515	0.0048	0.01	0.8944	0.47
48	107	1.515	0.0047	0.01	0.8990	0.48
49	104	1.515	0.0045	0.01	0.9035	0.49
50	100	1.515	0.0044	0.01	0.9079	0.51
51	97	1.515	0.0042	0.01	0.9121	0.52
52	93	1.515	0.0041	0.01	0.9162	0.53
53	90	1.515	0.0039	0.01	0.9201	0.54
54	87	1.515	0.0038	0.01	0.9239	0.55
55	84	1.515	0.0037	0.01	0.9275	0.56
56	81	1.515	0.0035	0.01	0.9311	0.57
57	78	1.515	0.0034	0.01	0.9345	0.58
58	76	1.515	0.0033	0.01	0.9378	0.59
59	73	1.515	0.0032	0.01	0.9410	0.60
60	70	1.515	0.0031	0.01	0.9440	0.61
61	68	1.515	0.0030	0.01	0.9470	0.62
62	66	1.515	0.0029	0.01	0.9498	0.63
63	63	1.515	0.0028	0.01	0.9526	0.64
64	61	1.515	0.0027	0.01	0.9552	0.65
65	59	1.515	0.0026	0.01	0.9578	0.66
66	56	1.515	0.0025	0.01	0.9602	0.67
67	54	1.515	0.0024	0.01	0.9626	0.68
68	52	1.515	0.0023	0.01	0.9649	0.69
69	50	1.515	0.0022	0.01	0.9671	0.70
70	48	1.515	0.0021	0.01	0.9692	0.71
71	46	1.515	0.0020	0.01	0.9712	0.72
72	45	1.515	0.0019	0.01	0.9731	0.73
73	43	1.515	0.0019	0.01	0.9750	0.74
74	41	1.515	0.0018	0.01	0.9768	0.75
75	39	1.515	0.0017	0.01	0.9785	0.76
76	38	1.515	0.0016	0.01	0.9801	0.77
77	36	1.515	0.0016	0.01	0.9817	0.78
78	34	1.515	0.0015	0.01	0.9832	0.79
79	33	1.515	0.0014	0.01	0.9846	0.80
80	31	1.515	0.0014	0.01	0.9860	0.81
81	30	1.515	0.0013	0.01	0.9873	0.82
82	28	1.515	0.0012	0.01	0.9885	0.83
83	27	1.515	0.0012	0.01	0.9897	0.84
84	25	1.515	0.0011	0.01	0.9908	0.85
85	24	1.515	0.0010	0.01	0.9918	0.86
86	22	1.515	0.0010	0.01	0.9928	0.87
87	21	1.515	0.0009	0.01	0.9937	0.88
88	20	1.515	0.0009	0.01	0.9945	0.89
89	18	1.515	0.0008	0.01	0.9953	0.90
90	17	1.515	0.0007	0.01	0.9961	0.91
91	16	1.515	0.0007	0.01	0.9967	0.92
92	14	1.515	0.0006	0.01	0.9974	0.93
93	13	1.515	0.0006	0.01	0.9979	0.94
94	12	1.515	0.0005	0.01	0.9984	0.95
95	10	1.515	0.0004	0.01	0.9989	0.96
96	9	1.515	0.0004	0.01	0.9993	0.97
97	7	1.515	0.0003	0.01	0.9996	0.98
98	6	1.515	0.0003	0.01	0.9998	0.99
99	4	1.515	0.0002	0.01	1.0000	1.00

Layer	k, md	h, m	Flow capacity, fraction	Storage capacity, fraction	Fn	Cn
10 Layers : Equal Flow Capacity						
1	2517	1.4	0.100	0.009	0.100	0.009
2	1705	2.0	0.100	0.014	0.200	0.023
3	1207	2.9	0.100	0.019	0.300	0.042
4	873	4.0	0.100	0.027	0.400	0.069
5	642	5.4	0.100	0.036	0.500	0.105
6	471	7.4	0.100	0.049	0.600	0.154
7	338	10.3	0.100	0.069	0.700	0.223
8	231	15.0	0.100	0.100	0.800	0.323
9	141	24.6	0.100	0.164	0.900	0.487
10	45	76.9	0.100	0.513	1.000	1.000
10 Layers : Equal Storage Capacity						
1	1134	15.0	0.489	0.100	0.489	0.100
2	423	15.0	0.182	0.100	0.671	0.200
3	255	15.0	0.110	0.100	0.781	0.300
4	171	15.0	0.074	0.100	0.854	0.400
5	119	15.0	0.051	0.100	0.906	0.500
6	85	15.0	0.036	0.100	0.942	0.600
7	59	15.0	0.026	0.100	0.968	0.700
8	40	15.0	0.017	0.100	0.985	0.800
9	24	15.0	0.010	0.100	0.995	0.900
10	11	15.0	0.005	0.100	1.000	1.000
5 Layers : Equal Flow Capacity						
1	2033	3.4	0.200	0.023	0.200	0.023
2	1013	6.9	0.200	0.046	0.400	0.069
3	544	12.8	0.200	0.085	0.600	0.154
4	275	25.3	0.200	0.169	0.800	0.323
5	69	101.6	0.200	0.677	1.000	1.000
5 Layers : Equal Storage Capacity						
1	778	30.0	0.671	0.200	0.671	0.200
2	213	30.0	0.183	0.200	0.854	0.400
3	102	30.0	0.088	0.200	0.942	0.600
4	50	30.0	0.043	0.200	0.985	0.800
5	18	30.0	0.015	0.200	1.000	1.000
6 Layers : equal flow capacity (3) & equal storage capacity (3)						
1	2175	2.7	0.167	0.018	0.167	0.018
2	1202	4.8	0.167	0.032	0.333	0.050
3	706	8.2	0.167	0.055	0.500	0.105
4	277	44.8	0.356	0.298	0.856	0.403
5	87	44.8	0.112	0.298	0.968	0.702
6	25	44.8	0.032	0.298	1.000	1.000

Table B-5 — Effect of reservoir heterogeneity on reservoir performance (depletion cases).

Cases		AFTER 3 YEARS			AFTER 5 YEARS			AFTER 10 YEARS		
		FOPR Sm^3/d	FGOR Sm^3/Sm^3	RF_o %	FOPR Sm^3/d	FGOR Sm^3/Sm^3	RF_o %	FOPR Sm^3/d	FGOR Sm^3/Sm^3	RF_o %
Permeability Distribution (Depletion)										
BASE (GOC fluid)	99 HBKS	1199	2118	15.7	612	3200	19.5	73	4905	23.3
High k at bottom	5 HBKF	1138	2247	15.3	583	3371	18.9	62	5342	22.4
	5 HBKS	940	2751	14.1	483	4097	17.0	48	5775	20.0
High k at top	99 HTKS	894	2902	13.6	458	4323	16.4	38	6033	19.2
	5 HTKF	896	2894	13.6	459	4317	16.4	10	6032	19.3
	5 HTKS	895	2897	13.6	459	4318	16.4	39	6035	19.3
High k in middle	99 HMKS	909	2862	13.7	463	4289	16.5	38	6029	19.4
	5 HMKF	914	2834	13.9	468	4232	16.7	41	5958	19.7
	5 HMKS	905	2865	13.8	462	4288	16.6	40	6018	19.5
6 layers (3F & 3S)		1161	2203	15.3	610	3219	19.0	66	5164	22.7
Effect of dip (angle=0)	99 HBKS	1079	2366	14.9	563	3483	18.3	207	4826	22.0
	5 HBKF	1086	2353	14.7	547	3595	18.1	181	5523	21.5
	5 HBKS	913	2824	13.6	470	4198	16.4	49	5908	19.3
Vertical Permeability kz=0	99 HBKS	869	3001	12.9	456	4363	15.6	47	5217	18.2
	5 HBKF	901	2886	13.2	462	4298	16.0	51	5932	18.9
	5 HBKS	878	2967	12.9	458	4329	15.7	48	5558	18.3
Harmonic Average	5 HBKF	1113	2301	15.2	567	3475	18.7	58	5541	22.1
	5 HBKS	938	2757	14.1	482	4108	17.0	48	5792	20.0
Effect of Average Reservoir Permeability (Depletion)										
Kavg = 232 md	99 HBKS	1199	2118	15.7	612	3200	19.5	73	4905	23.3
	99 HTKS	894	2902	13.6	458	4323	16.4	38	6033	19.2
Kavg = 50 md	99 HBKS	1002	2570	13.8	515	3830	16.9	74	4995	20.0
	99 HTKS	859	3018	12.5	446	4437	15.2	59	5927	17.9
Kavg = 10 md	99 HBKS	812	2399	9.2	479	3085	11.9	162	4172	15.0
	99 HTKS	695	2909	8.4	402	3779	10.7	135	5027	13.3
Effect of number of layers (Depletion)										
BASE (GOC fluid)	99 HBKS	1199	2118	15.7	612	3200	19.5	73	4905	23.3
	5 HBKF	1138	2247	15.3	583	3371	18.9	62	5342	22.4
	5 HBKS	940	2751	14.1	483	4097	17.0	48	5775	20.0
10-layers case	99 HBKS	1199	2118	15.7	612	3200	19.5	73	4905	23.3
	10 HBKF	1189	2137	15.6	603	3252	19.3	76	4660	23.1
	10 HBKS	991	2602	14.3	523	3775	17.4	55	5295	20.7
Effect of Fluid Composition (Depletion)										
BASE (GOC fluid)	99 HBKS	1199	2118	15.7	612	3200	19.5	73	4905	23.3
	5 HBKF	1138	2247	15.3	583	3371	18.9	62	5342	22.4
	5 HBKS	940	2751	14.1	483	4097	17.0	48	5775	20.0
Rich GC (4740 m)	99 HBKS	1199	2127	15.6	611	3219	19.4	76	4954	23.2
(Vromax=43%)	5 HBKF	1138	2255	15.2	585	3374	18.8	64	5364	22.3
	5 HBKS	948	2739	14.1	486	4091	17.0	50	5803	20.1
	99 HBKS	1199	2127	15.6	611	3219	19.4	76	4954	23.2
	10 HBKF	1192	2139	15.5	602	3272	19.2	78	4739	23.1
	10 HBKS	994	2606	14.3	522	3799	17.4	57	5355	20.7
Rich GC (4700 m)	99 HBKS	994	2686	18.0	521	4009	22.0	185	6000	26.3
(Vromax=27%)	5 HBKF	997	2689	18.0	522	4016	22.1	185	6002	26.3
	5 HBKS	999	2690	18.0	524	4015	22.1	185	6002	26.4
Oil Sample (4800m)	99 HBKS	2305	958	21.5	1293	1325	27.1	170	2295	32.2
	5 HBKF	2061	1089	20.4	1082	1596	25.2	136	2406	29.4
	5 HBKS	1805	1263	19.7	855	2047	23.7	111	2683	26.9
	99 HBKS	2305	958	21.5	1293	1325	27.1	170	2295	32.2
	10 HBKF	2199	1013	20.9	1222	1409	26.2	146	2480	31.0
	10 HBKS	2340	952	21.4	978	1795	26.4	125	2835	30.0
Oil Sample (5000m)	99 HBKS	3543	502	24.2	2016	690	31.0	0	0	36.1
	5 HBKF	3173	573	23.2	1751	803	29.1	0	0	33.6
	5 HBKS	3493	515	24.0	1685	845	30.3	0	0	34.1
Effect of Fluid Composition on 99 layers(Depletion)										
Rich GC (4500 m)	99 HBKS	1103	2497	25.2	595	3718	32.5	212	5851	40.5
(Vromax=12%,pg=433.542)	99 HTKS	1096	2526	25.1	595	3748	32.4	212	5865	40.4
Rich GC (4700 m)	99 HBKS	994	2686	18.0	521	4009	22.0	185	6000	26.3
(Vromax=27%,pg=433.542)	99 HTKS	996	2704	17.7	524	4032	21.7	186	6007	26.1
Rich GC (4740 m)	99 HBKS	1199	2127	15.6	611	3219	19.4	76	4954	23.2
(Vromax=43%,pg=477.243)	99 HTKS	905	2877	13.6	463	4301	16.4	40	6034	19.4
Rich GC (4750 m)	99 HBKS	1199	2118	15.7	612	3200	19.5	73	4905	23.3
(Vromax=55%,pg=478.027)	99 HTKS	894	2902	13.6	458	4323	16.4	38	6033	19.2
Oil Sample (4800m)	99 HBKS	2324	952	21.4	1301	1321	27.1	0	0	32.3
	99 HTKS	792	3010	12.2	388	4512	14.0	0	0	15.5
Oil Sample (5000m)	99 HBKS	3543	502	24.2	2016	690	31.0	0	0	36.1
	99 HTKS	787	2580	13.9	373	3861	15.2	0	0	16.0
Oil Sample (6000m)	99 HBKS	3980	166	24.1	1376	160	28.8	205	123	31.5
	99 HTKS	1033	1167	16.3	20	2334	17.1	0	0	17.1

Table B-6 — Effect of reservoir heterogeneity on reservoir performance (gas injection cases).

Cases		AFTER 3 YEARS			AFTER 5 YEARS			AFTER 10 YEARS		
		FOPR Sm^3/d	FGOR Sm^3/Sm^3	RF_o %	FOPR Sm^3/d	FGOR Sm^3/Sm^3	RF_o %	FOPR Sm^3/d	FGOR Sm^3/Sm^3	RF_o %
Permeability Distribution (Injection)										
BASE (GOC fluid)	99 HBKS	3543	955	27.4	2716	1295	41.2	1239	2996	61.5
High k at bottom	5 HBKF	3538	955	27.8	2406	1484	41.0	1623	2250	60.5
	5 HBKS	3044	1147	29.5	2526	1411	41.4	1300	2852	60.9
High k at top	99 HTKS	2423	1489	23.6	1632	2275	32.4	866	4336	44.9
	5 HTKF	2541	1409	24.1	1795	2049	33.2	827	4530	46.6
	5 HTKS	2164	1694	27.7	1550	2416	35.2	880	4269	49.0
High k in middle	99 HMKS	3075	1131	25.5	2249	1604	37.2	994	3758	53.3
	5 HMKF	3011	1157	26.7	2409	1480	37.8	1476	2493	59.0
	5 HMKS	2473	1455	28.4	1806	2040	37.0	1307	2838	55.2
6 layers (3F & 3S)		3949	834	28.4	2731	1287	43.4	1240	2994	60.9
Effect of dip (angle=0)	99 HBKS	3194	1074	25.6	2442	1452	37.9	1096	3393	56.4
	5 HBKF	3169	1083	26.0	2262	1580	38.0	1323	2775	55.1
	5 HBKS	2595	1368	28.3	2426	1464	39.0	1122	3315	57.3
Vertical Permeability kz=0	99 HBKS	2637	1352	25.0	1688	2195	34.4	777	4847	46.5
	5 HBKF	2657	1341	25.2	1722	2149	34.8	670	5639	47.4
	5 HBKS	2498	1445	28.8	1407	2690	36.1	918	4095	49.0
Average Reservoir Permeability variation (Injection)										
Kavg=232	99 HBKS	3543	955	27.4	2716	1295	41.2	1239	2996	61.5
	99 HTKS	2423	1489	23.6	1632	2275	32.4	866	4336	44.9
Kavg=50	99 HBKS	2221	1635	22.0	1616	2284	30.3	965	3869	43.8
	99 HTKS	2040	1798	21.0	1431	2602	28.4	845	4433	40.2
Kavg=10	99 HBKS	2248	1570	15.6	1825	2176	24.6	1062	3799	39.7
	99 HTKS	2220	1591	15.2	1807	2204	24.1	1041	3884	39.0
Effect of number of layers (Injection)										
BASE (GOC fluid)	99 HBKS	3543	955	27.4	2716	1295	41.2	1239	2996	61.5
	5 HBKF	3538	955	27.8	2406	1484	41.0	1623	2250	60.5
	5 HBKS	3044	1147	29.5	2526	1411	41.4	1300	2852	60.9
10 layers case	99 HBKS	3543	955	27.4	2716	1295	41.2	1239	2996	61.5
	10 HBKF	3567	946	27.6	2640	1337	41.2	1152	3231	60.1
	10 HBKS	3325	1031	27.8	2691	1310	41.1	1336	2775	62.0
Effect of Fluid Composition (Injection)										
BASE (GOC fluid)	99 HBKS	3543	955	27.4	2716	1295	41.2	1239	2996	61.5
	5 HBKF	3538	955	27.8	2406	1484	41.0	1623	2250	60.5
	5 HBKS	3044	1147	29.5	2526	1411	41.4	1300	2852	60.9
Rich GC (4700 m)	99 HBKS	2789	1274	27.6	2188	1668	41.6	1086	3471	63.7
(Vromax=27%)	5 HBKF	2788	1274	28.0	2084	1758	41.7	1459	2542	63.9
	5 HBKS	2467	1469	29.6	1965	1882	41.6	1083	3490	62.2
	99 HBKS	2789	1274	27.6	2188	1668	41.6	1086	3471	63.7
	10 HBKF	2798	1269	27.8	2165	1686	41.7	983	3841	62.2
	10 HBKS	2596	1384	27.9	2177	1678	41.4	1118	3368	63.6
Oil Sample (4800m)	99 HBKS	4378	712	25.2	3421	962	37.9	1520	2360	57.0
	5 HBKF	4263	737	26.4	3338	987	38.4	1898	1838	58.2
	5 HBKS	3923	821	29.8	2909	1165	40.2	1519	2352	56.6
	99 HBKS	4378	712	25.2	3421	962	37.9	1520	2360	57.0
	10 HBKF	4386	711	25.6	3264	1015	38.0	1873	1866	57.4
	10 HBKS	3876	834	27.0	3184	1048	38.6	1603	2222	56.8
Effect of Fluid Composition on 99 layers, Kavg = 232 md (Injection)										
Rich GC (4500 m)	99 HBKS	1659	2281	27.7	1285	2986	41.0	628	6214	61.8
(Vromax=12%,pg=)	99 HTKS	1335	2879	25.7	951	4096	35.9	526	7422	51.8
Rich GC (4640 m)	99 HBKS	2250	1630	27.7	1745	2145	41.5	861	4458	63.1
(Vromax=20%,pg=403.429)	99 HTKS	1703	2213	25.2	1217	3152	35.0	681	5659	50.6
Rich GC (4700 m)	99 HBKS	2789	1274	27.6	2188	1668	41.6	1086	3471	63.7
(Vromax=27%,pg=433.542)	99 HTKS	2020	1833	24.6	1450	2608	34.1	822	4626	49.3
Rich GC (4740 m)	99 HBKS	3540	956	27.2	2743	1281	41.1	1245	2982	61.8
(Vromax=43%,pg=477.243)	99 HTKS	2429	1485	23.5	1665	2229	32.4	870	4314	45.2
Rich GC (4750 m)	99 HBKS	3552	952	27.2	2728	1289	41.0	1239	2995	61.4
(Vromax=55%,pg=478.027)	99 HTKS	2436	1480	23.5	1641	2262	32.3	866	4335	44.9
Rich GC (4800 m)	99 HBKS	4389	710	25.1	3434	958	37.7	1520	2359	57.0
	99 HTKS	2827	1221	20.9	2073	1717	28.7	1174	3112	41.4
Effect of Fluid Composition on 99 layers, Kavg = 50 md (Injection)										
Rich GC (4640 m)	99 HBKS	1717	2190	24.8	1280	2985	35.0	729	5266	51.6
(Vromax=20%,pg=403.429)	99 HTKS	1624	2328	24.3	1186	3237	33.8	685	5622	49.2
Rich GC (4700 m)	99 HBKS	2041	1809	24.2	1541	2440	34.1	886	4269	50.4
(Vromax=27%,pg=433.542)	99 HTKS	1910	1946	23.5	1405	2693	32.7	818	4639	47.6
Rich GC (4740 m)	99 HBKS	2243	1618	22.0	1627	2268	30.4	966	3863	44.0
(Vromax=43%,pg=477.243)	99 HTKS	2064	1776	21.1	1440	2586	28.6	843	4445	40.4
Rich GC (4750 m)	99 HBKS	2221	1635	22.0	1616	2284	30.3	965	3869	43.8
(Vromax=55%,pg=478.027)	99 HTKS	2040	1798	21.0	1431	2602	28.4	845	4433	40.2
Oil Sample (4800m)	99 HBKS	2827	1218	20.3	2081	1705	28.2	1150	3149	40.7
	99 HTKS	2590	1348	19.5	1886	1908	26.6	1030	3544	37.8
Effect of number of grids - changed well position, 10 vertical layers (Injection)										
	100x10	4198	764	30.5	3284	1033	47.0	1291	2884	67.8
	50x10	4140	778	30.3	3269	1048	46.6	1294	2871	67.4
	10x10	3855	856	29.5	2931	1185	44.3	1311	2829	65.4
	50x50	4340	730	31.0	3491	956	48.3	1400	2661	70.1
	50x10	4140	778	30.3	3269	1048	46.6	1294	2871	67.4
	50X5	3865	856	29.1	2974	1166	44.2	1293	2869	64.8
	50X3	3493	972	27.7	2667	1322	41.2	1252	2968	60.8
	10x10	3855	856	29.5	2931	1185	44.3	1311	2829	65.4
	10X5	3617	928	28.4	2756	1269	42.2	1364	2701	63.2
	10X3	3318	1030	27.0	2530	1398	39.7	1275	2894	59.3
Half Model (half of the area) - Injector and Producer placed at corners										
	50X10	2138	745	30.6	1695	993	47.5	647	2881	68.9
	50X20	2166	732	30.9	1732	965	48.2	691	2698	69.8

Table B-7 — Black-oil versus compositional - Geologic unit properties.

Numerical Layer	Top geologc unit (GU1)		Middle geologic unit (GU2)		Bottom geologic unit (GU3)	
	k, md	Thickness, m	k, md	Thickness, m	k, md	Thickness, m
1	0.975	76.95	9.747	76.95	38.987	76.95
2	3.046	24.62	30.465	24.62	121.859	24.62
3	4.984	15.05	49.843	15.05	199.371	15.05
4	7.290	10.29	72.898	10.29	291.593	10.29
5	10.154	7.39	101.544	7.39	406.176	7.39
6	13.843	5.42	138.425	5.42	553.702	5.42
7	18.817	3.99	188.170	3.99	752.684	3.99
8	26.015	2.88	260.152	2.88	1040.610	2.88
9	36.756	2.04	367.558	2.04	1470.235	2.04
10	54.244	1.38	542.436	1.38	2169.750	1.38
k_{avg}, md	5		50		200	
Porosity	0.15		0.15		0.15	
Top, m	4500 - 4700		4550 - 4750		4600 - 4800	
Bottom	4550 - 4750		4600 - 4800		4650 - 4850	
Thickness, m	50		50		50	
Dip angle, degree	3.8		3.8		3.8	
PV, E6 m3	22.5		22.5		23	
HCPV, E6 m3	16.65		16.65		16.65	
Swi, %	26		26		26	
Sgc, %	2		2		2	
Sorg, %	22.7		22.7		22.7	
Sorw, %	21.5		21.5		21.5	
NX	50		50		50	
NY	10		10		10	
NZ	10		10		10	
DX, m	60		60		60	
DY, m	10		10		10	

Table B-8 — Black-oil versus compositional – Potential simulation parameters and naming convention.

Identifier	Parameters	1	2	3	4	5	6
A	Geologic Unit	GU3	GU2	GU1	GU4		
B	Production Control	DEP	INJ	0.5-Reinj	0.8-Reinj	1.0-Reinj	Dep+inj
C	Fluid Model	EOS6A	EOS8A	EOS22A	EOS3A		
D	Reservoir Fluid	NCO (4750)	RGC(-50)	VO(+50)	MGC(-250)	SVO(+250)	RS50
E	Res. Fluid Composition	Constant	Gradient from EOS 22	Gradient from Used EOS			
F	Permeability Distribution	High Bottom	High Top	High Middle			
G	Inclination (Dip)	3.8	0				
H	Perm variation, V	0.75					
I	Perm Pseudoization	Fn	Cn				
J	Injection Gas	RG	LG	Sep. Gas	C1N2	CO2	WATER
K	Vertical Permeability factor	0.1					
L	Relative Permeability	RP1					
M	Resevoir Pressure	Pr=495 P@GOC)	Pr=Psat@GOC				
N	Grid X	50	15	10	100	200	
O	Grid Y	10	5	50	100		
P	Grid Z	10	5	99			
Q	Simulator	ECL					
R	Reservoir Model	FULL					
S	Production Constraint	RESV	BHP				
T	Injection Constraint	RESV	BHP				
U	Production Limitation	TIME	GOR	Qg	Qo		
V	Geometry	CAR					
W	Separator Conditions	2-Stage					
Y	Swelling	Eclipse	swelling				
Z	Gravity		Stable				

Table B-9 — Black-oil versus compositional – Depletion cases.

Case Name	Description	Black-oil	EOS
EOS, Model			
A1C1*	Near critical fluid from GOC 4750 m ($V_{ro,max}$ =55%), EOS6		x
A1C3	Near critical fluid from GOC 4750 m ($V_{ro,max}$ =55%), EOS22		x
E2A4C3X	All three geologic units with reservoir fluid gradient, EOS22		x
D1F2C3	Near critical fluid, permeability high-top, EOS22		x
Initial Fluid, Constant			
A1C1	Near critical fluid from GOC 4750 m($V_{ro,max}$ =55%)	x	x
D2	Rich gas condensate from 4700 m($V_{ro,Max}$ = 28% and r_s = 0.00115 Sm^3/Sm^3)	x	x
D3	Volatile oil from 4800 m (B_{ob} = 2.3 and R_S = 407 Sm^3/Sm^3)	x	x
D4	Medium-rich gas condensate from 4500 m ($V_{ro,Max}$ = 12% and r_s = 0.00066 Sm^3/Sm^3)	x	x
D5	Slightly volatile oil from 5000 m (B_{ob} = 1.8 and R_S = 256 Sm^3/Sm^3)	x	x
Initial Fluid, Variable			
E2A1	Oil and some gas-condensate with fluid gradient as in bottom layer	x	x
E2A2	Gas condensate and oil with fluid gradient as in middle layer	x	x
E2A3	Only gas condensate fluid gradient as in top layer	x	x
E2A3_MODVO	Only gas condensate fluid gradient as in top layer, modified black-oil viscosity	x	x
E2A3_10	Only gas condensate fluid gradient as in top layer (k = 50 md)	x	x
E2A4	All three geologic units with reservoir fluid gradient	x	x
Permeability Variations			
D1F2	Near critical fluid, permeability high-top	x	x
D1F3	Near critical fluid, permeability high-middle	x	x
D3F2	Volatile oil, permeability high-top	x	x
D3F3	Volatile oil, permeability high-middle	x	x
D2F2	Rich gas condensate, permeability high-top	x	x
D2F3	Rich gas condensate, permeability high-middle	x	x
Saturated GOC			
D3M2	Volatile oil, constant oil and gas composition, saturated GOC	x	x
D3M2E2	Oil and gas gradient, saturated GOC	x	x
D3M2E2_3W	Oil and gas gradient, saturated GOC, 3 producers	x	x

* : A1C1.DATA (Black-oil simulation data file), A1C1X.DATA (Compositional Simulation data file)

Table B-10 — Black-oil versus compositional – Injection cases.

Case Name	Description	Black-oil	EOS
EOS models			
J2B2D1C3	Near critical fluid , lean gas injection, EOS22		x
J2B2E2A4C3	All three geologic units with reservoir fluid gradient, EOS22		x
J2B5D1C3	Near critical fluid, inject (lean gas) all produced gas, EOS22		x
Full Pressure Maintenance			
Gas condensate reservoirs with constant composition			
J2B2D1*	Near critical fluid, lean gas injection	x	x
J2B2D2	Rich gas condensate, lean gas injection	x	x
J2B2D4	Medium-rich gas condensate, lean gas injection	x	x
J2B2D1Z2	Near-critical fluid, lean gas injection, gravity stable	x	x
J2B2D2Z2	Rich gas condensate, lean gas injection, gravity stable	x	x
J1B2D1	Near critical fluid, rich gas injection	x	x
J2B2D1_99	Near critical fluid, lean gas injection, 99 numerical layers	x	x
Oil reservoirs with constant composition			
J2B2D5	Slightly volatile oil (SVO), lean gas injection	x	x
J2B2D5Y2	Slightly volatile oil (SVO), lean gas injection	x	x
J2B2D6T2Y2	Low GOR oil, lean gas injection	x	x
J2B2D6T2	Low GOR oil, lean gas injection	x	x
J2B2D6T2_200	Low GOR oil, lean gas injection (pr=200 bara)	x	x
J4B2D5	Slightly volatile oil, C1N2 injection	x	x
Compositional gradient reservoir			
J2B2E2A1	Fluid gradient as in bottom geologic unit, lean gas injection	x	x
J2B2E2A2	Fluid gradient as in middle geologic unit, lean gas injection	x	x
J2B2E2A3	Fluid gradient as in top geologic unit, lean gas injection	x	x
J2B2E2A4	All three geologic units with reservoir fluid gradient, lean gas injection	x	x
Permeability variations			
J2B2D1F2	High Perm at top,near critical fluid, lean injection gas	x	x
J2B2D1F3	High Perm at middle, near critical fluid, lean injection gas	x	x
Partial Pressure Maintenance			
Undersaturated gas reservoirs			
J2B5D1	Near critical fluid, inject (lean gas) all produced gas	x	x
J2B3D2	Rich gas condensate, inject (lean gas) 50% of produced gas	x	x
J2B4D2	Rich gas condensate, inject (lean gas) 80% of produced gas	x	x
J2B5D2	Rich gas condensate, inject (lean gas) all produced gas	x	x
J2B5D4	Medium-rich gas condensate, inject (lean gas) all produced gas	x	x
Undersaturated oil reservoirs			
J2B3D3	Volatile oil, inject (lean gas) 50% of produced gas	x	x
J2B4D3	Volatile oil, inject (lean gas) 80% of produced gas	x	x
J2B5D3	Volatile oil, inject (lean gas) all produced gas	x	x
Oil reservoirs with gas injection in gas cap			
J2B3E2A2	Layer 2 gradient, inject (lean gas) 50% of produced gas	x	x
J2B4E2A2	Layer 2 gradient, inject (lean gas) 80% of produced gas	x	x
J2B5E2A2	Layer 2 gradient, inject (lean gas) all produced gas	x	x
Permeability variations			
J2B5E2A2F2	Middle geologic unit, inject (lean gas) all produced gas, highest k at top	x	x
J2B5D3F2	Volatile oil, inject (lean gas) all produced gas, highest k at top	x	x
Depletion followed by injection			
J2B6D1	Near critical fluid, depletion followed by injection	x	x
J2B2D2	Rich gas condensate, depletion followed by injection	x	x
J2B2D4	Medium-rich gas condensate, depletion followed by injection	x	x
J2B2D3	Volatile oil, depletion followed by injection	x	x

Appendix C

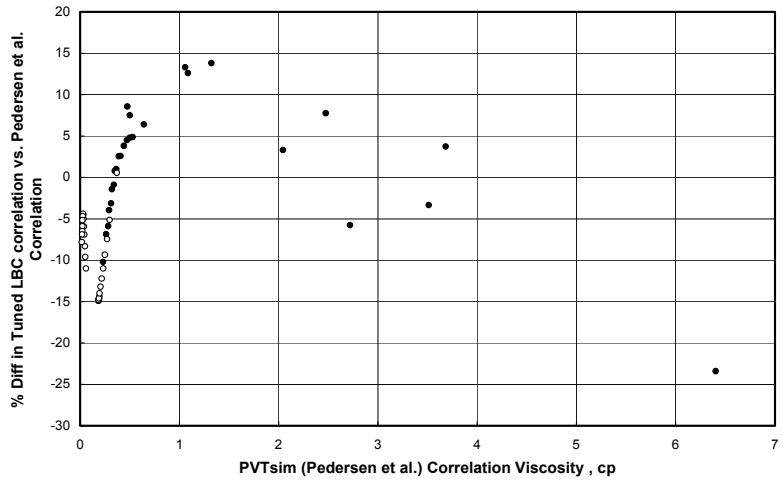

Fig. C-1 — Comparison of Viscosity Models — Pedersen et. al. versus LBC correlation.

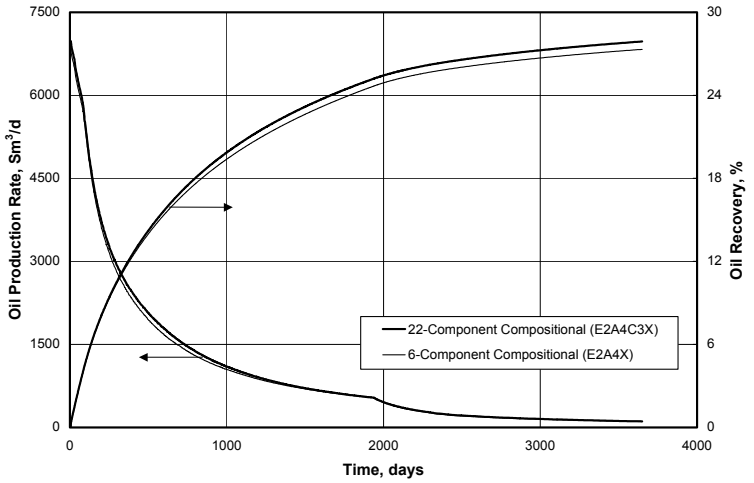

Fig. C-2 — Depletion Case – Near critical fluid system with compositional gradient and undersaturated GOC (three geologic unit), EOS22 vs. EOS6. (E2A4C3X.DATA, E2A4X.DATA).

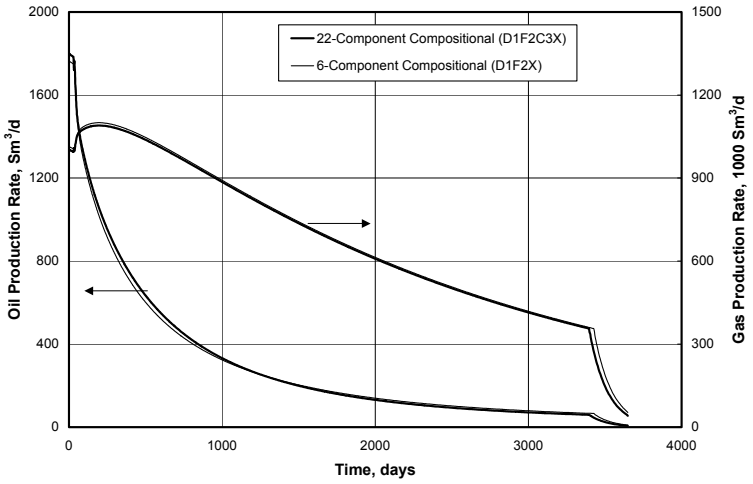

Fig. C-3 — Depletion Case – Near critical fluid with constant composition and the highest permeability at the top (bottom geologic unit), EOS22 vs. EOS6 (.D1F2C3X.DATA, D1F2X.DATA).

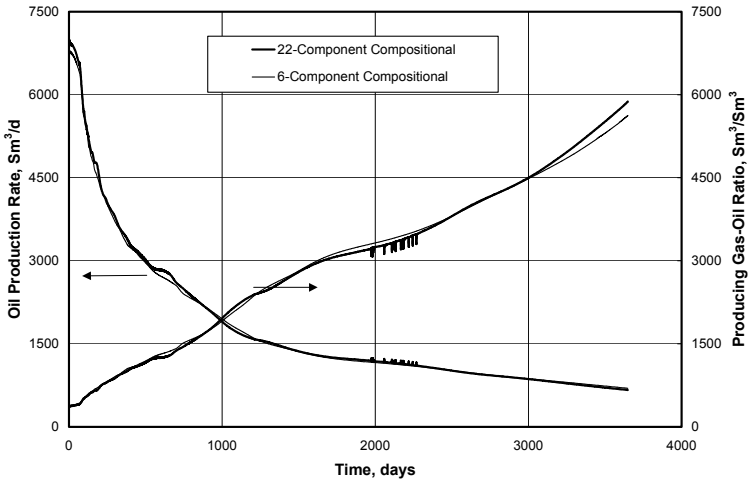

Fig. C-4 — Injection Case – Near critical fluid system with compositional gradient and undersaturated GOC (three geologic units), EOS22 vs. EOS6 (J2B2E2A4C3X.DATA, J2B2E2A4X.DATA).

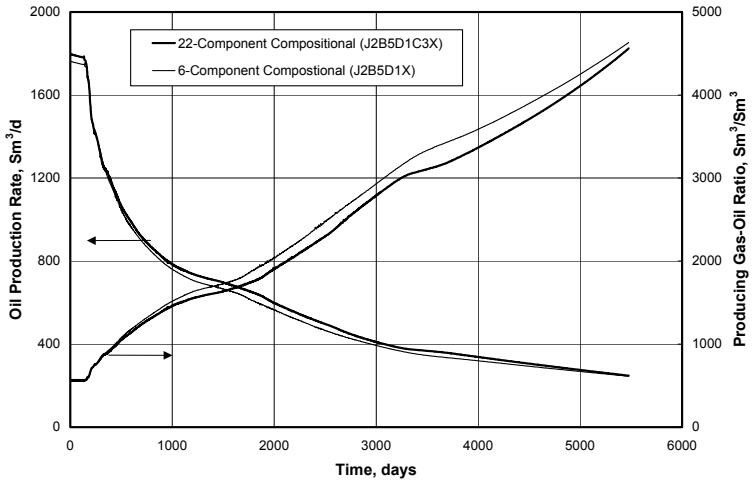

Fig. C-5 — Injection Case — Near critical fluid with constant composition and partial pressure maintenance (100% of the produced gas reinjected), EOS22 vs. EOS6 (J2B5D1C3X.DATA, J2B5D1X.DATA).

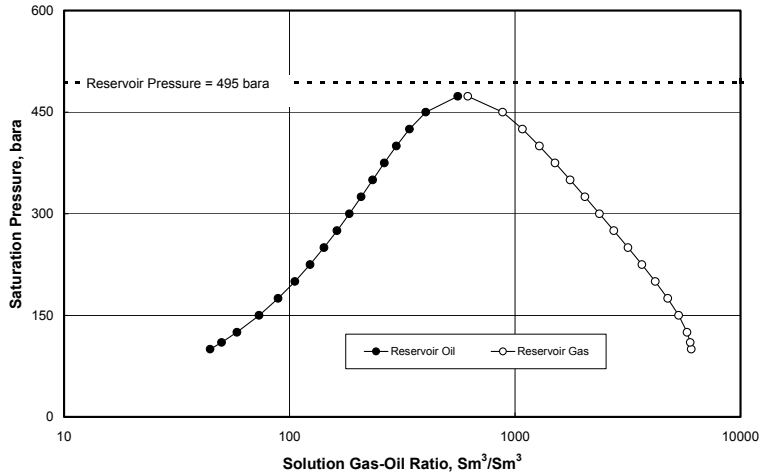

Fig. C-6 — Reservoir layering – Initial saturation pressure of different fluid systems.

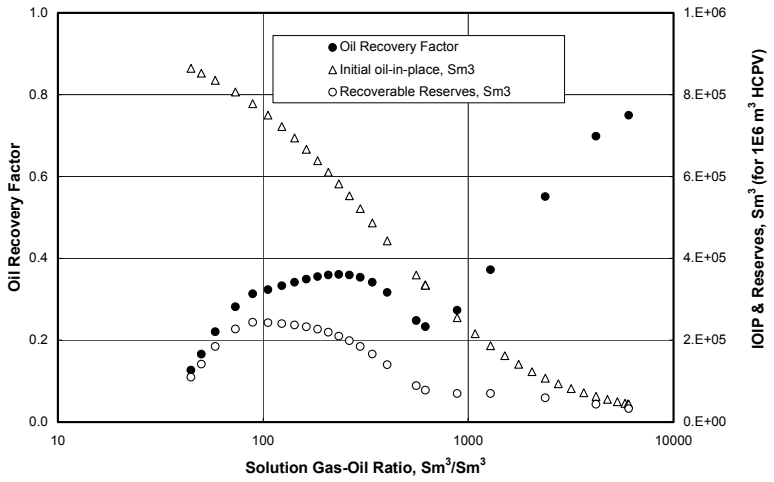

Fig. C-7 — Reservoir layering – Oil recovery factor, Initial oil in-place and recoverable reserves for different fluid systems, constant HCPV.

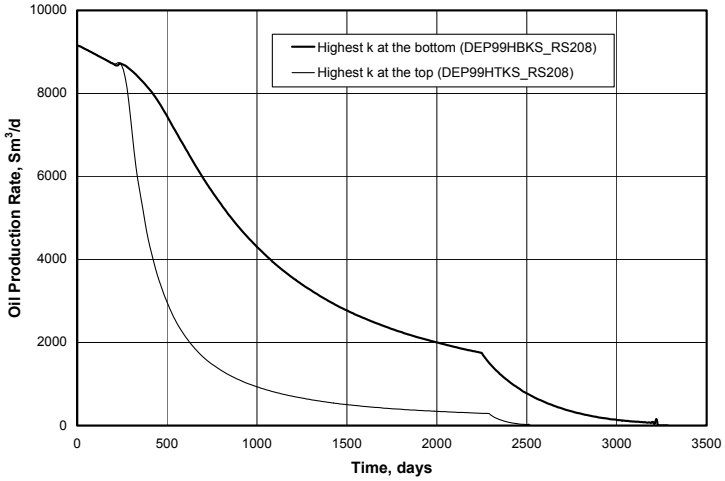

Fig. C-8 — Reservoir layering – Depletion performance of a constant composition oil (Rs=280 Sm^3/Sm^3) for (a) high permeability at the bottom (b) high permeability at the top.

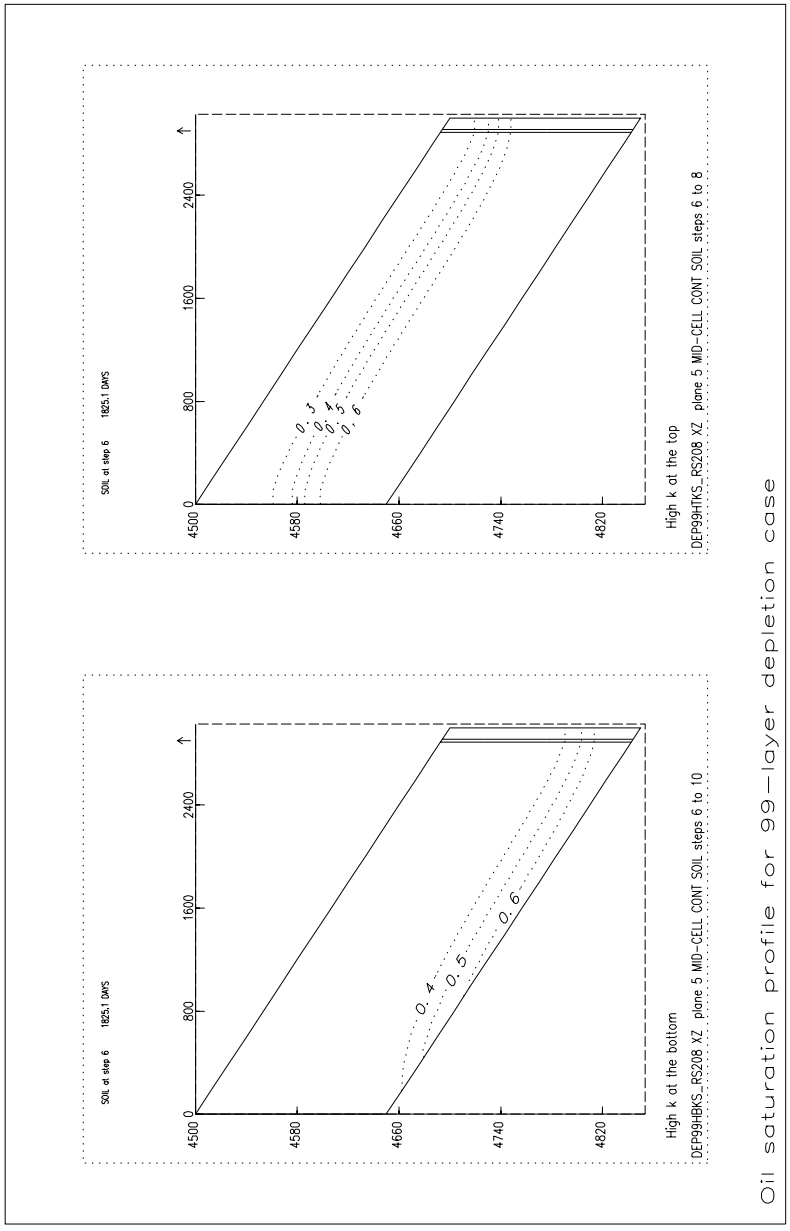

Fig. C-9 — Reservoir layering – oil saturation profile after 1825 days of depletion of constant composition oil (R_s=280 Sm^3/Sm^3) for (a) high permeability at the bottom (b) high permeability at the top.

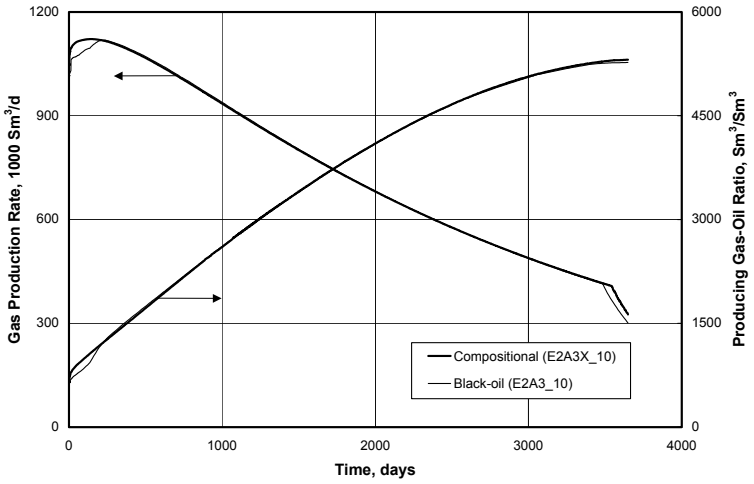

Fig. C-10 — Depletion Case – Top geologic unit with compositional gradient and increased average permeability; EOS6; (E2A3X_10.DATA, E2A3_10.DATA).

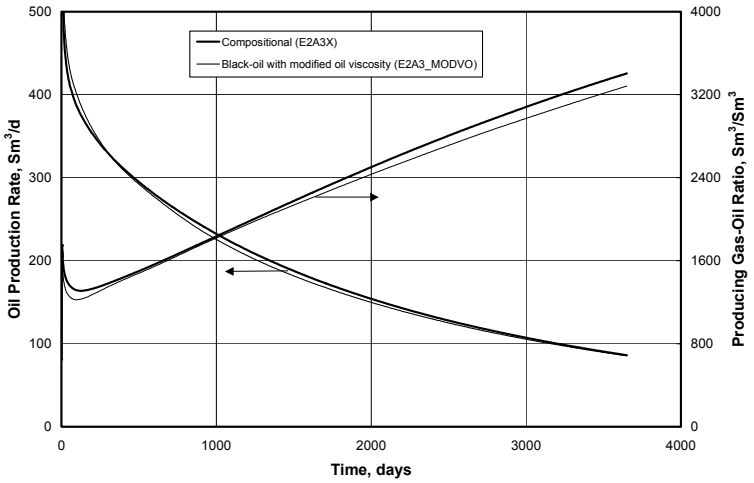

Fig. C-11 — Depletion Case – Top geologic unit with compositional gradient and modified oil viscosities in the black-oil model; EOS6; (E2A3X.DATA, E2A3_MODVO.DATA).

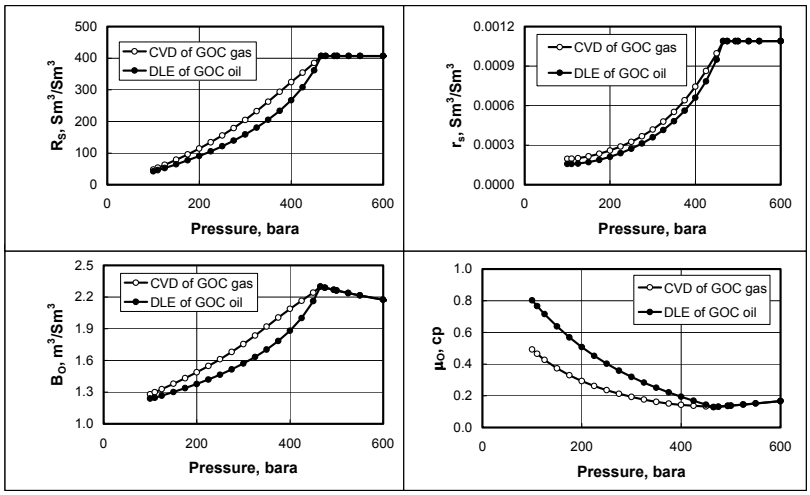

Fig. C-12 — Depletion Case – Black-oil PVT properties from a simulated DLE experiment with GOC oil and CVD experiment with GOC gas for a saturated GOC reservoir; EOS6.

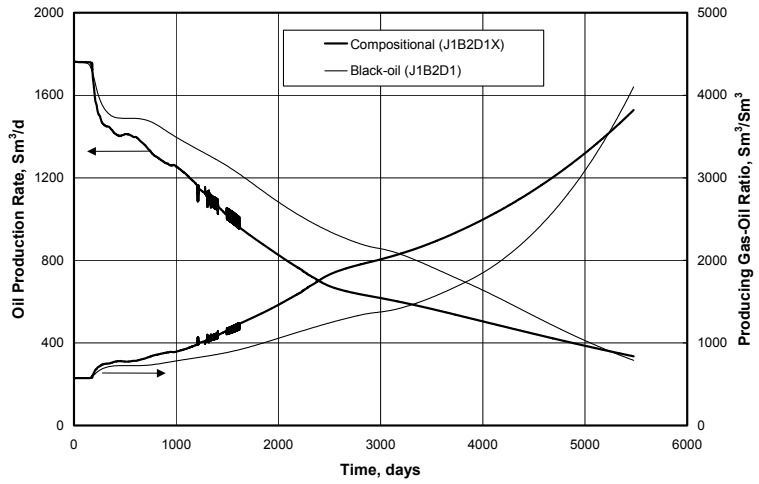

Fig. C-13 — Injection Case – Near critical fluid with constant composition and rich injection gas; EOS6 (J1B2D1X.DATA, J1B2D1.DATA).